

PDF hosted at the Radboud Repository of the Radboud University Nijmegen

The following full text is a publisher's version.

For additional information about this publication click this link.

<http://hdl.handle.net/2066/90819>

Please be advised that this information was generated on 2018-07-08 and may be subject to change.

Colofon

© Nasser Nadjmi, Antwerp, Belgium, 2011

Lay out	N. Nadjmi, C. Hellemans, Design Ivanhoe
NUR	877
ISBN	978-90-8174070-8
Printed by	Top Printing
Cover	Design Ivanhoe (www.ivan-hoe.be)

All rights reserved. No part of this publication may be reproduced or transmitted in any form by any means, electronically, mechanically by print or otherwise without written permission of the copyright author.

Financial support for the publication of this thesis was kindly provided by Nobel Biocare, Medicim NV, Titamed[®] Biomet 3i[™], Pevo-Dinkels, Aleamed

The evolution of 3D maxillofacial planning concepts in orthognathic surgery

Een wetenschappelijke proeve op het gebied van de Medische Wetenschappen

Proefschrift

Ter verkrijging van de graad van doctor
aan de Radboud Universiteit Nijmegen
op gezag van de rector magnificus prof. mr. S.C.J.J. Kortmann
volgens besluit van het college van decanen
in het openbaar te verdedigen op maandag 11 juli 2011
om 13.30 uur precies

door

Nasser Nadjmi

Geboren op 27 maart 1965
Te Shahrrey (Tehran), Iran

Promotoren

Professor dr. S.J. Bergé
Professor dr. A.M. Kuijpers-Jagtman

Copromotor

Dr. A.M. Ettema

Manuscriptcommissie

Professor dr. J. Jansen (voorzitter)
Professor dr. N. Verdonschot
Professor dr. M. Mommaerts (AZ Sint-Jan, Brugge)

This thesis was conducted at the department of Oral and Maxillofacial Surgery, Radboud University Nijmegen Medical Center, Nijmegen, The Netherlands. Current Head: Professor dr. S.J. Bergé

The studies presented in this thesis were conducted at the following departments:

1. Department of Oral and Maxillofacial Surgery, current head: Professor dr. J. Schoenaers, KUL, Leuven, Belgium
2. Department of Oral and Maxillofacial Surgery, current head: Dr. Herman Vercruyse, AZ Monica Antwerpen, Belgium
3. Department of Oral and Maxillofacial Surgery, current head: Dr. Nasser Nadjmi, AZ KLINA, Brasschaat, Belgium
4. Medical Image Computing (Radiology - ESAT/PSI), Faculties of Medicine and Engineering, University Hospital Gasthuisberg, Leuven, Belgium

The evolution of 3D maxillofacial planning concepts in orthognathic surgery

A accademic essay in Medical Sciences

Doctoral Thesis

To obtain the degree of doctor
from Radboud University Nijmegen
on the authority of the Rector magnificus, Prof. dr. S.C.J.J. Kortmann,
according to the decision of the Council of Deans
to be defended in public on Monday, 11 July 2011
at 13.30 hours

by

Nasser Nadjmi

born on the 27th of March 1965
in Shahrrey (Tehran), Iran

Supervisors

Professor dr. S.J. Bergé

Professor dr. A.M. Kuijpers-Jagtman

Co-supervisor

Dr. A.M. Ettema

Doctoral Thesis Committee

Professor dr. J. Jansen (chairman)

Professor dr. N. Verdonschot

Professor dr. M. Mommaerts (AZ Sint-Jan, Brugge)

Paranimfen

De heer P. Peeters

De heer M. Nadjmi

This work is affectionately dedicated to

my parents,

Ashraf & Shamsollah Shojaei-Nadjmi, for their patience, serene confidence and their unconditional love

and

my children,

Kian & Julie Nadjmi, the light and the hope of my life.

Table of contents

Introduction

<i>Chapter 1:</i>	<i>General introduction</i>	3
-------------------	-----------------------------	----------

Part I: Experimental studies (development of TS-MD®)

<i>Chapter 2:</i>	Maxillary distraction using a trans-sinusal distractor: technical note.	18
-------------------	---	-----------

Int J Oral Maxillofac Surg 2003: 31: 553-9

<i>Chapter 3:</i>	Cephalometric evaluation of maxillary advancement with an internal distractor in an adult boxer dog.	33
-------------------	--	-----------

Orthod Craniofacial Res 2003: 6: 104-11

Part II: Preliminary clinical results of TS-MD®

<i>Chapter 4a:</i>	Predictability of maxillary distraction with the transsinusoidal distractor.	50
--------------------	--	-----------

Rev Stomatol Chir Maxillofac 2004: 105: 9-12

<i>Chapter 4b:</i>	Transsinusoidal maxillary distraction in three cleft patients.	56
--------------------	--	-----------

Int J Oral Maxillofac Surg 2006: 35: 954-960

Part III: Long-term clinical results of TS-MD®

<i>Chapter 5:</i>	Trans-Sinusal Maxillary Distraction for correction of midfacial hypoplasia: Long – term clinical results.	70
-------------------	---	-----------

Int J Oral Maxillofac Surg 2006 : 35: 885-896

Part IV. Soft tissue prediction with a biomechanical model

- Chapter 6:* Soft tissue deformations for a maxillofacial surgery planning system: from computational strategies to a complete clinical validation. **98**

Medical Image Analysis 2007: 11: 282-301

Part V. Virtual occlusion planning

- Chapter 7:* Virtual occlusion in planning orthognathic surgical procedures. **144**

Int J Oral Maxillofac Surg 2010: 39: 457-462

Part VI. Validation of the soft tissue biomechanical model

- Chapter 8:* Quantitative validation of a computer aided maxillofacial planning system, focusing on soft tissue deformations. **160**

Submitted to Int J Oral Maxillofac Surg

Part VII. Discussion and conclusions

- Chapter 9:* General discussion **176**
- Chapter 10:* Samenvatting-summary **183**
List of abbreviations **190**
- Chapter 11:* Acknowledgement **191**
Curriculum Vitae **193**
List of publications **195**
Appendix **197**

1. Introduction

In the eighties and the nineties of the 20th century, distraction osteogenesis (DO) found its way into maxillofacial surgery and became a hot item. It was in those days that I saw many very young cleft patients with moderate to severe maxillary retrusion at the cleft consultation hours during my residency in Houston, Texas in 1997 and Southfield, Michigan in 1998. Most of the cleft patients with midfacial hypoplasia were treated with the Rigid External Device (RED II, KLS Martin Tuttlingen, Germany) developed by Polley and Figueroa, the only device available on the market for maxillary distraction¹¹ so far. This device produced satisfactory clinical results, but proved to be cumbersome and highly visible, while it had a strong impact on the patients both from an aesthetic and a psychosocial point of view. Moreover, its cranial fixation caused life-threatening intracranial complications in a number of patients². As a consequence, developing a safe distractor that was easy to apply, easy to activate, and that guaranteed predictable results became a personal challenge and by that, the topic of the first fase of this thesis.

2. Need for a different type of maxillary distractor

The RED-device (RED II, KLS Martin Tuttlingen, Germany) for maxillary distraction was a ground-breaking appliance when it first came on the market. It permitted easy device application and removal, and multidirectional movement. Its clinical application showed superiority to face mask protraction^{11,13,18}. However, soon it was recognized that the device had some serious disadvantages as well. Its clinical application proved to be cumbersome, and it was highly visible³⁴. In external maxillary distraction, the distraction hardware was rigidly fixed to the cranium and projected in the frontofacial midline, thus limiting oronasal airway access⁴⁶. Finally, its cranial fixation caused life-threatening intracranial complications in a number of patients².

It became obvious that one solution to the problems, mentioned above, would be the development of an intra-oral distractor. The first low profile, intraoral distraction device, used in an experimental study by Weinzweig et al was successfully used for midface distraction at the Le Fort I level. However, the distraction cylinder protruded through the buccal mucosa and had to be delivered through a skin incision in the nasolabial fold area⁴².

Another design was a subcutaneous distraction device, (Zurich Maxillary Distractor, KLS Martin Tuttlingen, Germany) placed in the malar region. With this type of intra-oral maxillary distractor, it was difficult to install the devices with a parallel axis to allow maximum distraction length. The distraction often resulted in a rotational more than in a gliding movement, causing loss of distraction distance at the level of occlusion. Delaire masks were used up to 1 year as a retention device to stabilize the results^{45,16}. Further there was less control of the vector of lengthening in

comparison to the extra-oral devices. An accurate three-dimensional correction could not be achieved because the vector of distraction could not be predicted preoperatively²⁹. At this point the need to develop an intraoral device that could be easy to apply, easy to activate, and that guaranteed predictable results became obvious. One important aspect in the design of the device was to accommodate the activation part in an area of the maxillofacial skeleton that would not interfere with the normal function of the patient during activation and callus maturation period. The sinus cavity appeared to be ideal, because the human sinus, even at the age of 6 to 8 years is deep enough to provide room for the distraction screw, and this is not significantly different in cleft patients¹⁴. Finally I designed a simple unidirectional trans-sinusal distraction device (TS-MD) that was used in an experimental animal study. Consequently a more suitable device (TS-MDTM) was developed for the clinical use (see appendix). The TS-MDTM was a unidirectional device. Therefore, the determination of the desirable position of the distractor and of the distraction vector was of paramount importance.

3. Vector prediction and planning

Control of the distraction vector when using an intra-oral device is more complicated than when an external device is used. In extra-oral devices simple modifications are often sufficient to change the vector. Swennen et al.³⁵ formulated a two-dimensional mathematical model for planning of maxillary distraction osteogenesis. Their model was used to calculate the distraction angle and the required distraction distance when using external maxillary distractors. They assumed that a proper vertical dimension would be achieved through a posterior autorotation of the mandible at the condylar pivot. However it has been shown in the literature that the center of mandibular autorotation is almost never at the condylar pivot and needs to be determined in each individual patient²¹.

The first computer assisted distraction of the maxilla was described by Watzinger et al. in an attempt to determine the final position of the bone fragment after the distraction procedure. They as well based their planning on two-dimensional lateral and frontal cephalograms and used a quite sophisticated and cumbersome technique for intra-operative control of the vector of distraction. Their system consisted of an electromagnetic tracking system and the computer program Virtual Patient System (ARTMA Medizintechnik, Vienna)^{40,41,39}. However in the only case of maxillary distraction they presented in their study, they evaluated the vector of distraction only after placement of the distraction device, and the postoperative lateral cephalograms proved a wrong prediction. Finally Nakagawa et al.²⁶ reported the use of a positioning device for the intra-operative parallel positioning of the Zurich Pediatric Maxillary distractors in a case report. They used cephalometry and model surgery to plan the distraction of the maxilla and simultaneous vertical ramus osteotomy in a severe Class III patient. At this point in time the development of a real three-dimensional planning software became the objective of my further

research. As the TS-MD™ was a unidirectional device, the determination of the desirable position of the distractor and of the distraction vector is of utmost importance. In cooperation with ESAT KU Leuven, Belgium, software that could virtually place the distractor device on the maxilla and calculate the precise vector of distraction was developed. Using CT-scan data, surface models of the bone were constructed. First a virtual Le Fort I osteotomy was performed, and the distractor was installed. During this procedure the vector of distraction was determined based on clinical examinations. The ideal position of the distraction screw inside the maxillary sinus was then indicated. The planning was then transferred to the patient by a stereolithographic model and custom-made templates.

4. Development of a soft tissue simulator

Once it was possible to predict and plan a complete DO procedure and transfer it to the operating theatre, the next step was to predict the soft tissue changes after moving the underlying bone, since a reliable prediction of the facial changes is of utmost importance in view of a better understanding of the (bi)maxillary changes in relation to the skull, a better preparation, an improved surgical outcome and a shorter operation time. This asks for the development of a biomechanical model that transfers the bony changes to the overlying soft tissue structures, which needs fundamental research and clinical validation. When the project described in the thesis started, research into these hard tissue – soft tissue models for orthognathic surgery was still in its infancy.

Advances in medical imaging and the onset of computers in this field, have promoted the development of medical planning software. The idea of predicting the new patient's facial outlook with a computer aided maxillofacial planning system, was originally introduced by Vannier et al.³⁸. At that moment, especially the computer animation world had expertise in facial modeling. Most of these facial modelers represented the face as a collection of regularly assembled mass-spring entities and were mainly focused on real-time output and realistic graphical behavior⁴⁷. The first maxillofacial soft tissue prediction systems were strongly inspired by these computer graphics facial modelers. Koch et al.¹⁷ presented a non-linear finite-element approach to simulate the new facial outlook, which provided a C1-continuous finite element surface. Linear springs were used to connect the facial surface with the underlying bone structures. They applied virtual maxillofacial interventions on the Visible Human Data Set1 and qualitatively validated the newly predicted facial outlook by visual inspection. Afterwards Keeve et al.¹⁴ compared the two most popular soft tissue models for maxillofacial surgery, namely the mass spring model that originated from the computer animation world and the finite element model that was assumed to be a more biomechanical relevant model. Their comparison was based on a qualitative visual inspection of the predicted facial outlook calculated with each model. They concluded that, although the mass spring model could never be biomechanically correct, the speed and the easy architecture

of this model could be a serious advantage over the more accurate but computationally intensive finite element model. At the same time Sarti et al.³⁰ presented a volumetric finite element model applied on a cubic grid that coincides with the voxel grid of the CT data. This voxel-based modeling is advantageous from an image processing point of view (the data remain available on a voxel grid), but demands a large number of finite elements, which is memory intensive. At that time they still needed a super computer to perform the calculations but they achieved good simulation results.

Despite these good results, it became clear that planning systems running on specially designed computers would never be accepted in daily clinical practice. Moreover, as already suggested for 2D soft tissue profile planning systems^{32,10}, it is important to incorporate changes in facial outlook during planning as well. The bone-related planning should be adjusted in function of the new predicted facial outlook, which implies that the soft tissue prediction step needs to become part of the complete treatment planning. Therefore it is necessary that predictions are calculated in a fast and accurate way. A new goal in the search of a good computer aided maxillofacial planning system became the speed in which the new facial outlook could be calculated. Also in other research fields, researchers tried to simulate accurately the deformation behavior of soft tissues and tried to find a golden mean between accuracy and speed. Especially for surgical simulators used for training, where real-time simulations have to be performed, this trade-off became very clear. In this research area a couple of novel computational strategies were presented^{4,9,27} in order to tackle this trade-off. More recent maxillofacial soft tissue planning systems were strongly inspired by these novel models. Zachow et al.⁴⁸ presented in 2000 a tetrahedral volumetric FEM model. These tetrahedral elements, which have less degree of freedom than the prismatic elements that were often used before, are assumed to be better suited for simulation of the deformation of biological objects. By making a trade-off between the number of elements and the accuracy of the model, they were able to compute the new facial outlook of a real patient in less than 5 minutes. They noted that thanks to these short calculation times their model became appropriate for use in daily clinical practice. Two years later Teschner et al.^{36,19} reported on a multi-layer non-linear mass spring model. In their work they introduced the combination of using a mass spring model with a static constraint to calculate the soft tissue deformations. Until then mass spring models were typically combined with a time-integration scheme of the Newtonian motion equation to find the deformation of the soft tissues. Teschner et al.^{36,19} suggested that only the deformation of the tissues was important and not the animation from the original position to the new deformed position. Consequently they proposed the use of an iterative scheme to directly find this new deformed position. By doing so and by lowering the number of mass points, they could reduce the simulation time of their mass spring model to less than 20 seconds. They used the planning system to predict the new facial outlook of one real patient and compared qualitatively the prediction result and the real postoperative facial outlook.

Other important work in the field of maxillofacial soft tissue prediction systems was realized by Chabanas et al.⁵. They were one of the first to present a complete maxillofacial planning system that incorporated the bone-related planning and the prediction of the new facial outlook. To overcome the difficult meshing step, they used a generic model that was elastically registered with patient specific data. A finite element solution was used to simulate the soft tissue deformation. The generic mesh contained 2284 mesh nodes and also muscle specific structures were incorporated in the mesh. This enabled not only prediction of the new facial outlook, but also simulation of the post-operative facial functional behavior. This functional simulation of the facial expressions after surgery was introduced by Gladilin et al.¹² at the same moment. More and more it became clear that before a maxillofacial soft tissue prediction system can be used in clinical practice, not only a qualitative validation of the predicted facial outlook is necessary, but also a real quantitative validation. Schutyser et al.³¹ was the first to note that this quantitative validation should be a numerical comparison between the predicted and real post-operative facial skin surface. After first registering the predicted and actual post-operative facial skin surface based on an unaltered subpart of the face, they quantified distances between both surfaces in 3D. Later the relevance of this idea was confirmed by Chabanas et al.⁶. In their work they quantitatively validated soft tissue predictions for three patients by measuring distances between the predicted facial surface and the real post-operative outcome. More recently Zachow et al.^{49,44} reported on a quantitative validation for one relevant patient. They compared simulation results for different model parameters and concluded that a mean prediction error of 1 to 1.5 mm could be achieved with their model.

As discussed before, only a few maxillofacial planning systems that simulate the post-operative facial appearance have been proposed in the past^{48,36,5,30}. However, before such a planning system could be applicable in daily practice it should first allow for fast or real-time calculations of the post-operative outlook, on a standard personal computer. The surgeon should be able to immediately verify, in 3D, the deformation of the facial soft tissues caused by the displacement of a certain bone patch. These fast simulations should be achieved by the implementation of efficient computational models for soft tissue modeling, without implying a significant decrease in the precision of the prediction and without the need for specialized computing hardware. Second, before such planning system is acceptable for clinical use, the accuracy of the generated predictions has to be investigated. This validation should include a quantitative and a qualitative comparison between the predicted and actual post-operative facial outlook. Quantitative validation evaluates the absolute accuracy of the predicted facial surface, while a qualitative validation step assesses the satisfaction of the surgeon about the agreement between his perception of the surgical outcome and the prediction generated by the system.

Finally, the planning system should be complete. To simulate the post-operative facial appearance, a number of subtasks has to be performed. Five subroutines can

typically be distinguished: data acquisition, building a patient specific soft tissue model, performing a bone-related planning, calculation of the soft tissue deformations based on the generated planning data and finally, visualization of the predicted post-operative facial appearance. The presented system should offer an automatic or semi-automatic solution for each task. In this work, we propose a soft tissue planning system that tries to fulfill all of these specific requirements.

5. Occlusion in virtual orthognathic surgery

The remaining missing link was the development of a three dimensional virtual occlusion tool in order to perform the model surgery in a virtual OR-environment. This would allow not only the planning and predicting of the final occlusion, but also show the influence of the occlusion on the soft tissue changes after virtual orthognathic surgery.

Until now, there have been few reports of how occlusal planning can be combined with a computer-aided planning system. Bettega et al.³ presented a complete computer-aided planning system, and used plaster casts to define the occlusion. After manually positioning the lower and upper casts so that the desired occlusion was obtained, the relative movement of the lower cast was transferred to the virtual planning by means of a 3D optical localizer. Later, Chapuis et al.⁷ used the same concept and presented some case results. They showed that an occlusion could easily be defined with this concept, but their approach and the Bettega system have limitations. First, plaster casts of the upper and lower dentition are still necessary because they are used to define the occlusion. Second, a 3D optical localizer is necessary to transfer the defined occlusion to the computer-aided planning system. These optical systems are expensive and not available in every clinical practice. Third, errors arise in their systems when transferring the manually defined occlusion to the computer-aided planning process.

Pongracz & Bardosi²⁸ tried to omit the use of plaster casts and created a fully virtual occlusal planning tool. To define a good occlusion, they aligned upper and lower dental models based on corresponding points that were manually indicated. The accuracy of their method is hard to confirm since the contact behavior between the upper and lower dentition is not modeled and the impenetrability of teeth is not guaranteed.

In this thesis a novel method that virtually defines the occlusion is presented.

6. Aims and overview of the thesis

1. Design and development of a prototype of an intraoral maxillary distraction device, and its application in an experimental animal study (Chapter 2 and 3)^{22,33}.
2. Development of software that would enable virtual placement of the distractor device on the maxilla and prediction of the desired vector of distraction. Secondly, a method should be implicated in order to transfer the predicted vector intra-operatively (Chapter 4a, 4b)^{23,43}.
3. Follow up of the long-term results of maxillary distraction (Chapter 5)²⁴.
4. Development of a biomechanical model that would transfer the bony changes during orthognathic and distraction procedures to the overlying soft tissue structures (Chapter 6)²⁰.
5. Development of a three-dimensional virtual occlusion tool in order to perform the model surgery in a virtual OR-environment. This would allow not only planning and prediction of the final occlusion, but also show the influence of the occlusion on the soft tissue changes after virtual orthognathic surgery. Therefore, an occlusion tool was developed and clinically validated (Chapter 7)²⁵.
6. A quantitative validation study into the accuracy of the soft tissue simulation module of this novel virtual planning software (Chapter 8).

References

1. Ackermann MJ. The visible human project. Proceedings of the IEEE : Special Issue on Virtual and Augmented Reality in Medicine 1998; 86: 504–511
2. Le BT, Eyre JM, Wehby MC, Wheatley ML. Intracranial migration of halo fixation pins: a complication of using an extra oral distraction device. Cleft Palate Craniofac J 2001; 38:401-404
3. Bettega G, Payan Y, Mollard B, Boyer A, Raphaël B, Lavallee S. A simulator for maxillofacial surgery integrating 3D cephalometry and orthodontia. Comput Aided Surg 2000; 5: 156–165
4. Bro-Nielsen M, Cotin S. Real-time volumetric deformable models for surgery simulation using a finite elements and condensation. Computer Graphics Forum (Eurographics) 1996; 15:57–66
5. Chabanas M, Luboz V, Payan Y. Patient specific finite element model of the face soft tissues for computer-assisted maxillofacial surgery. Med Image Anal 2003; 7:131–151
6. Chabanas M, Marecaux C, Chouly F, Boutault F, Payan Y. Evaluating soft tissue simulation in maxillofacial surgery using preoperative and postoperative CT scans. Proceedings of CARS 2004: 419–424
7. Chapuis J, Schramm A, Pappas I, Hallermann W, Schwenger-Zimmerer K, Langlotz F, Caversaccio M. A new system for computer-aided preoperative planning and intraoperative navigation during corrective jaw surgery. IEEE Trans Inform Technol Biomed 2006; 11: 274–287
8. Le BT, Eyre JM, Wehby MC, Wheatley MJ. Intracranial migration of halo fixation pins: a complication of using an extraoral distraction device. Cleft PalateCraniofac J2001; Vol. 38 No. 4: 401-404
9. Cotin S, Delingette H, AyacheN. Real-time elastic deformations of soft tissues for surgery simulations. IEEE Trans Vis Comput Graph 1999; 5(1):62–73
10. Cousley RR, Grant E, Kindelan JD. The validity of computerized orthognathic predictions. J Orthod 2003 Jun; 30(2):149-154
11. Figueroa AA, Polley JW. Management of severe cleft maxillary deficiency with distraction osteogenesis: procedure and results. Am J Orthod Dentofacial Orthop 1999; 115: 1-12

12. Gladilin E. Biomechanical Modeling of Soft Tissue and Facial Expressions for Craniofacial Surgery Planning. PhD thesis, Fachbereich Mathematik und Informatik der Freien Universität Berlin, Konrad-Zuse-Zentrum für Informationstechnik Berlin (ZIB): October 2002
13. Harada K, Baba Y, Ohyama K, Enomoto S. Maxillary distraction osteogenesis for cleft lip and palate children using an external, adjustable, rigid distraction device: a report of 2 cases. *J Oral Maxillofac Surg* 2001; 59: 1492-6
14. Harvold E. Cleft lip and palate. Morphologic studies of the facial skeleton. *Am J Orthod* 1954; 40: 493
15. Keeve E, Girod S, Kikinis R, Girod B. Deformable modeling of facial tissue for craniofacial surgery simulation. *Comput Aided Surg* 1998; 3(5): 228–238
16. Kessler P, Wiltfang J, Schultze-Mosgau S, Hirschfeld U, Neukam FW. Distraction osteogenesis of the maxilla and midface using a subcutaneous device: report of four cases. *Br J Oral Maxillofac Surg* 2001; 39: 13-21
17. Koch RM, Gross MH, Carls FR, von Buren DF, Frankhauser G, Parish YIH. Simulating facial surgery using finite element models. In *Proc. of SIGGRAPH* 1996: 421–428
18. Krimmel M, Cornelius CP, Roser M, Bacher M, Reinert S. External distraction of the maxilla in patients with craniofacial dysplasia. *J Craniofac Surg* 2001; 12: 458-463
19. Meehan M, Teschner M, Girod S. Three-dimensional simulation and prediction of craniofacial surgery. *Ortho Craniofac Res* 2003; 6(Suppl 1):102–107
20. Mollemans W, Schutyser F, Nadjmi N, Maes F, Suetens P. Predicting soft tissue deformations for a maxillofacial surgery planning system: from computational strategies to a complete clinical validation. *Med Image Anal* 2007;11(3): 282-301
21. Nadjmi N, Mommaerts MY, Abeloos JVS, De Clercq CAS, Neyt LF. Prediction of mandibular autorotation. *J Oral Maxillofac Surg* 1998; 56: 1241-1247
22. Nadjmi N, Van Erum R, Schoenaers J, Schepers E. Maxillary distraction using a trans-sinusal distractor: technical note. *Int J Oral Maxillofac Surg* 2003; 31: 553-559
23. N. Nadjmi. Prédicibilité de la distraction du maxillaire supérieur avec distracteur transsinusien. *Rev Stom Chir Maxillofac* 2004; 105: 9-12

24. Nadjmi N, Schutyser F, Van Erum R. Trans-Sinusal Maxillary Distraction for correction of midfacial hypoplasia: Long-term clinical results. *Int J Oral Maxillofac Surg* 2006; 35: 885-896
25. Nadjmi N, Mollemans W, Daelemans A, Van Hemelen G, Schutyser F, Bergé S. Virtual occlusion in planning orthognathic surgical procedures. *Int J Oral Maxillofac Surg* 2010 May; 39(5): 457-62
26. Nakagawa K, Ueki K, Takatsuka S, Marukawa K, Yamamoto E. A device for determining the position of intraoral distractors for protracting the maxilla. *J Craniomaxillofac Surg* 2003; 31: 234-237
27. Picinbono G, Delingette H, Ayache N. Non-linear anisotropic elasticity for real-time surgery simulation. *Graphical Models* 2003; 65(5):305–321
28. Pongracz F, Bardosi Z. Dentition planning with image-based occlusion analysis. *Int J CARS* 2006; 1: 149–156
29. Rachmiel A, Aizenbud D, Peled M. Long-term results in maxillary deficiency using devices. *Int J Oral Maxillofac Surg* 2005; 34: 473–479
30. Sarti A, Gori R, Lamberti C. A physically based model to simulate maxillo-facial surgery from 3D CT images. *Future Generation Computer Systems* 1999; 15(2):217–221
31. Schutyser F, Van Cleynenbreugel J, Ferrant M, Schoenaers J, SuetensP. Image-based 3D planning of maxillofacial distraction procedures including soft tissue implications. *Lecture Notes In Computer Science (MICCAI)* 2000: 1935:999–1007
32. Smith JD, Thomas PM, ProffitWR. A comparison of current prediction imaging programs. *AmJ Orthod Dentofacial Orthop* 2004; 125(5):527–536
33. Stalmans K, Van Erum R, Verdonck A, Nadjmi N, Schepers E, Schoenaers J, Carels C. Cephalometric evaluation of maxillary advancement with an internal distractor in an adult boxer dog. *Orthod Craniofacial Res* 2003; 6: 104-11
34. Swennen G, Colle F, De May A, Malevez C. Maxillary distraction in cleft lip palate patients: a review of six cases. *J Craniofac Surg* 1999; 10: 117-22
35. Swennen G, Figureoa AA, Schierle H, Polley JW, Malevez C. Maxillary distraction osteogenesis: a two-dimensional mathematical model. *J Craniofac Surg* 2000; 11: 312-7

36. Teschner M. Direct Computation of Soft-Tissue Deformation in CranioFacial Surgery Simulation. PhD thesis, Shaker Verlag, Aachen, Germany, Jan 2000
37. Terzopoulos D, Walters K. Physically-based facial modeling, analysis and animation. *Vis Comp Anim* 1990: 1(4):73–80
38. Vannier MW, Gado MH, Marsh JL. Three-dimensional display of intracranial soft-tissue structures. *Am J Neurorad* 1983: 4(3): 520–521
39. Wagner A, Ploder O, Enislidis G, Truppe M, Ewers R. Image-guided surgery. *Int J Oral Maxillofac Surg* 1996: Apr: 25(2):147-151
40. Watzinger F, Wanschitz F, Waner A, Enislidis G, Millesi W, Baumann A, Ewers R. Computer-aided navigation of post-traumatic deformities of the zygoma. *J Craniomaxillofac Surg* 1997: 25: 198-202
41. Watzinger F, Wanschitz F, Rasse M, Millesi W, Schopper Ch., Kremser J, Birkfellner W, Sinko K, Ewers R. Computer-aided surgery in distraction osteogenesis of the maxilla and mandible. *Int. J. Oral Maxillofac Surg* 1999: 28: 171-175
42. Weinzweig J, Baker SB, Mackay GJ, Whitaker LA, Barlett SP. Immediate versus delayed midface distraction in a primate model using a new intraoral internal device. *Plast Reconstr Surg* 2002: 15: 1600-1610
43. Wenghoefer M, Martini M, Najmi N, Schutyser F, Jagtman AK, Berge S. Transsinusoidal maxillary distraction in three cleft patients. *Int J Oral Maxillofac Surg* 2006: 35: 954–960
44. Westermarck A, Zachow S, Eppley B. Three-dimensional osteotomy planning in maxillofacial surgery including soft tissue prediction. *J Craniofac Surg* 2005: 16(1): 100–104
45. Wiltfang J, Hirschfelder U, Neukam FW, Kessler P. Long-term results of distraction osteogenesis of the maxilla and midface. *Br J Oral Maxillofac Surg* 2002: 40: 473-479
46. Wong GB, Nargoizian C, Padwa BL. Anesthetic concerns of external maxillary distraction osteogenesis. *J Craniofac Surg* 2004 : 15: 78-81
47. Lee Y, Terzopoulos D, Walters K. Realistic modeling for facial animation. *Computer Graphics, 29(Annual Conference Series)* 1995: 55–62

48. Zachow S, Gladiline E, Hege HC, Deuffhard P. Finite-element simulation of soft tissue deformation. In Proc. of CARS 2000: 23–28
49. Zachow S, Hierl Th, Erdmann B. A quantitative evaluation of 3D soft tissue prediction in maxillofacial surgery planning. In Proc. of 3 Jahrestagung der Deutschen Gesellschaft für Computer- und Roboter-assistierte Chirurgie 2004 October: 75–79, München

CHAPTER 2

Maxillary distraction using a trans-sinusal distractor: Technical Note

N. Nadjmi¹, R. Van Erum², J. Schoenaers³, E. Schepers⁴

1. Department of Cranio-Maxillofacial Surgery, AZ Monica, Antwerp, Belgium.
2. Department of Orthodontics, Catholic University of Leuven, Belgium.
3. Department of Oral and Maxillofacial Surgery, Catholic University of Leuven, Belgium.
4. Department of Prosthodontic Dentistry, Catholic University of Leuven, Belgium.

Int J Oral Maxillofac Surg 2003; 31: 553-9

Abstract

In this pilot study, the principle of distraction osteogenesis was used to advance the mid face of a boxer dog. A modified high Le Fort I-type osteotomy was performed. Following a latency period of 5 days the maxilla was distracted 14 mm in 14 consecutive days at a rate of 1 mm per day. Ten weeks after the completion of the distraction, multiple biopsies were taken across the distraction gap. Histological observation showed bone deposition in the osteotomy sites. Soft and hard tissue formation resulted in complete healing across the distraction gap. The maxillary sinus was used to accommodate the distraction device. Superimposition of the standardised lateral cephalograms taken at the end of distraction and 14 months after the removal of the distractors showed no sign of relapse in the achieved sagittal advancement of the maxilla. This small, intraoral / trans-sinusal placed, distractor has a completely new conceptual design, and may be helpful in distraction of maxilla in children and adults with midfacial hypoplasia.

Keywords: Distraction osteogenesis; midface; maxillary sinus; cleft lip and palate; bone tissue.

Introduction

Maxillary DO can find its indication in severe Angle class III malocclusions, and severe maxillary hypoplasia among some cleft patients and other craniofacial deformities. Attempts were made to treat these malocclusions through the use of maxillary protracting appliances with chin caps, with conflicting opinions about the treatment results^{4, 5}. Several external distraction devices, such as the traction mask of Molina and Ortiz-Monasterio and the rigid external distraction system of Polley and Figueroa, permit easy device application and removal, and multidirectional movement. But, the reverse headgear and rigid external distraction apparatus are cumbersome and highly visible^{9, 15}. A low profile, intraoral distraction device, used in an experimental study by Weinzweig et al¹⁶ was successfully used for midface distraction at the Le Fort I level. However, the distraction cylinder protruded through the buccal mucosa and had to be delivered through a skin incision in the nasolabial fold area. In a clinical study by Kessler et al⁷ four patients were treated by high Le Fort I osteotomies and insertion of a subcutaneous distraction device, placed in malar region. The range of the distraction was limited (7-14 mm) due to the distractor design, and the distraction rods led to injuries at the angle of the mouth and swelling of the lips. Delaire masks had to be used to stabilise the results. An ideal distractor should be easy to apply, easy to activate, and guarantee predictable results. It should not result in any physical, or psychosocial complaints, and should allow normal function during the distraction and the retention period.

The aim of this experimental pilot-study is to evaluate the effectiveness of a new maxillary distractor, an intraoral – trans sinus placed device.

Material and Methods

Animal selection: Clearance of the study protocol was obtained by the Ethical Committee of the Catholic University of Leuven-Belgium for performing the experimental distraction in a 2-year-old boxer dog. This dog fulfilled the requirements for a good experimental model: - a maxillary sinus, deep enough to provide space for placement of the distraction screw, - a short splanchnocranium (short snout) and an inherent hypoplastic mid face, comparable to the class III malocclusion in humans.

Distractor design: The distractor was made out of three main parts: two plates and a distraction screw. The distraction screw was the axis of a joint formed by the lower plate, which was connected to it and could move around it. All parts of the device were made out of a Titanium alloy (Ti-6Al-4V). The device was fabricated by Titamed[®], Belgium. The upper plate was fixed cranial to the osteotomy line with two screws (Fig.1).

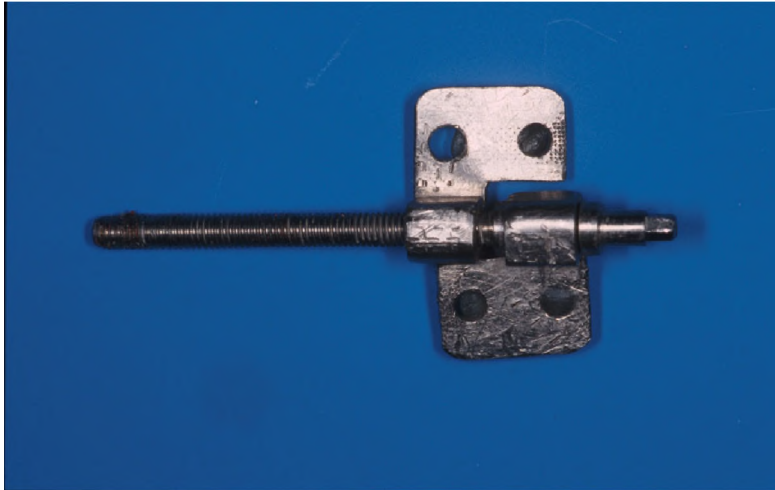


Fig. 1. Trans-Sinus-Maxillary-Distractor (TS-MD), with 2 fixing plates and the distraction screw that makes an axis of a joint formed by the lower plate.

Only two screws per plate were used to see whether the minimal fixation of the plates would be sufficient to withstand the forces applied during the distraction process. The distractor was fixed on the lateral aspect of the nasal wall and the distraction screw, which was almost perpendicular to the frontal plane, entered the maxillary sinus through the anterior wall of the sinus. The other end of the distraction screw (activation head) found its way through the soft tissue covering the anterior wall of the maxillary sinus, and was hidden behind the upper lip. The activation head (AH) was hexagonal, with a matching screwdriver. A 360 degrees counter clockwise rotation of the AH gave a displacement of 0.5 mm.

Animal experiment: The boxer dog was put under general anaesthesia. A modified Le Fort I type osteotomy was then performed, and the distraction devices were placed bilaterally (day one). After a latency period of 5 days the distraction started at a ratio of 1 mm per day during 14 consecutive days (distraction phase). Activation was performed under light sedation, using Thalamonal[®] and Pentothal[®].

The distractors were removed under general anaesthesia after another 10 weeks (retention phase). During the same session multiple bone biopsies were taken at the site of distraction.

A standard lateral cephalogram was taken on day 1, day 5 (start of distraction), day 12, day 19 (end of distraction), day 33, day 47, day 61, day 75 (end of retention), and 14 months after removal of the distractors. A cephalostat was used to ensure the standardisation of the lateral cephalometric radiographs. A fixed distance of 74 cm between the source (90 kV and 60 ms) and the middle of the skull was maintained. All cephalograms were taken under light sedation.

Surgical technique: A 2 years old boxer dog was premedicated with IV injection of 0.5 ml Thalamonal[®] (fentanyl, 0.05 mg/ml + droperidol 2.5 mg/ml; Janssen Pharmaceutics, Beerse, Belgium) and 0.5 ml atropine (atropine sulphate 0.5 mg/ml). Five hundred-milligram Augmentin[®] (SK Beecham) IV was given preoperatively. A daily maintenance dose of Augmentin was given during latency and distraction period. The dog was placed on the operating table in a supine position with his head in slight extension. The animal was inducted with IV injection of 30 mg/kg Narcovet[®] (sodium pentobarbital 60 mg/ml; Apharmo, Arnhem, Nederland). An orotracheal tube was placed and anaesthesia maintained with Ethrane[®] (enflurane 15 mg/ml; Abott, Amstelveen, Nederland). A throat pack was placed, and the oral mucosa and dentition were rinsed with chlorhexidine digluconate 1 % in water.

First, the crowns of the lower canines were lowered to the gingival level, and were treated endodontically in order to minimise the chance of interference during the maxillary protrusion.

Local anaesthesia Xylocaine[®] 1% in 1/100.000 epinephrine was injected submucosally. A Le Fort I type incision was made with electrocautery. Care was taken not to damage the infraorbital nerve. The incision was then carried down to the bone. Next, a subperiosteal dissection was carried out to expose the midface structures. In order to free the posterior maxillary wall from the skull base the orbital floor had to be osteotomised, because this part forms the orbital floor in dogs. Therefore a subperiosteal tunnel was made from the most medial point of the inferior rim (medial to infraorbital nerve) over the orbital floor towards the corner made by the horizontal and the perpendicular lamina of the palatinal bone.



Fig. 2. Illustration of the high Le Fort I type osteotomy and the entry hole to the maxillary sinus.

The posterior maxilla was separated from the rest of the skull via a transpalatinal approach in contrast to the human anatomy where the posterior maxilla can easily be separated via an upper buccal sulcus incision. A modified high Le Fort I type osteotomy was then performed. The cut started from the osseous corner made by the horizontal and perpendicular lamina of the palatinal bone (as described above), continued over the orbital floor and ended 4-mm posterior to the infraorbital rim. Then an osteotomy cut was made starting midway from the zygomatico-alveolar crest to a point midway between the infraorbital rim and the superior border of the infraorbital foramen. This osteotomy line was continued parallel to the hard palate through the lateral nasal wall, approximately 1 cm cranial to the nasal floor.

A small hole with a diameter of approximately 4-mm was made in the anterior wall of the maxillary sinus on the right side, through which the distraction screw would enter the sinus. This opening was located at the most medial point of the anterior wall of the maxillary sinus and was part of the anterior osteotomy line (Fig. 2). The maxilla was slightly mobilised making sure there was no interference between the maxilla and the rest of cranium. At this stage the distractor was fixed to the lateral nasal wall (Figs 3-4). The lower plate moves in the same direction as the distraction vector and therefore is fixed to the lateral nasal wall at the lower border of the osteotomy line. Each plate was fixed to the underlying bone with two screws. The same procedure was performed at the contra lateral side. The distractors were activated for 4-mm to make sure there were no interferences, and then reversed.

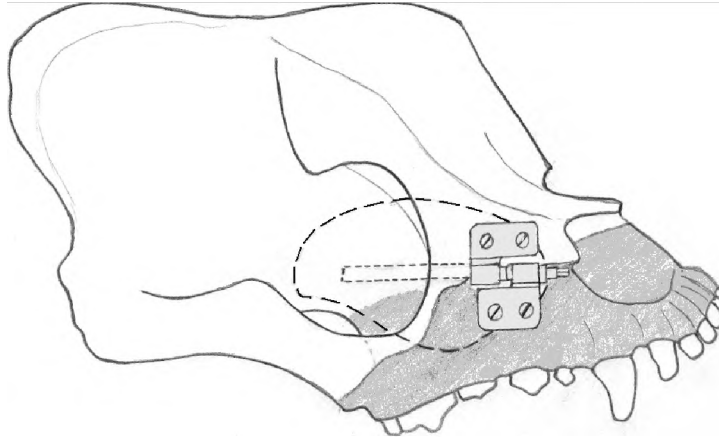
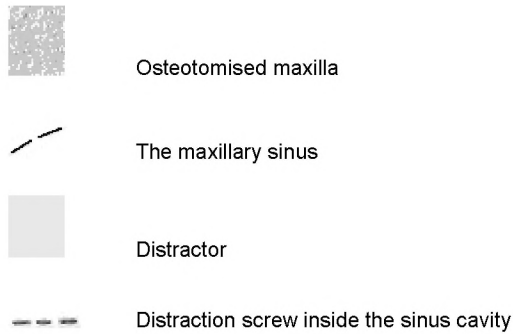


Fig. 3. Schematic diagram showing the position of TS-MD on the right maxilla and the distraction screw inside the sinus cavity.



The distractor on the right side was opened for a few mm (before fixation of the lower plate) in order to be distinguished on radiographs. An osteosynthesis screw (diameter 1.5 mm, length 5 mm) was placed in the midline on the frontal bone, as a landmark for the cephalometric analysis. Two small class-5 amalgam fillings were placed on the upper molars on the left side, as additional landmarks for cephalometric analysis.

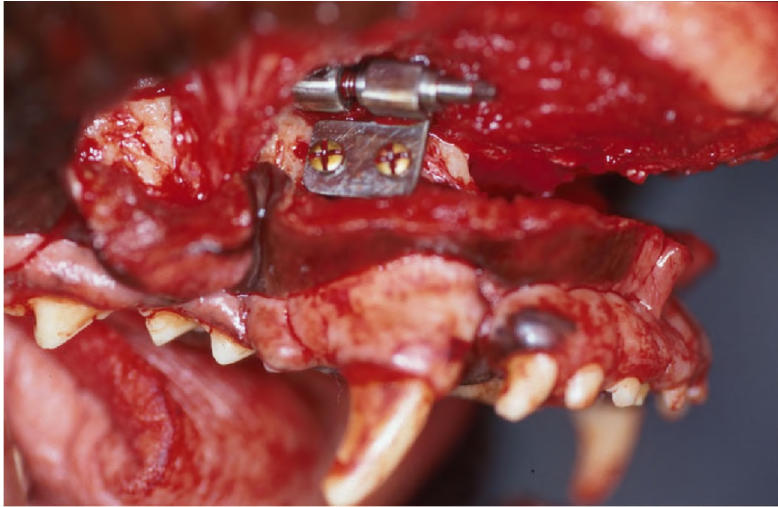


Fig. 4. TS-MD fixed on the right side. The distraction screw is located inside the maxillary sinus, while the upper plate of the device is buried behind the inferior orbital nerve.

The distraction head was too short to be exposed into the oral cavity (right behind the upper lip). Therefore a hard silicon tube approximately 2 cm in length and with a diameter that matched the head of the distraction screw was pulled over it and fixed with Ethilon 2/0 to the surrounding periosteum, thus allowing for activation of the distractors. The intraoral incision was sutured with Ethilon 2/0 (Fig. 5). Postoperative diet consisted of soft food.

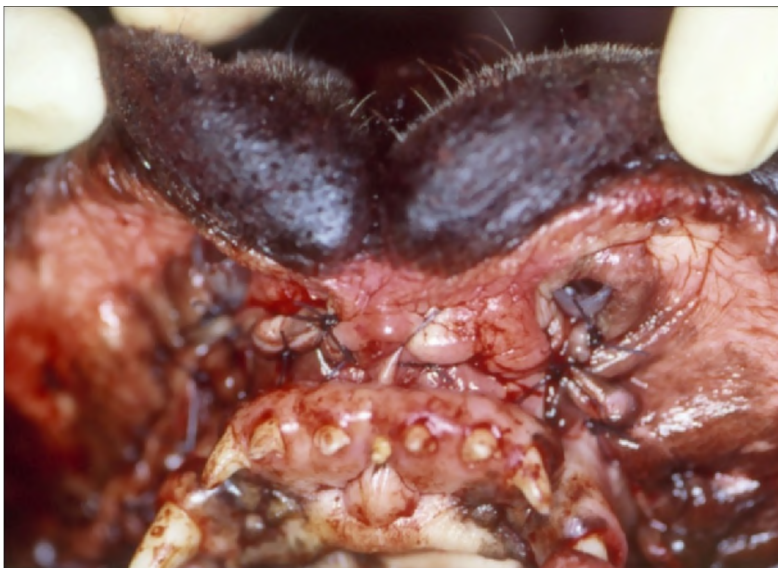


Fig. 5. White arrows show hard silicon tubes approximately 2 cm in length and with a diameter that matched the head of the distraction screw. The distractors were activated intraorally through the silicone tube.

Removal of the distractors: The animal was put under general anaesthesia following the same protocol as described above. A small incision was made at the level of the distractor. A subperiosteal dissection was performed at the level of the distracted area. Subsequently, the distractors were removed very easily. Multiple bone biopsies were taken at the site of distraction.

Histological evaluation: At the time of distractor removal biopsies were taken and immediately fixated in a solution of one part formaldehyde (Merck, Darmstadt, Germany), neutralised with 50 g CaCO₃/l, and two parts 80% ethanol. The samples were dehydrated in graded alcohols and embedded in methylmethacrylate. Non-decalcified serial sections were prepared in a sawing microtome (Leitz 1600, Wetzlar, Germany) and ground and polished to a thickness of approximately 30 to 50 µm (Minimet[®], Buehler Inc., Lake Bluff, IL, U.S.A.). Finally, the sections were stained with a combination of Stevenel's blue and Von Gieson's picrofuchsine for light microscopical evaluation.

Results

Insertion of the trans-sinusal maxillary distractor was easy. The monocortical screw fixation gave sufficient stability and the distraction devices were well tolerated by the animal. No signs of infection were observed. The animal tolerated the soft diet very well. Although the expected linear increase of the cephalometric points was supposed to be 14 mm, an average increase of 8,7 was found. The superimposition showed a downward tipping of the maxilla the first five days of the distraction period. A standard lateral cephalogram was taken 14 months after removal of the distractors. The superimposition of this cephalogram with the one taken immediately after removal of the distractors showed no sign of relapse (Figs 7-10).

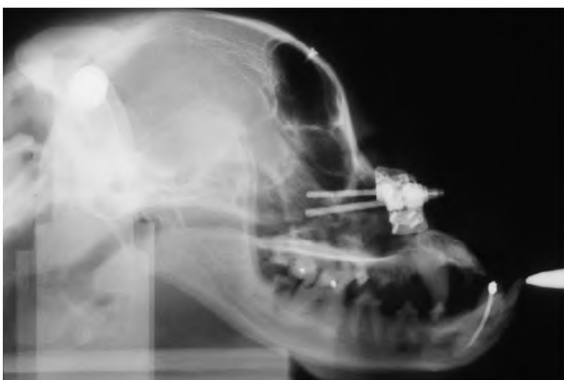


Fig. 7. Lateral cephalogram at the beginning of the distraction



Fig. 8. Lateral cephalogram at the end of the distraction.



Fig. 9. Lateral cephalogram 14 months after removal of the distractors.

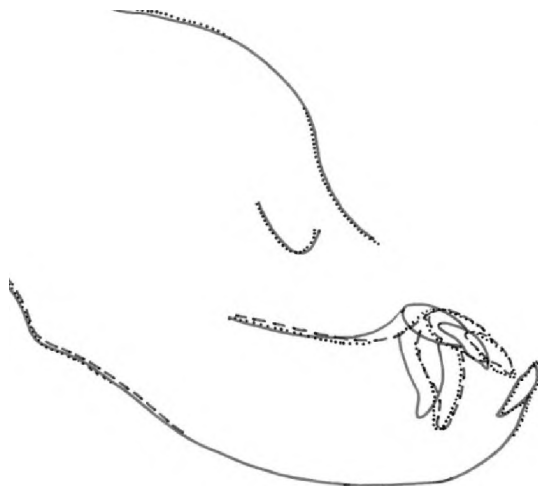


Fig. 10. Superimposition of the lateral cephalograms taken at well-defined time-intervals.

- At the start of the distraction
- - - - - At the end of distraction
- After 14 months

Histological examination showed an almost completely filled distraction gap with newly formed bone with a typical woven structure that could clearly be distinguished from the bone at the border of the gaps that had a mature lamellar nature. Two

types of ossification were observed. Most of the new bone was formed by appositional bone growth. Within some areas, where the gap was not yet completely filled, the newly formed bone was covered with a layer of osteoid tissue and a row of active osteoblasts. In other areas endochondral bone formation was observed; here the bone formation was preceded by cartilage formation. Islands of active remodelling could be observed in the newly formed bone, with osteoclasts lying in resorption lacunae and at the other side active osteoblasts (Fig. 6).

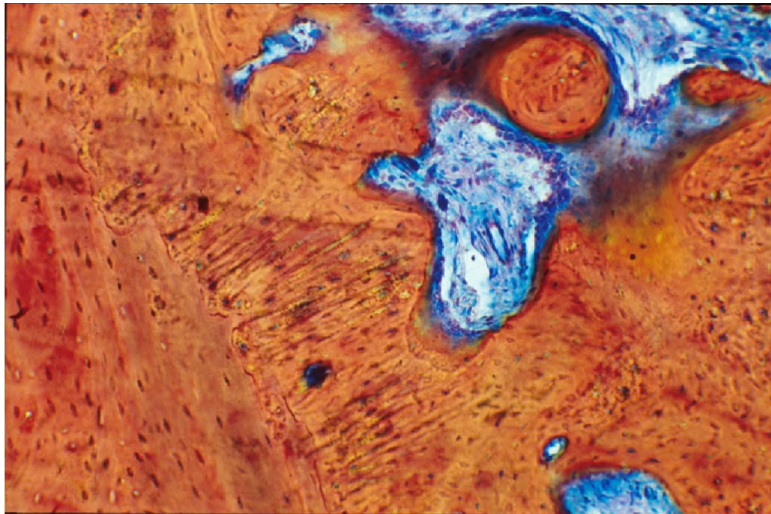


Fig. 6. The difference between the new and old bone is clear. In the newly formed bone islands of active remodelling with osteoclasts and osteoblasts are visible.

Discussion

Distraction osteogenesis is of particular interest in patients with midfacial hypoplasia as they lack both bone and soft tissue. The subcutaneous, intraoral devices present several advantages over external distraction devices currently used, which are cumbersome, highly visible, and potentially not well tolerated by patients¹⁷. The intraoral devices have certain disadvantages. At present, they are all unidirectional. This implicates a perfect preoperative vector planning. The removal of the devices must be performed under general anaesthesia, and can be difficult⁷. This is due to the fact that the current devices are still too bulky, and are placed under the periosteum. The activation rods are either in continuous contact with lips, causing pain and irritation, or have to be delivered through the skin in the nasolabial region^{3,7,17}. In this study the distraction screw was placed inside the maxillary sinus rather than in the subperiosteal area. The volume of the sinus cavity provides enough room for positioning of the distraction screw, which determines the vector of distraction. In this way a bulky and movable part of the device is accommodated in an empty cavity, and does not interfere with the surrounding soft tissue and periosteum. Although the linear increase of the cephalometric points was expected

to be 14 mm, an average of only 8,7 mm was found. This could be explained biomechanically by the influence of several factors f.e. distractor design, distractor placement, and the possible movement of the screws in the fixation plates. Secondly, the superimposition of the lateral cephalograms shows a clockwise tipping of the maxilla during the first 5 days of the distraction period, which can contribute to the difference between the expected and the effective gain in sagittal displacement of the maxilla. Apparently the fixation of the distractor plates, each with only two screws did not provide sufficient stability of the device to withstand the forces applied during the initial distraction process.

Histologically two types of ossification were observed in the distraction gap. Endochondral bone formation, which was preceded by cartilage formation, was observed in some areas. This can be due to instability of the bone segments and the distraction rate, but it does not influence the final result^{8,12,15}. Islands of active remodelling could be observed in the newly formed bone tissue, with osteoclasts lying in resorption lacunae and at the other side active osteoblasts (Fig. 6). These observations are in accordance with other studies^{8,15,16}.

Because of a potential communication between the oral cavity and the maxillary sinus a strict protocol with antibiotics was maintained during the distraction period. Brånemark et al¹ showed that the insertion of implants where sinus or even nasal cavity penetration could not be avoided, was justified, as titanium screws penetrating the bone of sinus or nasal cavity did not cause undesirable side effects¹. In this study no clinical or radiological sign of infection or fistula formation were found. This distraction device provided skeletal anchorage and relapse was not seen up to 14 months post distraction.

The potential advantages of this distractor can be mentioned as follows. The distractor is easy to place and is positioned intraorally. The distraction screw goes backward into the sinus rather than forward into the lip, which would implicate the transcutaneous delivery of the distraction barrels in the nasolabial folds bilaterally¹⁷. It can serve as a retention device and be left in place as long as necessary. This is in contrast with distraction performed using extra-oral devices or a facial mask with elastic forces. Other studies report on dental anchorage for the fixation of the distraction device^{2,10,13,14,16}, but this resulted often in a significant dento-alveolar displacement.

Distraction can be achieved in horizontal, vertical, and sagittal planes, simply by changing the inclination of the distraction screw. Correction of the midline can be done by distracting one side more than the other.

The clinical prototype was designed by N. Nadjmi in cooperation with Martin Medizin-Technik, Tuttlingen, Germany, and has successfully been applied in a clinical study for the treatment of 10 patients with moderate to severe midfacial hypoplasia¹¹. A detailed report is in progress.

Acknowledgements. The authors acknowledge with thanks the kind assistance of Dr. Karen Stalmans, Dr. An Verdonck, Orthodontic Department, and Professor Lambrechts, Endodontic Department of the Catholic University of Leuven. Special thanks to Dr. Joel Defrancq, Craniofacial Association Antwerp, for his advise on the choice of material used to make the distractors.

References

1. Brånemark PI, Adell R, Albreksson T, Lekholm U, Lindstrom J, Rockler B. An experimental and clinical study of osseintegrated implants penetrating the nasal cavity and maxillary sinus. *J Oral Maxillofac Surg* 1984; 42: 497-505
2. Figueroa AA, Polley JW. Management of severe cleft maxillary deficiency with distraction osteogenesis: procedures and results. *Am J Orthod Dentofacial Orthop* 1999; 115: 1-5
3. Guerrero CA, Bell WH, Meza LS. Intraoral distraction osteogenesis: maxillary and mandibular lengthening. *Atlas Oral Maxillofac Surg Clin North Am* 1999; 7: 111-51
4. Hathaway R. Maxillary and midface deformity. In: Bell WH.: *Modern practice in orthognatic and reconstructive surgery*. Philadelphia: WB Saunders 1992: Chap. 63-6
5. Ishii H, Morita S, Takeuchi Y, Nakamura S. Treatment effect of combined maxillary protraction and chin cap appliance in severe skeletal Class III cases. *Am J Orthod Dentofac Orthop* 1987; 92: 304-12
6. Karp NS, McCarthy JG, Schreiber JS, Sissons HA, Thorne CH. Membranous bone lengthening: a serial histological study. *Ann Plast Surg* 1992; 29: 2-7
7. Kessler P, Wiltfang J, Schultze-Mosgau S, Hirschfelder U, Neukam FW. Distraction osteogenesis of the maxilla and midface using a subcutaneous device: report of four cases. *Br J Oral Maxillofac Surg* 2001; 39: 13-21
8. Komuro Y, Takato T, Harii K, Yonehara Y. The histologic analysis of distraction osteogenesis of the mandible in rabbits. *Plast Reconstr Surg* 1994; 94: 152-157
9. Molina F, Ortiz-Monasterio F. Maxillary distractor: Three years of clinical experience. *Plast Surg Forum* 1996; 19:54
10. Molina F, Ortiz-Monasterio F, de la Paz Aquilar M, Barrera J. Maxillary distraction: aesthetic and functional benefits in cleft lip palate and prognathic patients during mixed dentition. *Plast Reconstr Surg* 1998; 101:951-963
11. Nadjmi N. The state of the art in the planning and performance of midfacial distraction osteogenesis. *J Cranio-Maxillofac Surg* 2002; 30:143

12. Peterka M, Peterkova R, Likovský Z. Timing of exchange of the maxillary deciduous and permanent teeth in boys with three types of orofacial clefts. *Cleft Palate-Craniofacial J* 1996; 33-4: 318-323
13. Polley JW, Figueroa AA. Management of severe maxillary deficiency in childhood and adolescence through distraction osteogenesis with external, adjustable, rigid distraction device. *J Craniofac Surg* 1997; 8:181-185
14. Rachmiel A, Aizenbud D, Ardekian L, Peled M, Laufer D. Surgically assisted orthopedic protraction of the maxilla in cleft lip and palate patients. *Int J Oral Maxillofac Surg* 1999; 28: 9-14
15. Sawaki Y, Ohkubo H, Yamamoto H, Ueda M. Mandibular lengthening by intraoral distraction using osseointegrated implants. *Int J Oral Maxillofac Implants* 1996; 11 :186-193
16. Swennen G, Colle F, De Mey A, Malevez C. Maxillary distraction in cleft lip and palate patients: a review of six cases. *J Craniofac Surg* 1999; 10: 117-122
17. Weinzweig J, Baker SB, Mackay GJ, Whitaker LA, Bartlett SP. Immediate versus delayed midface distraction in a primate model using a new intraoral internal device. *Plast Reconstr Surg* 1999; 109: 1600-10

CHAPTER 3

Cephalometric evaluation of maxillary advancement with an internal distractor in an adult boxer dog

**K. Stalmans¹, R. Van Erum¹, A. Verdonck¹, N. Nadjmi²,
E. Schepers⁴, J. Schoenaers³, C Carels¹**

1. Department of Orthodontics, Catholic University of Leuven, Belgium.
2. Department of Cranio-Maxillofacial Surgery, Eeuwfeestkliniek, Antwerp, Belgium.
3. Department of Oral and Maxillofacial Surgery, Catholic University of Leuven, Belgium.
4. Department of Prosthodontic Dentistry, Catholic University of Leuven, Belgium.

Structured Abstract

Objective – The aim of the study was to evaluate cephalometrically the effects of distraction of the maxilla over a 1-year period by means of an internal distractor applied in a boxer dog. **Design** – Internal distractors were placed bilaterally in the internal cavity of the maxillary sinus of a 2-year-old boxer dog after a Le Fort I osteotomy. Distraction was started 5 days after surgery and activations were continued for 14 days at a rate of 1 mm/day. Standardized lateral cephalograms were taken with an external source of 90 kV, 60 mS immediately pre-surgery, at day 1 after the start of the distraction (dp) and at day 5 dp, day 7 dp, day 10 dp, day 14 dp (end of distraction), at 14 days of consolidation period (cp), at 28 days cp and at 56 days cp (removal of the distractors). One year after the removal of the distractor, a final lateral cephalogram was taken. Cephalometric analysis was performed and superimpositions were used for the evaluation of the sagittal position of the maxilla.

Results The linear measurements, as well as the superimposition showed evidence for a significantly advanced position of the maxilla, which was stable 1 year after removal of the distractor.

Conclusion The application of the internal maxillary distractor in a boxer dog resulted in a sagittal advancement of the midface that was still present after 1 year.

Keywords: Cleft lip and palate; distraction osteogenesis; maxillary internal distractor; maxillary sinus; midface

Introduction

The concept of lengthening bones is not new: distraction osteogenesis was introduced in medicine by Ilizarov¹⁻³ and was further developed by several clinicians and researchers over the past 30 years. The application of distraction osteogenesis in the craniofacial skeleton was first reported by Snyder et al.⁴, describing the use of an extraoral distractor to lengthen the mandible. In the last 10 years distraction osteogenesis has undergone a rapid evolution^{5, 6}. The introduction of intraoral and miniature devices substantially improved the clinical application and widened its field of application. Distraction osteogenesis of the maxilla and the midface as a treatment objective in congenital craniofacial malformations, such as hemi-facial microsomia, Treacher-Collins syndrome, Apert and Crouzon syndrome, has proved its clinical usefulness at short term⁷⁻¹⁰.

Treatment of maxillary retrusion in cleft lip and palate patients by distraction osteogenesis is a new approach in treating the skeletal disproportion or disharmony in these patients. Several treatment strategies have already been delineated, such as the use of miniature systems after a midfacial osteotomy for midface distraction in young children⁹, an external, adjustable device for maxillary distraction osteogenesis in patients with severe maxillary hypoplasia, and a facial mask with elastic traction to intraoral fixed appliances after an incomplete Le Fort I osteotomy¹¹⁻¹³. One of the specific indications of internal maxillary distraction is severe hypoplasia of the maxilla in cleft lip and palate patients at an early age.

Traditionally, a combined orthodontic and orthognathic treatment is performed, but in some cases this has resulted in an incomplete long-term correction. Moreover, because of the large displacement needed to correct the reversed overjet, the surgical procedure has often to be performed in both jaws, with a setback of the mandible, despite a normal sagittal position¹¹. In addition, traditional osteotomies may not be performed until growth has fully ceased, and a considerable relapse may be expected due to soft tissue and muscular tension and/or resorption of the bone graft. Distraction osteogenesis overcomes these surgical problems and enables improvement of the child's psychological maturation due to an earlier facial improvement. For this specific application the usefulness of an internal maxillary distraction device is evaluated in this pilot study with bilateral distractors in the maxilla of a boxer dog. In this article, the complete distraction process and consolidation period were documented cephalometrically.

Materials and methods

The distractor

The prototype was a concept of the fourth author. The two fixation plates caudally and cranially to the osteotomy line were placed on the lateral nasal wall. The body of

the screw was located in the maxillary sinus. The hexagonal head of the screw lies in the vestibulum under the upper lip, a position that makes the activations easy (Fig. 1).

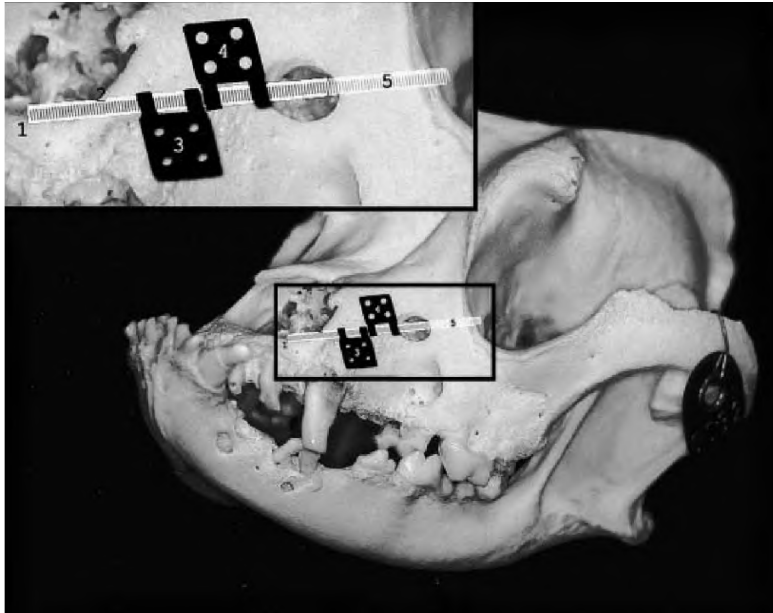


Fig. 1. The internal maxillary distractor: 1. The activation part of the screw ending in the vestibulum. 2. The screw of the distractor. 3. The fixation plate under the osteotomy line. 4. The fixation plate above the osteotomy line. 5. The body of the screw ending in the cavity of the maxillary sinus.

The animal

A 2-year-old female boxer dog was used in this study. The protocol and the guidelines for this in vivo animal study were approved by the ethical commission of the Faculty of Medicine. The pre- and post-operative care was supervised by the University's animal centre.

The choice of this animal was influenced by physiological and anatomical considerations in order to create the best experimental model. The anatomy of the boxer's snout showed several advantages. First, the maxillary sinus is large enough to provide sufficient space to contain the end of the screw of the distractor. Secondly, the boxer dog has a short splanchnocranium comparable to the human. Thirdly, the typical hypoplastic maxilla of the boxer dog is comparable to human class III conditions with reversed overjet and in cleft lip and palate patients.

Surgical protocol

A modified Le Fort I osteotomy was performed and the maxilla was mobilized (Fig. 2). The distractors were fixed on each side by four titanium screws and activated peroperatively to ensure the advancement of the maxilla.



Fig. 2. Lateral cephalogram with an indication of the osteotomy line (modified Le Fort I in the boxer dog) and the bilateral distractors.

The surgical procedure was under general anaesthesia [with Pentothal® (Abbott, Chicago, Illinois, USA) and Fluothane® (Astra-Zeneca, Wilmington, Delaware, USA)]. Amoxicilline® (Merck, Whitehouse Station, New Jersey, USA) was used pre- and post-operatively during the activation period of one week after termination of the distraction. The dog was put on a soft diet during the whole experimental period. During surgery the lower canines were reduced to the gingival level and treated endodontically to prevent any dental interference during the anterior movement of the upper jaw. At the same time, a screw was placed in the crown of the skull on the midline to guarantee a fixed reference point for the cephalometric analysis.

Distraction protocol

After a healing period of five days, distraction was initiated. The intraoral activations were performed under sedation [with Thalamonal® (Innovar, Bogota, Colombia) and Pentothal® (Abbott)]. An activation of 14 mm was aimed to obtain a clinically observable result. The distraction was therefore performed daily for 14 consecutive days at the rate of 1 mm a day. The active distraction period was followed by a consolidation period of two months.

Finally, the distractors, as well as the reference screw were removed under general anaesthesia. At that time samples of the newly formed bone in the distracted area were taken for histological analysis.

Cephalometric analysis

Standardised lateral cephalograms were taken at welldefined time intervals. The first cephalogram was taken prior to surgery, and five cephalograms were taken during distraction (days 1, 5, 7, 10 and 14) and three cephalograms were taken during the consolidation period (days 14, 28 and 56). The last cephalogram was taken one year post-consolidation. To ensure the standardization of the lateral radiographs, a cephalostat was designed so that the head of the boxer dog could be placed in relation to the film in a reproducible way. A fixed distance of 74 cm between the source (90 kV and 60 mS) and the middle of the skull was maintained.

The analysis of the lateral cephalograms was performed using standard tracing and superimposition techniques. To this end eight cephalometric points and lines were defined (Table 1). Beside the skeletal reference points the screw in the crown of the skull was used as fixed reference point. Sagittal displacement was assessed with five linear measurements – the perpendicular distance between ANS, PNS, PI, Ca, Inc and the line A. The crown of the skull and the fixed reference point (screw) were used for superimpositions (Fig. 3).

Table 1. The points and lines used in the cephalometric analysis

Points	Definition
ANS	Anterior nasal spine
PNS	Posterior nasal spine
Ref _S	Reference point skull (screw)
Po	Most superior point of the internal porion
Or	Most inferior point of the orbital ridge
Inc	Incisal edge of the upper central incisor
Ca	Incisal edge of the upper canine
PI _{C/D}	Point of intersection of C and D
Lines	Definition
A	Perpendicular from the middle of Ref _S on FFH
B	Frankfort horizontal
C	Tangent at the most prominent point of the upper incisor
D	Tangent at the palate through PNS

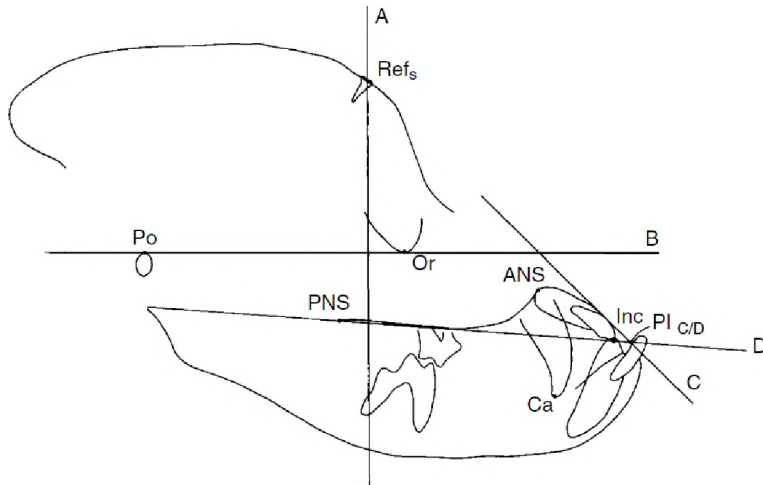


Fig. 3. Tracing showing the points of Table 1 used in the cephalometric analysis.

The tracings as well as the superimpositions were made by one investigator (first author). Repeated measurements were statistically analysed using the Dahlberg formula and showed no significant intraobserver differences.

Results

The operation was performed without any complications and the dog began eating the first day postoperatively. The distractors remained stable during the entire experimental period. Because of the communication between the oral cavity and the maxillary sinus, a strict antibiotic protocol was maintained.

Cephalometric analysis

The results of the linear measurements are summarized in Table 2.

Table 2. The displacements of the reference structures during the distraction* and the consolidation† period

	Distance from ANS to A (ref line) in mm	Distance from PNS ⊥ A (in mm)	Distance from Pl _{C/D} ⊥ A (in mm)	Distance from Ca ⊥ A (in mm)	Distance from Inc ⊥ A (in mm)
Day 1*	43	14	72	51	68
Day 5*	47	12	72	53	70
Day 7*	48	11	76	54	71
Day 10*	51	9	78	55.5	73.5
Day 14*	52.5	5.5	82	59	75.5
Sag. Displ*	+9.5	-8.5	+10	+8	+7.5
Day 14†	53	5	82	59	76
Day 28†	53	5	83	59	76.5
Day 56†	53	5	83	59	77
Sag. Displ	0.5	+ 0.5	+1	0	+1.5

For all the linear measurements an increase was found, except for PNS (the pre-distraction distance of PNS to A was 14 mm and the post-operative distance was 7.5 mm, resulting in a decrease of 6.5 mm). The sagittal position of the maxilla remained stable and the linear measurements did not change during the consolidation period.

The advancement during the active distraction period could also be evaluated radiographically by evaluating the widening of the radiolucent area adjacent to the osteotomy line. A progressive radio-opacity caused by calcification of the distracted tissue was observed during the consolidation period. This calcification started at both ends of the distracted bony parts towards the centre of the distracted area. The one year post-operative data show total calcification of the distracted area.

The radiographs of the active distraction period and the consolidation period, up to one year post-surgery, were traced and superimposed on the crown of the skull and the screw to reveal the gradual anterior movement of the maxilla. One year after removal of the distractors, no sagittal relapse was evaluated by superimposition (Fig. 4).

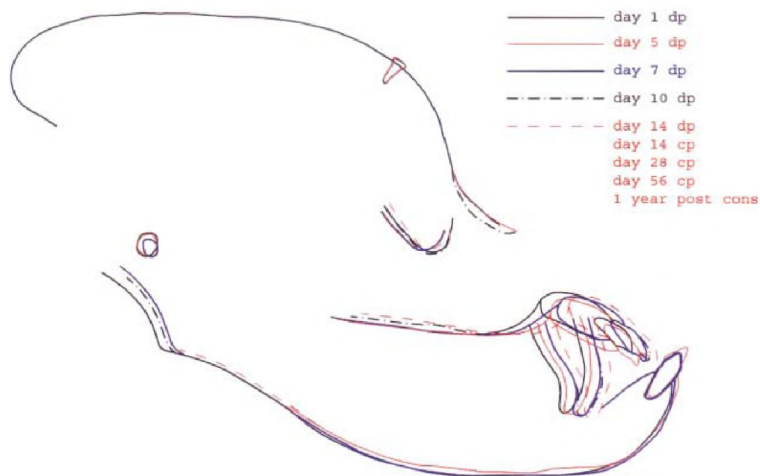


Fig. 4. Superimpositions of the tracings made from cephalograms respectively at days 1, 5, 7, 10 and 14 after the start of the distraction and at days 14, 28, and 56 after the start of the consolidation period with the distractor in place. The final cephalogram was made 1 year after the removal of the distractor.

Histological analysis

Histological examination shows a distraction gap almost completely filled with newly formed bone. Most of this new bone was formed by intramembranous ossification and only a little by endochondral ossification (Figs 5 and 6).

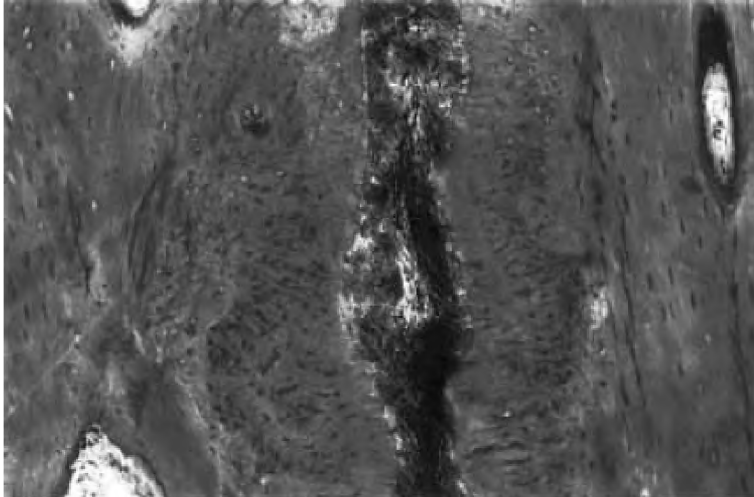


Fig. 5. New bone is appositioned to both borders of the osteotomy line, approximately in the middle of the histological section. It can be distinguished from the pre-existing bone by its woven structure instead of a mature lamellar structure.

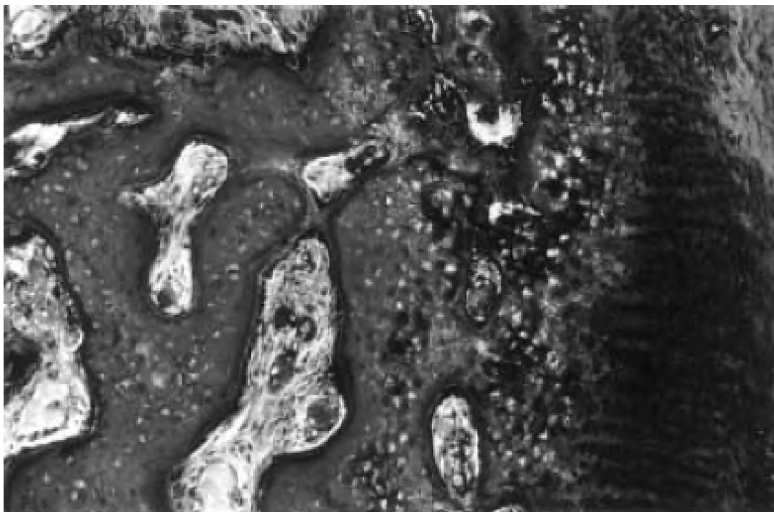


Fig. 6. Apparent chondrocytes differentiated in the distracted area, giving rise to endochondral bone formation (on the right side of the section).

This enchondral ossification can be due to instability of the bone segments and the distraction rate, but it does not influence the final result. These observations (ossification through two mechanisms) are in accordance with other studies¹⁴⁻¹⁶.



Fig. 7. (a) A clear radiolucent gap (area) next to the osteotomy line during distraction.



Fig. 7 (b) A progressive radio-opacity caused by calcification during consolidation period.

Discussion

In this study, a mature boxer dog with natural maxillary hypoplasia was chosen to exclusively evaluate the effects of distraction effects without confounding growth influences. The absence of a cephalometric analysis in the literature that could be used to interpret the maxillary advancement in boxer dogs necessitated the development and evaluation of landmarks for the cephalometric analysis. Of these, ANS, PNS, upper Ca, upper Inc and PIC/D were the most stable. The landmarks located in the mandible seemed unstable, probably due to occlusal interferences and the resulting minimal shifts. For the superimpositions, the crown of the skull and the screw were used as a registration point.

A latency period of five days was employed. The recommended latency period in the literature for limb lengthening is between 0 and 10 days^{2,3,17,18}, depending on the patient's age: the younger the individual, the shorter the period^{7,8,19,20}. The distraction rate was 1 mm/day. Due to practical considerations, the activations were performed once a day. Slow activations can result in premature ossification and fusion, faster activations can result in fibrous tissue within the distraction gap and unstable consolidation. Some authors claim that a more uniform hard and soft tissue response is obtained when the activations are performed twice a day²¹⁻²⁴. In our study a uniform hard and soft tissue response was seen radiologically and histologically.

Both distractors were placed symmetrically under the same conditions, the rate and latency period were identical, and activations were performed by one investigator. After removal of the distractors, the activation of both devices was identical. The use

of two individual distractors, however, introduces the possibility of asymmetrical activations in the sagittal plane. The orientation of the distractors therefore provides an opportunity to also correct minor transversal and vertical maxillary disproportions.

The active distraction period was 14 days. The expected linear advancement of the cephalometric points was 14 mm; however, an average advancement of only 8.7 mm was found. The largest increases, 9.5 and 10 mm, were found at ANS and PIC/D. This failure to achieve a 14-mm gap could be explained biomechanically by the influence of several factors like the distractor design, distractor placement, the possible movement of the screws in the fixation plates and maybe other environmental influences^{25, 26}. First, the overall difference between 8.7 and 14 mm perhaps was due to incorrect activations. To gain 1 mm, two rotations of 360° had to be performed. Secondly, the superimposition shows a downward tipping of the maxilla during the first 5 days of the distraction period, an effect that can contribute to the difference between the expected and the effective gain in sagittal displacement of the maxilla. Soft tissue resistance could be a third factor explaining the difference between the expected and the effectively gained displacement.

There are a number of advantages to the distractor (prototype) used. Its internal location makes it psychologically much more acceptable than the external location. It was also confirmed in this study that implants accidentally perforated into the sinus do not necessarily show complications^{27,28}. In contrast to distraction performed using, for example, the RED system or a facial mask with elastic forces, the same device can be used during the whole retention period. In previous studies, dental anchorage was often used for the fixation of the distraction device^{11-13,29,30}. This resulted in a limited skeletal advancement and a significant dento-alveolar displacement. With this distractor prototype, there is a skeletal anchorage and up to a year following distraction, no relapse could be observed.

Therefore, the results seem promising for extrapolation to the human clinical situation for treatment of moderate to severe class III relations, especially in young patients with cleft lip, and palate patients with maxillary hypoplasia. Further experimental and clinical studies, however, are needed to confirm these findings.

Acknowledgements. We are indebted to Prof. Lambrechts (K.U. Leuven), Prof. Simoens (R.U. Gent), Prof. Van Bree (R.U. Gent), H. De Fraye, I. Laermans and L. Hendrickx for their practical help in the experiments.

References

1. Ilizarov GA. Basic principles of transosseus compression and distraction osteosynthesis. *Orthop Traumatol Protez* 1975; 10:7–15
2. Ilizarov GA. The tension-stress effect on the genesis and growth of tissues: I. The influence of stability of fixation and soft-tissue prevention. *Clin Orthop* 1989; 238:249–81
3. Ilizarov GA. The tension-stress effect on the genesis and growth of tissues: II. The influence of the rate and frequency of distraction. *Clin Orthop* 1989; 239:263–85
4. Snyder CC, Levine GA, Swanson HM, Browne EZ. Mandibular lengthening by gradual distraction: preliminary report. *Plast Reconstr Surg* 1973; 51:506–8
5. McCarthy JG, Schreiber J, Karp N. Lengthening the human mandible by gradual distraction. *Plast Reconstr Surg* 1999; 89:1-10
6. Ortiz-Monasterio F, Molina F. Mandibular distraction in hemifacial microsomia. *Oper Tech Plast Reconstr Surg* 1994; 1:105–11
7. Cohen SR, Rutrick RE, Burnstein FD. Distraction osteogenesis of the human craniofacial skeleton: initial experience with a new distraction system. *J Craniofacial Surg* 1995; 6:368–74
8. Chin M, Toth BA. Distraction osteogenesis in maxillofacial surgery using internal devices: review of five cases. *J Oral Maxillofac Surg* 1996; 54:45–54
9. Cohen SR, Burstein FD, Stewart MB, Rathburn MA. Maxillary midface distraction in children with cleft lip and palate: a preliminary report. *Plast Reconstr Surg* 1997; 99:1421–8
10. Do Amaral CMR, Di Domizio G, Tiziani V. Gradual bone distraction in craniosynostosis. *Scand J Plast Reconstr Hand Surg* 1997; 31:25–37
11. Polley JW, Figueroa AA. Management of severe maxillary deficiency in childhood and adolescence through distraction osteogenesis with external, adjustable, rigid distraction device. *J Craniofacial Surg* 1997; 8:181–5
12. Molina F, Ortiz-Monasterio F, de la Paz Aquilar M, Barrera J. Maxillary distraction: aesthetic and functional benefits in cleft lip palate and prognathic patients during mixed dentition. *Plast Reconstr Surg* 1998; 101:951–63

13. Swennen G, Colle F, De Mey A, Malevez C. Maxillary distraction in cleft lip and palate patients: a review of six cases. *J Craniofacial Surg* 1999; 10:117–22
14. Karp NS, McCarthy JG, Schreiber JS, Sissons HA, Thorne CH. Membranous bone lengthening: a serial histological study. *Ann Plas Surg* 1992; 29:2–7
15. Komuro Y, Takato T, Harii K, Yonehara Y. The histologic analysis of distraction osteogenesis of the mandible in rabbits. *Plast Reconstr Surg* 1994; 94:152–7
16. Sawaki Y, Ohkubo H, Yamamoto H, Ueda M. Mandibular lengthening by intra oral distraction using osseointegrated implants. *Int J Oral Maxillofac Implants* 1996; 11:186–93
17. De Bastiani G, Aldegheri R, Renzi-Brivio L, Trivella G. Limb lengthening by callus distraction. *J Pediatr Orthop* 1987; 7:129–34
18. Stanitski DF. The effect of limb lengthening on articular cartilage: an experimental study. *Clin Orthop* 1994; 301:68–72
19. White SH, Kenwright J. The timing of distraction of an osteotomy. *J Bone Joint Surg* 1990; 72:356–61
20. Tetsworth K, Pabe D. Basic science of distraction histiogenesis. *Cur Opin Orthop* 1995; 6:61–8
21. Aldegheri R, Renzi-Brivia L, Agostini S. The callostasis method of limb-lengthening. *Clin Orthop* 1989; 241:137–45
22. Price CT, Cole JD. Limb lengthening by callotasis for children and adolescents: early experience. *Clin Orthop* 1990; 250:105–11
23. Young JWR, Kostrubiak IS, Resnik CS, Paley D. Sonographic evaluation of bone production at the distraction site in Ilizarov limb-lengthening procedures. *Am J Reconstr* 1990; 154:125–8
24. Dahl MT, Gulli B, Berg T. Complications of limb lengthening: a learning curve. *Clin Orthop* 1994; 30:10–8
25. Ahn JG, Figueroa AA, Braun S, Polley JW. Biomechanical considerations in distraction of the osteotomized dentomaxillary complex. *Am J Orthod Dentofacial Orthop* 1999; 116:264–70
26. Grayson BH, Santiago PE. Treatment planning and biomechanics of distraction osteogenesis from an orthodontic perspective. *Sem Orthod* 1999; 5:9–24

27. Brånemark PI, Adell R, Albrektsson T, Lekholm U, Lindtroöm J, Rockler B. An experimental study of osseointegrated implants penetrating the nasal cavity and maxillary sinus. *J Oral Maxillofac Surg* 1984; 42:497–505
28. Timmenga NM, Raghoobar GM, Boering G, van Weissenbruch R. Maxillary sinus function after sinus lifts for the insertion of dental implants. *J Oral Maxillofac Surg* 1997; 55:936–9
29. Figueroa AA, Polley JW. Management of severe cleft maxillary deficiency with distraction osteogenesis: procedure and results. *Am J Orthod Dentofacial Orthop* 1999; 115:1–5
30. Rachmiel A, Aizenbud D, Ardekian L, Peled M, Laufer D. Surgically assisted orthopedic protraction of the maxilla in cleft lip and palate patients. *Int J Oral Maxillofac Surg* 1999; 28:9–14

CHAPTER 4a

Predictability of maxillary distraction with the trans-sinusoidal distractor

Original title:

Prédictibilité de la distraction du maxillaire supérieur avec distracteur transsinusiené

N. Nadjmi

Department of Cranio-Maxillofacial Surgery, AZ MONICA, Antwerp, Belgium.

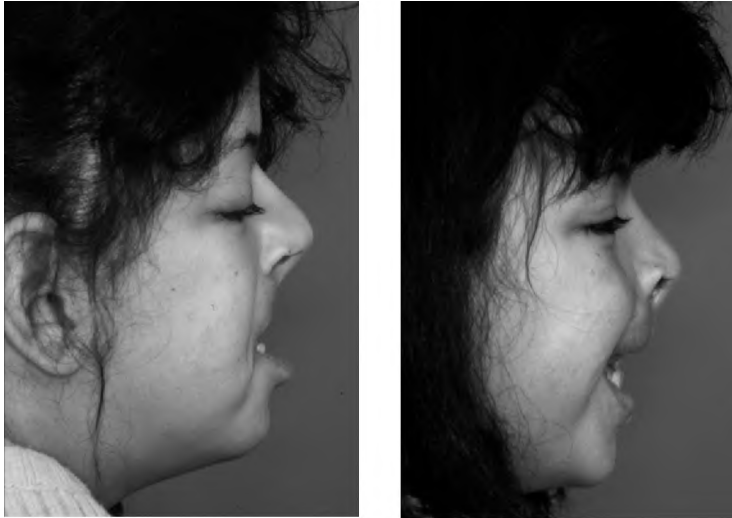
Rev Stomatol Chir Maxillofac. 2004; 105: 9-12

Introduction

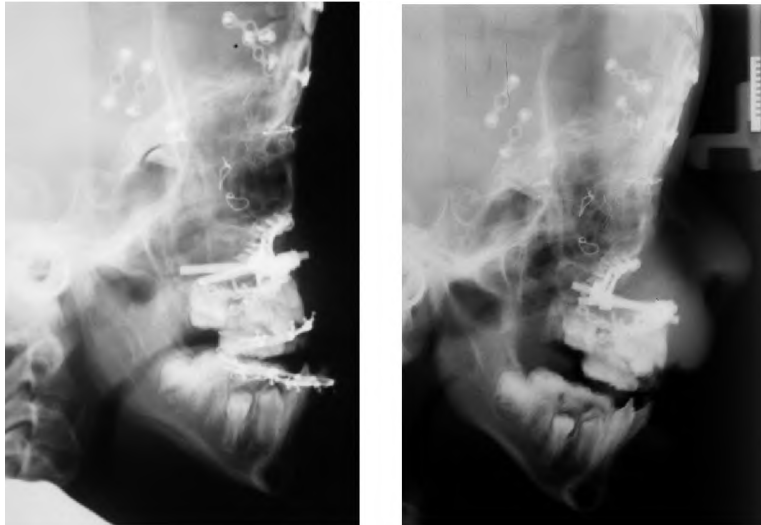
Maxillary distraction is indicated in severe angle Class III malocclusions and severe maxillary hypoplasia among some cleft patients, and for other craniofacial deformities. The latter group of patients show Class III malocclusions at a young age. Miniature intraoral distractors can now be used at earlier ages and these are therefore beneficial for children's psychological and emotional development. According to the literature, at 8 years of age the maxillary sinus is sufficiently developed to house the activation screw of the intraoral distractor device that has been presented in this study. The anatomy of the sinus cavity allows the axis of the distraction vector to be positioned without limitation.

Patients and methods

Fourteen patients aged 8 to 55 years with severe maxillary and mid-facial hypoplasia were treated in our centre between June 2000 and September 2002. The maxillary hypoplasia was caused by repaired unilateral (5 cases) or bilateral cleft lip and palate (4 cases) (Fig. 1 and 2, 3 and 4), Class III malocclusions in four patients (Fig. 5 and 6), and an acromegaly in one patient. Five patients received pre-operative orthodontic treatment.



Figs. 1 and 2. Young 8-year-old girl with maxillary hypoplasia associated with cleft lip and palate. Clinical profile views before and after maxillary distraction.



Figs. 3 and 4. Profile X-rays before and after distraction (16 mm). Notice the advancement and rotation of the maxilla with correction of the open bite.



Fig. 5. Young 12-year-old girl with a Class III dental and skeleton malocclusion and open bite.

Fig. 6. Six months after distraction and reduction genioplasty.

A CT-scan was performed one month prior to surgery. Medicim[®] (NV Belgium) prediction and simulation software was used to process the digital data. These data were used to transfer the distraction vector into a stereolithographic (STL) model of the midface containing a tube in each maxillary sinus into which the distraction screws fit. The position of the distraction screws in the STL model defines the distraction vector. This STL model was then used for bending the upper and lower plates of the device. After preoperative positioning of the TSMD on the STL model

by the surgeon, a methyl-methacrylate template was manufactured by a dental technician. The template was used intraoperatively for positioning the upper plate of the distractor. A high Le Fort I type osteotomy was performed in all cases. An intraoral trans-sinusoidal maxillary distractor was placed on either side of the maxilla. The only visible part of the distractor was the tip of the activation rod, which was concealed behind the upper lip. Activation commenced after a 5-day latency period and was performed at the rate of 1 mm per day. The distraction period lasted 7-22 days, after which the activation rods were removed under local anaesthesia. The distractors were left in place until callus maturation (showed on the ultrasound and/or the CT-scanner) generally after two months.

Results

All the procedures were performed by the same surgeon. There were no immediate complications. In the first two patients, problems arose during distraction. The first patient had a temporary prototype and the screw had to be introduced directly on the activation axis, which required local anaesthesia. Thereafter, a flexible activation rod was used. In the second patient, who had an acromegaly, the flexible activation proved to be insufficiently strong after 8 mm advancement. In the other 12 patients, the distraction was completed with a rigid activation rod, either by the patient or, in the case of children, by the patient's parents. All the patients were able to resume normal activity after one week. The intra-sinusoidal positioning in the maxillary sinus was well tolerated by all patients. The advancement obtained at the distractor level varied from 7 to 22 mm.

Discussion

In this paper, the use of a novel intra-sinusoidal distractor (TS-MD) is suggested. The latest prototype of the TS-MD distractor has permitted distraction to be brought to a successful conclusion with up to 22 mm advancement. According to the anthropological literature, the maxillary sinus in humans appears at age of 6 to 8 years, even in patients with cleft lip and palate¹. Harvolds¹ compared the maxillary sinus' growth curve in patients with clefts to the normal population and concluded that there was no significant difference. Duerinckx² retrospectively compared the evolution of paranasal sinuses in 80 children from birth to age 17 years and was able to show that 2/3 of the sinusoidal pneumatization occurred at the age of 4 years. Few changes occur after the age of 11 years. Branemark³ showed the feasibility of using implants when intra-sinusoidal penetration was inevitable. The results of these clinical studies show no morbidity due to titanium implants, even in the cases of sinusoidal perforation. In an anatomical study of 102 paediatric skulls, Wolf showed that the size of the maxillary sinus had increased significantly towards the age of 8 years⁴. The maxillary sinus ventrocaudal dimension varied between 34 and 38 mm. Maxillary hypoplasia makes patients with a bilateral lip and palate cleft, candidates for a distraction at age 8-10 years. The benefits of the trans-sinusoidal TS-MD distractor are:

- It is well tolerated by patients because the most voluminous part is placed within the maxillary sinus.
- The device does not interfere with the patient's social life and is, therefore, more readily accepted than a halo type external distractor⁵.
- It does not require alveolo-dental fixation, and therefore nonalveolo-dental displacement caused by external traction⁶⁻⁸.

The TS-MD distractor can also prevent the need for bone grafting in cases with major maxillary advancement and extrusion. The precise positioning of the vector is crucial. Correction of the midline can be done by distracting one side more than the other.

References

1. Harvold E. Cleft Lip and Palate. Morphologic studies of the facial skeleton. *Am J Orthod* 1954; 40:493-7
2. Duerinckx AJ; Hall TR, Whyte AM, Lufkin R, Kangaroo H. Paranasal sinuses in pediatric patients by MRI: normal development and preliminary findings in disease. *Eur J Radiol* 1991; 13:107-12
3. Branemark PI, Adell R, Albrektsson T, Lekholm U, Lindstrom J, Rockler B. An experimental and clinical study of osseointegrated implants penetrating the nasal cavity and maxillary sinus. *J Oral Maxillofac Surg* 1984; 42:497-505
4. Wolf G, Anderhuber W, Kuhn F. Development of the paranasal sinuses in children: implication for paranasal surgery. *Ann Otol Rhinol Laryngol* 1993; 102:705-11
5. Polley JW, Figueroa AA. Management of severe maxillary deficiency in childhood and adolescence through distraction osteogenesis with external, adjustable, rigid distraction device. *J Craniofac Surg* 1997; 8:181-5
6. Molina F, Ortiz-Monasterio F, De La Paz Aguilar M, Barrera J. Maxillary distraction: aesthetic and functional benefits in cleft lip palate and prognathic patients during mixed dentition. *Plast Reconstr Surg* 1998; 101:951-63
7. Figueroa AA, Polley JW. Management of severe cleft maxillary deficiency with distraction osteogenesis: procedure and results, *Am J Orthod Dentofacial Orthop* 1999 115:1-12
8. Swennen G, Colle F, De May A, Malevez C. Maxillary distraction in cleft lip and palate patients: a review of six cases. *J Craniofac Surg* 1999; 10:117-22

CHAPTER 4b

Trans-sinusoidal maxillary distraction in three cleft patients (technical note)

**M. Wenghoefer¹, M. Martini¹, N. Nadjmi², F. Schutyser³,
A. K. Jagtman³, S. Berge^{1,3}**

1. University of Bonn, Sigmund-Freud-Str. 25, Bonn 53105, Germany;
2. Department of Oral & Maxillofacial Surgery, AZ MONICA Antwerpen, Harmoniestraat 68, Antwerpen 2018, Belgium;
3. Department of Oral & Cranio-Maxillofacial Surgery, Radboud University Nijmegen, Geert Grooteplein-Zuid 14, 6525 GA Nijmegen, The Netherlands

Int J Oral Maxillofac Surg 2006; 35: 954–960.

Abstract

The trans-sinusoidal maxillary distractor (TS-MD) was used to achieve maxillary advancement in three patients with repaired cleft lip and palate. After preoperative computer-aided planning of the distraction vectors, each TS-MD was bent on a stereolithographic model of the maxilla of the patient. The devices were intraoperatively positioned using a methyl-methacrylate template. After standard Le Fort I osteotomy the devices were intraorally activated. After distraction the devices remained in situ for 3 months as rigid internal fixation of the maxilla. All patients were successfully distracted according to protocol. Maxillary advancement was 12, 8 and 11 mm. In two patients, additional maxillary widening of 6 and 8 mm was achieved by choosing divergent distraction vectors. After distraction a clockwise rotation of the maxilla was observed in two patients. There was no relapse during the 3 months of consolidation and 12-month follow-up. The TS-MD allows not only distraction but also rigid internal fixation after distraction. It was easy to apply but difficult to remove. Owing to preoperative 3D planning of the distraction vectors, the results were predictable, but clockwise rotation of the maxilla during distraction should be considered in planning. The distractor did not interfere with function or social activities during distraction and retention periods. After removal it left no extraoral scars.

Patients with cleft lip and palate often present with severe maxillary hypoplasia in vertical, horizontal and transverse dimensions. Treatment of maxillary hypoplasia or retrusion is primarily surgical¹⁵. Traditional protocols rely on a combined surgical–orthodontic approach including Le Fort I maxillary advancement, maxillary and alveolar bone crafting, and rigid internal fixation. Long-term results have however been disappointing, with relapse occurring in more than 20% of the cases^{10,16}. Apart from conventional orthognathic surgery, distraction osteogenesis^{11,13} has frequently been used in the treatment of various craniofacial deformities, including midface deficiencies, by means of internal as well as external distraction devices^{3,6,7,8,14}. External systems utilize a cranial fixed distraction device to achieve the desired vertical and horizontal reposition of the maxilla.

Most external devices are fully adjustable and offer the ability to change the vertical and horizontal vector of distraction at any time in the distraction process^{1,7}, but interfere with function during distraction and retention and have a strong impact on the patient aesthetically and socially^{6,14,19}.

In this study an internal device, the trans-sinusoidal maxillary distractor (TSMD, Gebrüder Martin GmbH & Co. KG, Tuttlingen, Germany) was used to achieve maxillary advancement in three cleft patients. Depending on the preoperative planning, the TS-MD allows maxillary advancement, clockwise rotation and maxillary widening¹⁴.

Patients, material and methods

Patients

All three patients presented with retrusion of the maxilla due to repaired unilateral (n = 2) or bilateral (n = 1) cleft lip and palate. The average age of the patients on presentation was 18.3 years. One patient was male and two were female.

Patient EE: A 19-year-old male patient with a repaired left unilateral cleft lip and palate. On presentation, EE showed a severe sagittal and transverse maxillary deficiency with anterior open bite. Figure 1A and B shows the preoperative clinical photographs, Fig. 1C shows the preoperative dental occlusion and Fig. 1D shows the preoperative lateral cephalogram. Preoperative 12-mm maxillary advancement and 8-mm maxillary widening were planned.

Patient SK: An 18-year-old female patient with a repaired bilateral cleft lip and palate. On presentation, SK showed a class III malocclusion. Figure 2A and B shows the preoperative clinical photographs, Fig. 2C shows the preoperative dental occlusion and Fig. 2D shows the preoperative lateral cephalogram. Preoperative 8-mm maxillary advancement was planned.

Patient GS: An 18-year-old female patient with a repaired left unilateral cleft lip and palate. On presentation, GS showed a severe sagittal and transverse maxillary deficiency with anterior open bite and a deformity of the nose. Figure 3A and B shows the preoperative clinical photographs, Fig. 3C shows the preoperative dental occlusion and Fig. 3D shows the preoperative lateral cephalogram. Preoperative 11-mm maxillary advancement was planned.

Distractor

The TS-MD is an internal device consisting of two plates connected with a distraction screw that is positioned in the maxillary sinus (Fig. 4A). The screw is activated by an activation arm in the oral cavity. Fig. 4B shows the distractor on a stereolithographic (STL) model of the midface.

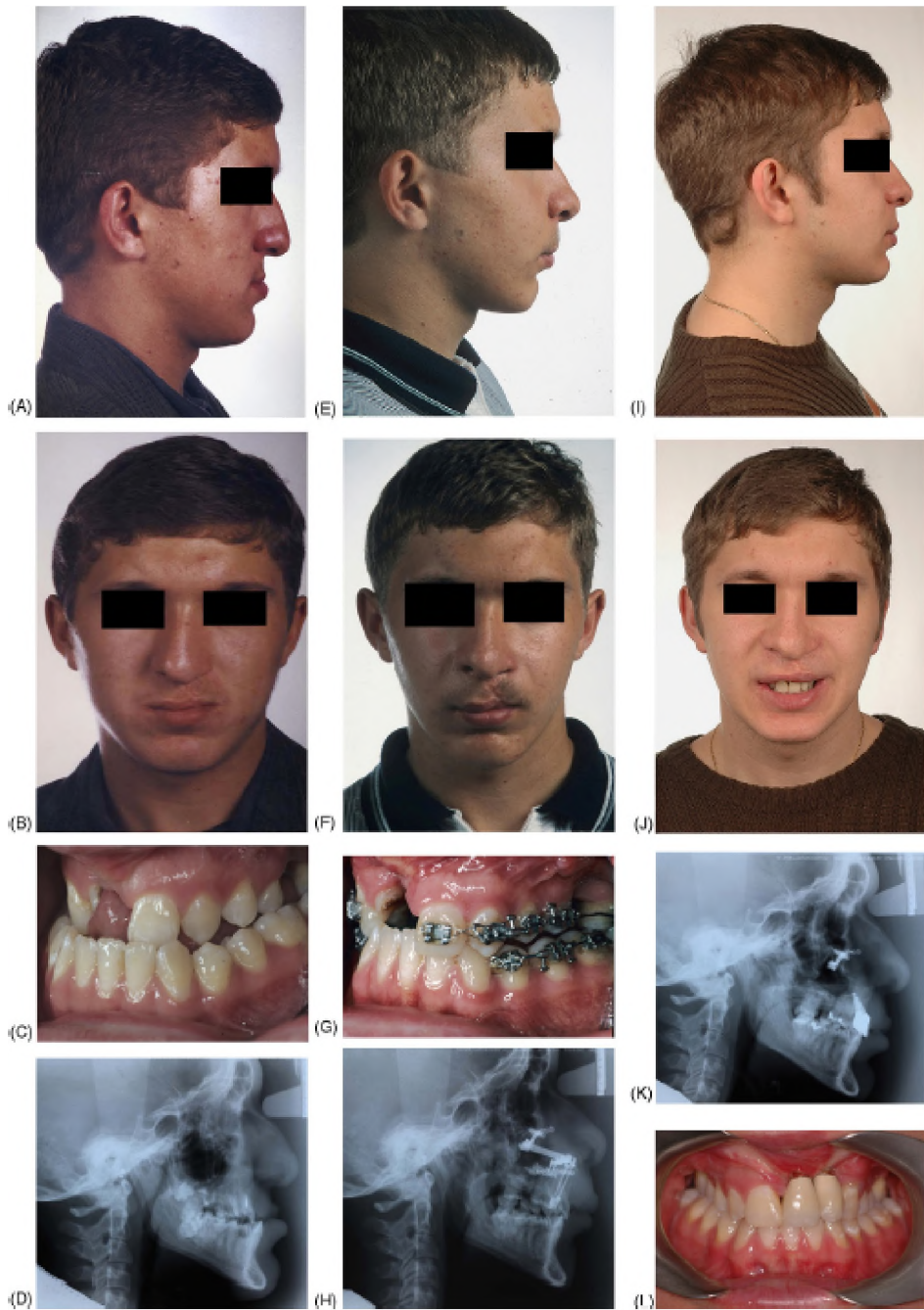


Fig. 1. Patient EE. Clinical photos before distraction: (A) lateral, (B) frontal, (C) intraoral views; (D) cephalogram. Clinical photos after distraction and retention: (E) lateral, (F) frontal, (G) intraoral views; (H) cephalogram. Clinical photos 2 years after distraction: (I) lateral, (J) frontal, (K) intraoral views; (L) cephalogram.



Fig. 2. Patient SK. Clinical photos before distraction: (A) lateral, (B) frontal, (C) intraoral views; (D) cephalogram. Clinical photos after distraction and retention: (E) lateral, (F) frontal, (G) intraoral views; (H) cephalogram. Clinical photos 2 years after distraction: (I) lateral, (J) frontal, (K) intraoral views; (L) cephalogram.



Fig. 3. Patient GS. Clinical photos before distraction: (A) lateral, (B) frontal, (C) intraoral views; (D) cephalogram. Clinical photos after distraction and retention: (E) lateral, (F) frontal, (G) intraoral views; (H) cephalogram. Clinical photos 2 years after distraction: (I) lateral, (J) frontal views; (K) cephalogram.

Preoperative computer-aided planning

In a 3D planning environment generated from CT images the distraction was simulated with respect to the sagittal, transversal and horizontal planes (Fig. 4C–E). The desired distraction vector and the osteotomy line were defined by the surgeon in planning. These data were used to transfer the distraction vector into a STL model of the midface containing a tube in each maxillary sinus into which the distraction screws fit. The position of the distraction screws in the STL model defines the distraction vector (Fig. 4F). This STL model was then used for bending the upper and lower plates of the device (Fig. 4B and G). After preoperative positioning of the TSMD on the STL model by the surgeon, a methyl-methacrylate template was manufactured by a dental technician (Fig. 4H). The template was used intraoperatively for positioning the upper plate of the distractor.

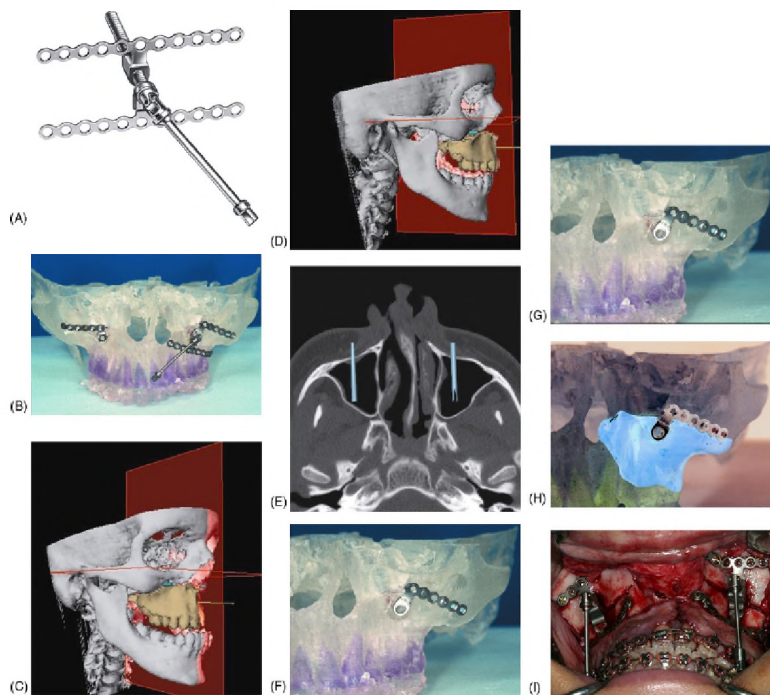


Fig. 4. (A) The TS-MD. (B) TS-MD on a stereolithographic (STL) model of the midface. (C–E) Distraction was simulated in a 3D planning environment generated from CT images. (F) The position of the distraction screws in the STL model defines the distraction vector. (G) STL model was used for positioning upper plate of device. (H) Methyl-methacrylate template used intraoperatively for positioning upper plate of distractor, manufactured by dental technician. (I) TS-MD in situ in patient GS after Le Fort I osteotomy.

Surgical technique

A maxillary vestibular incision from the first bicuspid on one side to the first bicuspid on the other side was followed by preparation of the maxilla for a Le Fort I osteotomy. By using the methyl-methacrylate template, an entry hole for the distraction screw was generated in the anterior maxillary wall and the pre-bent upper part of the distractor was fixed cranial to the desired osteotomy line. After Le Fort I osteotomy, the maxilla was mobilized without a complete down fracture, and the lower part of the distractor together with the distraction screw was positioned caudal to the osteotomy line (Fig. 4I). The distractor was activated bilaterally and then returned to the first position to exclude any interference. Via two stab incisions cranial to the maxillary vestibular incision, the activation arms were brought into the oral cavity, followed by wound closure.

Distraction protocol

After 5 days of latency, distraction was initiated at a rate of 2 mm - 0.5 mm per day and continued until the planned advancement of the maxilla was achieved; then the activation arms were removed. Distraction was followed by a retention period of 3 months using the TS-MD as retention device. The distractor was then removed under general anesthesia.

Results

There were no complications (no infections, problems with materials, etc.). Owing to postoperative fibrosis and osseointegration of the upper and lower plate and of the distraction screws it was particularly difficult to remove the distractor. In all patients, the upper plate of the distractor was not removed in order to prevent the infraorbital nerve from being damaged.

Patient EE: The TS-MDs were activated for 22 mm on each side. The planned advancement of 12 mm in combination with a maxillary widening of 8 mm was achieved because of divergent distraction vectors. A clockwise rotation of the maxilla was observed. Figure 1E and F shows the postoperative clinical photographs, Fig. 1G shows the postoperative dental occlusion and Fig. 1H shows the lateral cephalogram. Figure 1I and J shows the clinical photos, Fig. 1K shows the intraoral situation and Fig. 1L shows the lateral cephalogram 2 years after distraction. The upper plate of the TS-MD is still in situ.

Patient SK: The TS-MDs were activated for 8 mm on each side to achieve the planned advancement. Figure 2E and 2F shows the postoperative clinical photographs, fig. 2G shows the postoperative dental occlusion and fig. 2H shows the lateral cephalogram. As fig. 2I–K depicts, the maxillary advancement has been stable since then; fig. 2L shows the lateral cephalogram with the upper plate of the TS-MD in situ.

Patient GS: The TS-MDs were activated for 20 mm on each side to achieve the planned advancement. The planned advancement of 11 mm in combination with a maxillary widening of 6 mm was achieved because of divergent distraction vectors. A clockwise rotation of the maxilla was observed. Figure 3E and 3F shows the postoperative clinical photographs, Fig. 3G shows the postoperative dental occlusion and fig. 3H shows the lateral cephalogram. Within the next two years the patient received a rhinoplasty and a genioplasty. Figure 3I and 3J shows the final results, and fig. 3K shows the lateral cephalogram with the upper plate of the TS-MD in situ. The cephalometric measurements before and after treatment are given in Table 1.

Patient	Age (years)	Parameters	Before treatment	After treatment
EE	18	SNA	73.1°	83.0°
		SNB	75.0°	73.2°
		ANB	1.1°	3.4°
		Advancement		12 mm
		Widening		8 mm
		Rotation		Clockwise
SK	19	SNA	74.0°	85.0°
		SNB	86.0°	83.4°
		ANB	-2.0°	6.6°
		Advancement		8 mm
		Widening		-
		Rotation		-
GS	18	SNA	68.4°	76.6°
		SNB	71.6°	69.7°
		ANB	-3.2°	6.9°
		Advancement		11 mm
		Widening		6 mm
		Rotation		Clockwise

Table 1: Cephalometric measurements

Discussion

Traditional surgical approaches for correction of a midface deficiency in cleft patients include maxillary osteotomy, bone grafting and rigid internal fixation^{15,1,17}. Bone grafts in the posterior gap between the maxillary tuberosity and the pterygoid plates in combination with miniplate fixation help to reduce relapse after orthognatic surgery^{18,4}, but carry the potential risks of donor site morbidity, and resorption or infection of the bone graft^{17,12}. More than 20% of the cases that were treated traditionally showed a relapse¹⁶.

Distraction osteogenesis of the maxilla avoids autogenous bone transplants and achieves long-term skeletal stability after maxillary advancement by using a rigid external distraction device⁷. Disadvantages are discomfort and impairment of the patient's social life caused by the headframe- based extraoral device.

Trans-sinusoidal placement of a distractor in patients with cleft lip and palate is a possible alternative^{14,2,5,9}. The major part of the TS-MD is within the maxillary sinus and does not interfere with function during distraction and retention or with the patient's social life^{6,14,8}. Compared with head-frame-based extraoral devices for midface distraction, the TS-MD does not leave extraoral scars after removal¹⁹. In the present study, in order to protect the infraorbital nerve from damage, the upper plate of the distractor remained in situ; only the lower plate was removed.

A 3D planning environment enables planning of the distraction vector in three dimensions. This allows planning not only of a maxillary advancement, but also of a rotation and correction of a midline shift. As maxillary hypoplasia in cleft patients is a three-dimensional problem, transversal widening of the maxilla is often mandatory. This can be achieved by choosing divergent instead of parallel distraction vectors in the horizontal plane, as in patients EE and GS.

As described by Gateno et al.⁸ a clockwise rotation of the maxilla was observed in two patients. In future, clockwise rotation should be considered in the preoperative planning. A solution for this problem might be to define slightly counterclockwise distraction vectors preoperatively to compensate for the clockwise maxillary rotation during distraction.

The preoperative bending of the device reduced operation time and costs. The application of the distractors during the operation was quick and easy. After distraction the TS-MD is stable enough to be used as a retainer. In contrast to Gateno et al.⁸, no relapses of distraction were observed in the present study. Another advantage of the preoperative planning was that the procedure of distraction could be visualized and discussed with the patient, leading to greater acceptance and compliance.

References

1. Adlam DM, Banks P. A retrospective study of the stability of midface osteotomies in cleft lip and palate patients. *Br J Oral Maxillofac Surg* 1989; 27: 265–276
2. Bra°nemark PI, Adell R, Albreksson T, Lekholm U, Lindstrom J, Rockler B. An experimental and clinical study of osseointegrated implants penetrating the nasal cavity and maxillary sinus. *J Oral Maxillofac Surg* 1984; 42: 497–505
3. Cohen SR, Burstein FD, Williams JK. The role of distraction osteogenesis in the management of craniofacial disorders. *Ann Acad Med Singapore* 1999; 28: 728–738
4. Drommer R, Luhr HG. The stabilization of osteotomised maxillary segment with Luhr miniplates in secondary cleft surgery. *J Maxillofac Surg* 1981; 9: 166–169
5. Eckel W, Beisser D. Studies on the problem of the effect of harelip formation on the dimensions of the maxillary antra. *Z Laryngol Rhinol* 1961; 40: 23–31 in German.
6. EMPARANZA A, VELA A, LASAGABASTER F. Distraction osteogenesis in maxillary hypoplasia using internal devices: case reports. In: *Craniofacial Distraction Osteogenesis*. St. Louis: Mosby 2001: 535–540
7. Figueroa AA, Polley JW, Ko EW. Maxillary distraction for the management of cleft maxillary hypoplasia with a rigid external distraction system. *Semin Orthod* 1999; 5: 46–51
8. Gateno J, Engel ER, Teichgraeber JF, Yamaji KE, Xia JJ. A new Le Fort I internal distraction device in the treatment of severe maxillary hypoplasia. *J Oral Maxillofac Surg* 2005; 63: 148–154
9. Harvold E. Cleft lip and palate. Morphologic studies of the facial skeleton. *Am J Orthod* 1954; 40: 493. 10. Hochban W, Ganss C, Austermann KH. Long-term results after maxillary advancement in patients with clefts. *Cleft Palate Craniofac J* 1993; 30: 237–243
10. Ilizarov GA. The principles of the ilizarov method. *Bull Hosp Jt Dis Orthop Inst* 1988; 48: 1. 12. Laurie SW, Kaban LB, Mulliken JB. Donor site morbidity after harvesting rib and iliac bone. *Plast Reconstr Surg* 1984; 73: 933–938
11. Molina F, Ortiz Monasterio F. Mandibular elongation and remodeling by distraction: a farewell to major osteotomies. *Plast Reconstr Surg* 1995; 96: 825

12. Nadjmi N. Predictability of maxillary distraction with the trans-sinusoidal maxillary distractor. *Rev Stomatol Chir Maxillofac* 2004; 105: 9–12
13. Obwegeser HL. Surgical correction of small or retro-displaced maxillae: the 'dish-face' deformity. *Plast Reconstr Surg* 1969; 43: 351–365
14. Posnick JC, Dagens AP. Skeletal stability and relapse patterns after Le Fort I maxillary osteotomy fixed with miniplates: the unilateral cleft lip and palate deformity. *Plast Reconstr Surg* 1994; 94: 924–932
15. Rachmiel A, Aizenbud D, Peled M. Long-term results in maxillary deficiency using intraoral devices. *Int J Oral Maxillofac Surg* 2005; 34: 473–479
16. Stoelinga PJW. The prevention of relapse after maxillary osteotomies in cleft palate patients. *J Craniomaxillofac Surg* 1987; 15: 326–331
17. Stucki-McCormick SU, Drew S, Mizrahi RD. *Distraction Osteogenesis: Overcoming the challenges of a new technique*. St. Louis: Mosby 2001: 595–603

CHAPTER 5

Trans-Sinusal Maxillary Distraction for correction of midfacial hypoplasia: Long-term clinical results

N. Nadjmi¹, F. Schutyser², R. Van Erum³

1. Department of Cranio-Maxillofacial Surgery, AZ Monica, Antwerp, Belgium.
2. Medical Image Computing (Radiology - ESAT/PSI)
Faculties of Medicine and Engineering,
University Hospital Gasthuisberg, Herestraat 49, B-3000 Leuven,
Belgium
3. Department of Orthodontics, Catholic University of Leuven, Belgium.

Int J Oral Maxillofac Surg 2006; 35: 885-896

Abstract

Maxillary distraction osteogenesis finds its indication in severe Angle class III malocclusions, and severe maxillary hypoplasia among some cleft patients and other cranio-facial deformities. Twenty patients, 9 female and 11 male, age 8 to 48 years (mean 17,8 yrs \pm 10,5 SD) with moderate to severe maxillary and midfacial hypoplasia were treated in our centre from May 2000 to October 2005. The follow up period varied from 13 to 65 months (mean 35 months \pm 16,3 SD). One trans-sinusual maxillary distractor (TS-MD, KLS Martin, Tüttlingen, Germany) was placed intra-orally at each side of the maxilla. The distraction vector was predicted using MaxilimTM (Sint-Niklaas, Belgium) software, and was transferred to the patients using stereolithographic models and individual templates. A (high) Le Fort I type osteotomy was performed. The amount of activation varied from 8 to 17,5 mm (mean, 13,1 mm \pm 2,9 SD).

Soft and hard tissue formation resulted in complete healing across the distraction gaps. The maxillary movements and new bone formation in the sagittal, horizontal, and vertical planes could be predicted and achieved. The distractors are almost completely submerged, and can be left in place as long as necessary to avoid relapse. Due to the fact that cephalometric reference points used in this study change with time in growing individuals, as well as the position of the coordinate axes, the results of linear and angular measurements after six months were judged to be unreliable. Therefore Wits' appraisal was used to measure the stability of the long-term distraction results.

Results up to five years follow-up after distraction showed considerable maxillary advancement with long-term stability. Nevertheless, ongoing growth of the facial skeleton must be considered when distraction osteogenesis is chosen in growing patients.

Introduction

A possible treatment for patients suffering from maxillary hypoplasia or midface deficiency is maxillary distraction. This can be indicated in severe Angle class III malocclusions, and severe maxillary hypoplasia among cleft patients and other craniofacial deformities. Primary cleft lip and palate repair in infancy and early childhood often results in deficient maxillary growth in sagittal direction (Yu-Faung). This can lead to a pronounced maxillary hypoplasia already at a young age (13). Conventional treatment by Le Fort I type osteotomy proved to be difficult with unstable long-term results in CLP patients. Scarring from previous operations hampers to mobilize the maxilla, and the relapse is more significant and more frequent in cleft patients compared to non-cleft patients¹³. Although there are no conclusive data on any differences in surgical relapse, velofaryngeal function and speech between cleft maxillary osteotomy and distraction, distraction osteogenesis tends to be preferred to conventional osteotomy for younger CLP patients with more severe deformities²⁴.

Attempts to treat Class III malocclusions through the use of maxillary protracting appliances and chin caps are described, with conflicting opinions about the treatment results^{8, 14}.

Maxillary distraction osteogenesis by using external device (Delaire facial mask), with dental anchorage showed significant dentoalveolar compensations¹³.

The rigid external distraction system of Polley and Figueroa (RED II, KLS Martin Tuttlingen, Germany) permits easy device application and removal, and multidirectional movement. It has shown satisfactory clinical results, and its superiority to face mask protraction⁸. However, reverse headgear and rigid external distraction apparatus are cumbersome and highly visible¹³. In external maxillary distraction, the distraction hardware is rigidly fixed to the cranium and projects in the frontofacial midline, thus limiting oronasal airway access²¹.

A low profile, intraoral distraction device, used in an experimental study by Weinzweig et al was successfully used for midface distraction at the Le Fort I level. However, the distraction cylinder protruded through the buccal mucosa and had to be delivered through a skin incision in the nasolabial fold area¹⁷.

A subcutaneous distraction device, (Zurich Maxillary Distractor, KLS Martin Tuttlingen, Germany) placed in the malar region, was clinically evaluated^{7, 19}. One distractor is installed at the left and one at the right hand side of the patient. With this type of intra-oral maxillary distractor, it was difficult to install this pair with a parallel axes to allow maximum distraction length. The distraction often resulted in a rotational more than in a gliding movement, causing loss of distraction distance at the level of occlusion⁷. Delaire masks were used up to one year as a retention device to stabilize the results^{7, 19}.

A recent study showed that the maxilla in young cleft patients can be lengthened successfully using intraoral distraction devices (Zurich Maxillary Distractor, KLS Martin Tuttlingen, Germany) with long term stability. There was less control of the vector of lengthening in relation to the extraoral devices, and a three dimensional correction could not be achieved. With this type of distractor, the distraction length is limited to maximum 15 mm²².

In our previously published animal study the potential of using a trans-sinusal distractor for the correction of maxillary hypoplasia was discussed^{11, 12}. Based on those results a novel maxillary distractor has been designed with following objectives. The device should be easy to apply, easy to activate, and guarantee predictable results. It should be submerged to minimize social hindrances, and should allow normal function during the distraction and the retention period. Correction of severe maxillary deficiency in a young age (6-8 y) should be possible, before the time the child may experience any psychosocial harm of its facial disharmony.

We have already published the early results of the clinical applicability of this new maxillary distractor, with an activating system introduced into the maxillary sinus¹¹. The aim of this study was to assess the long-term results of trans-sinusal maxillary distraction in a heterogeneous group of patients with moderate to severe midfacial hypoplasia.

Materials and methods

Patient selection

Twenty patients age 8 to 48 years with moderate to severe maxillary and midfacial hypoplasia were treated in our centre since May 2000. The observation period ended in October 2005. Only patients with a minimum follow up of 12 months were included in our study. The follow up period varied from 13 to 65 months (mean 35 months \pm 16,3 SD). The preoperative cephalometric measurements, dental relationship and soft tissue analysis, reveal the anteroposterior maxillary hypoplasia, due to, unilateral (9 patients) or bilateral cleft lip and palate (6 patients), class III malocclusion (2 patients), acromegaly (1 patient), Treacher Collins (1 patient), and Trisomy 21 (1 patient). Nine patients underwent preoperative orthodontic treatment (see Table I).

Case nr.	Sex (M/F)	Retention period	Diagnosis	Age (years)	Orthodontic treatment (yes/no)	Follow-up (months)
1	M	6	UCLP	19	Y	30
2	M	3	UCLP	21	Y	23
3	M	4	BCLP	18	Y	18
4	M	3	BCLP	22	Y	31
5	F	2.5	BCLP	9	Y	24
6	F	2.5	UCLP	10	N	20
7	F	4.5	UCLP	12	N	13
8	M	6	Trisomie 21	17	Y	29
9	M	6	BLCP	12	N	18
10	M	2	UCLP	10	N	30
11	F	6	UCLP	8	N	54
12	F	6.5	UCLP	15	Y	55
13	F	4	Treacher Collins	18	Y	19
14	M	3	BCLP	48	N	41
15	M	5	Class III	39	Y	54
16	F	3	UCLP	9	N	31
17	M	(24)	Acromegaly	31	N	30
18	F	4	Class III	14	N	60
19	M	4.5	UCLP	14	N	55
20	F	3.5	BCLP	10	N	65

Table I. Patient table with indication of age, diagnosis, sex, orthodontic treatment status and follow-up time. UCLP = Unilateral Cleft Lip and Palate; BCLP = Bilateral Cleft Lip and Palate.

Distractor design

The distraction device consisted of two parts: an upper plate, fixed cranial to the osteotomy line, which is attached to a cylinder in which screw rods are tapped. The second part consists of a distracting screw, which is attached to a plate and the activating rod by a universal joint (see Fig. 1).

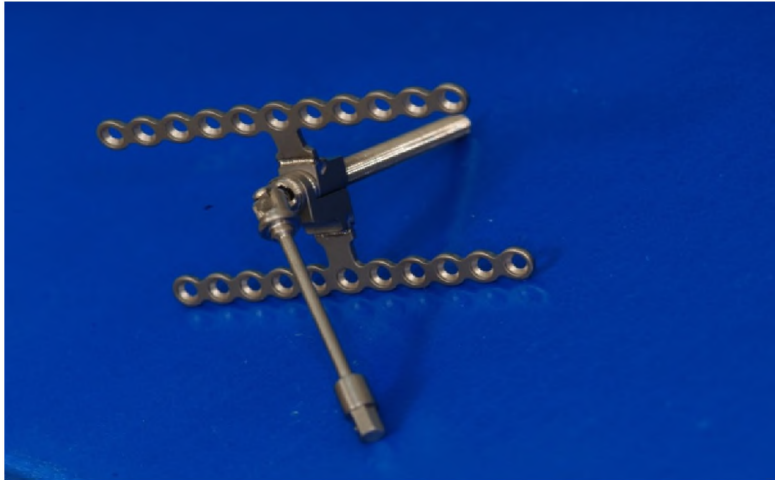


Fig. 1. The distractor consisted of two parts: an upper plate, and a lower plate holding the distraction screw. The distraction screw is place inside the maxillary sinus, while the activation arm is brought into the oral cavity.

This plate is fixed caudal to the osteotomy line. The distraction screw is placed inside the maxillary sinus, while the activation arm is brought into the oral cavity through a stab incision cranial to the Le Fort I incision. After the activation period, the intraoral part of the activation arm is cut, so that the device becomes completely submerged.

Preoperative planning

The TS-MDTM is a unidirectional device. Therefore, the determination of the desirable position of the distractor and of the distraction vector is of utmost importance. A preoperative CT-scan was obtained following the MaxilimTM CT-protocol. The imaged volume extends from 1 cm caudal to supra-orbital bar to the entire mandible (see Fig 2).

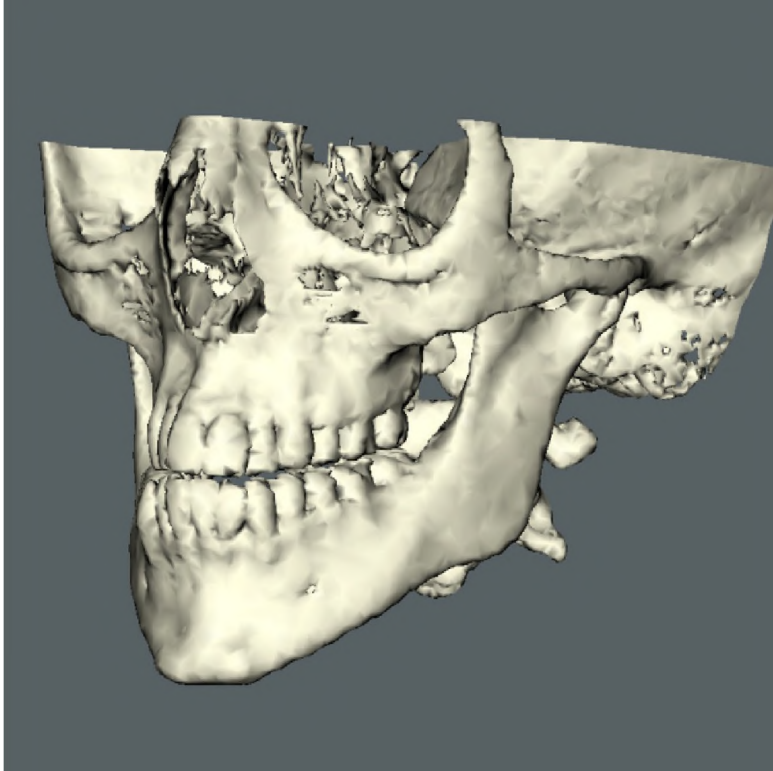


Fig. 2. This schematic picture indicates the region imaged by the CT-scanner.

The X-ray tube voltage is 120 kV and the effective tube current is 90 mAs. The pitch was set to 0.6 for multi-slice CT scanners. The axial slices were reconstructed with a slice interval of 1 mm with a bone kernel.

The CT-data were sent to Medicim on a CD-ROM for conversion to Maxilim data. During this step, surface models of the bone are constructed.

These data are loaded into Maxilim™ (Maxilim™ v1.3.0, Medicim, Sint-Niklaas, Belgium) to perform the planning. First a virtual LeFort I osteotomy is performed, and the distractor is installed (see Fig 3).

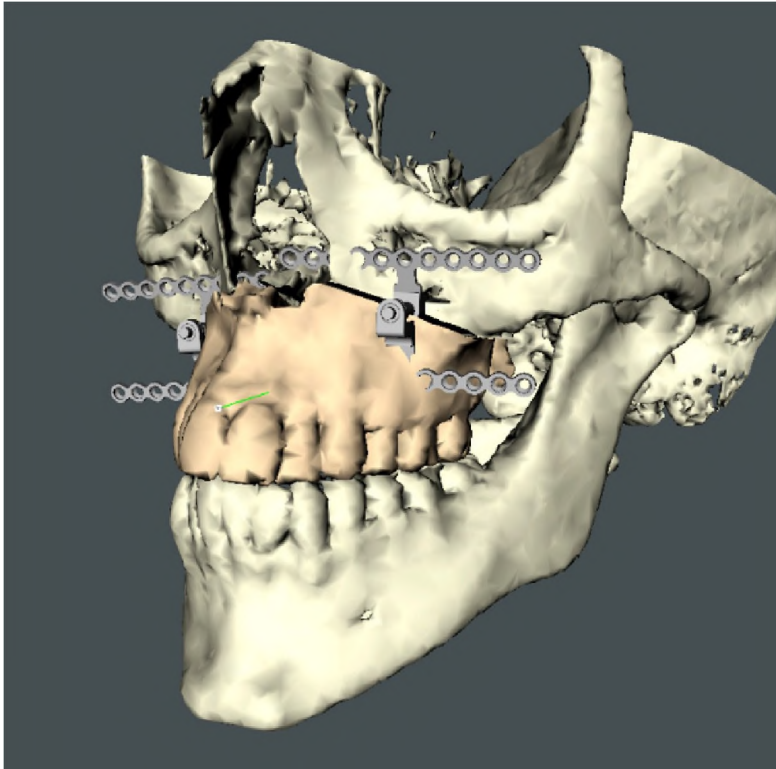


Fig. 3. The distraction is planned and simulated in Maxilim™. The distraction vector is virtually determined. The position of the distractor with respect to the sinus, and nerve is controlled.

During this procedure the vector of distraction is determined based on clinical examinations. The software guides you through the whole procedure on a step-by-step fashion. The ideal position of the distraction screw inside the maxillary sinus is then indicated. At this stage the entry point of the screw, the depth of the sinus, the position of the tooth buds and or the roots of the teeth are studied carefully. The bone movements are measured with respect to the Frankfurter plane and the mid-sagittal plane (see Fig. 4).

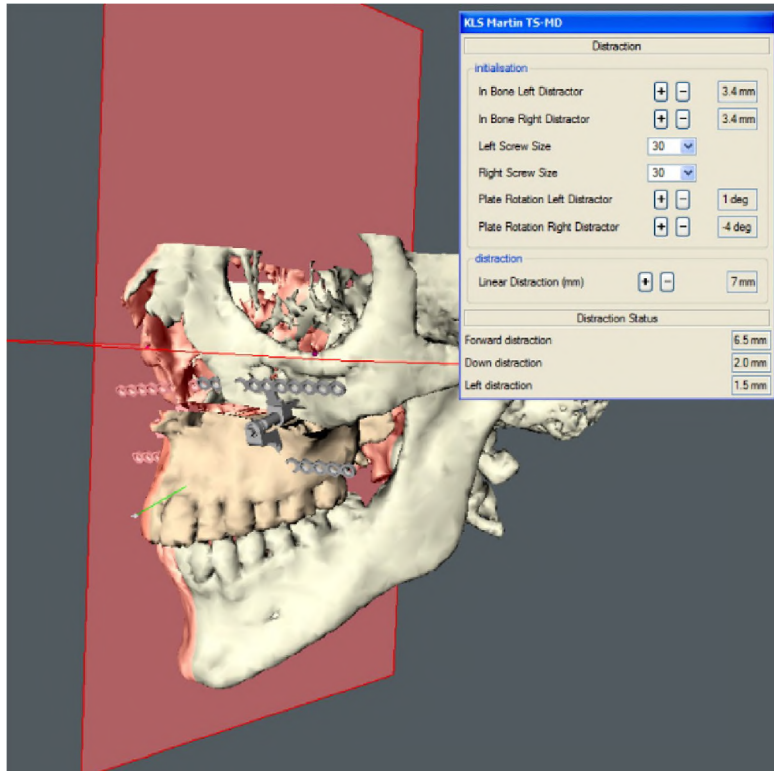


Fig. 4. The movement of the osteotomized maxilla is measurement with respect to the Frankfurter and mid-sagittal plane.

From this planning, a stereolithographic model comprising the maxillary region is fabricated. It contains a tube in the maxillary sinus into which the distraction screw fits, and shows the distraction vector.

The predicted vector is transferred to the patient by a stereolithographic model and custom-made templates (see Fig. 5.a, 5.b and 5.c).



Fig. 5.a. Distractor placed on the stereolithographic model according the predetermined vector and the plates are pre-bended.



Fig. 5.b. The position of the upper plate determines the vector of distraction.



Fig. 5.c. Template is used to determine the position of the upper plate in vivo

Surgical technique

All patients were operated under general anaesthesia. The maxilla was prepared for a (high) LeFort I type osteotomy. The maxillary template for the exact positioning of the upper plate of the TS-MD was placed on the anterior surface of the maxilla. An entry hole for the distraction screw on the anterior maxillary wall was made using a round bur. The pre-bended upper plate of TS-MD was placed and fixed (see Fig. 6).

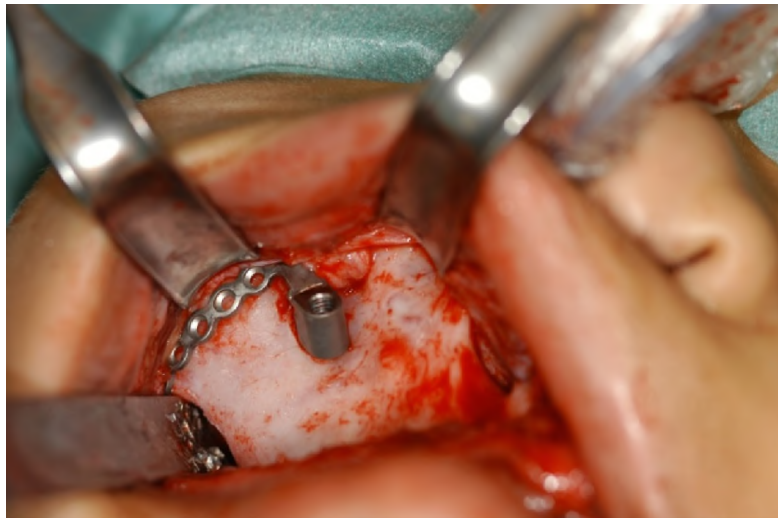


Fig. 6. Step 1 of the surgery: an entry hole for the distraction screw on the anterior maxillary wall was made using a round bur. The pre-bended upper plate of the TS-MD™ is positioned.

Then the lower plate with the distraction screw is placed and temporarily fixed with a few screws. Next, the desired osteotomy line is drawn. Then the lower plate with the distraction screw is removed. The desired osteotomy is then performed, using a

reciprocating saw. The pterygoid process is separated from the tuberosity, and the nasal septum is then separated from the maxilla.

The maxilla is then mobilized without complete down fracturing in growing patients. The lower plate together with the distraction screw is then placed and fixed. The stereolithographic model study indicated the safe positioning of the lower plate in respect to the tooth buds.

The distractors are activated bilaterally for about 4 to 5 mm to check if there is any interference (see Fig. 7).

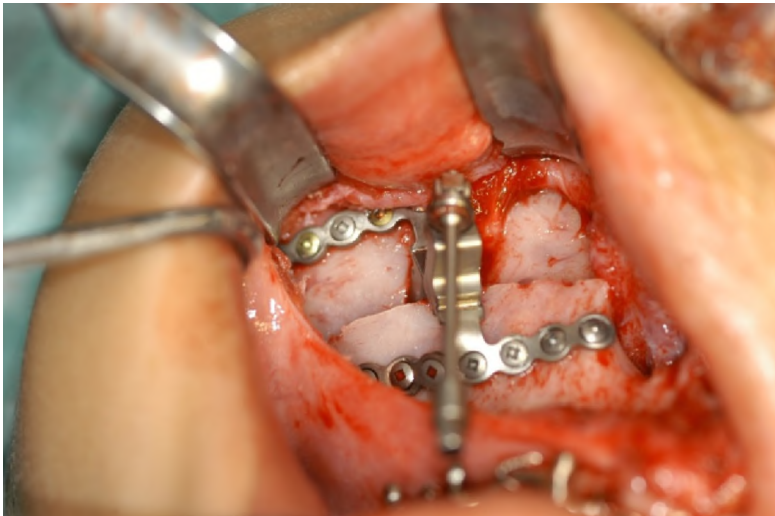


Fig. 7. The distractor is activated bilaterally for about 4 to 5 mm to check whether there is any interference or not.

Then the devices are put back to the zero position.

A stab incision cranial to the LeFort I incision at the desirable place (usually cranial to the root of the canines) is then made. The activation arm is then brought to the oral cavity through this incision.

The intra-oral wound is then closed in two layers. The only visible part of the distractor device is the activation head, which is hidden behind the upper lip. The activation started after a latency period of 5 days at a rate of 0.5 mm twice a day, till the planned correction was achieved. The activation was performed either by the patient or the parents. At the end of distraction period the intra-oral part of the devices (activation heads) were cut off under local anaesthesia. The devices were left in place till complete callus maturation was achieved. No manipulation was done after the end of distraction period, however some patients received (further) orthodontic treatment 6 weeks after activation period. The retention period varied from 2 to 6.5 months (mean 4.2 ± 1.4 SD), except one patient who was lost from follow up for two years. The distraction devices gave sufficient stabilization during the retention period. The lower parts of the distractors were removed through two

lateral incisions at the level of the same intraoral incisions. All surgical procedures were done under general anaesthesia by one surgeon (first author).

All patients received antibiotic prophylactics during the first postoperative week. Soft diet was prescribed during the activation phase and six weeks thereafter.

Cephalometric analysis

Standardised lateral cephalograms were obtained preoperatively and at well-defined time intervals (before distraction, end of distraction, six months after distraction) and for each patient at different moments in time during the further follow-up period. Five hard tissue landmarks and a coordinate axes passing through nasion (N) were defined (see Fig. 8).

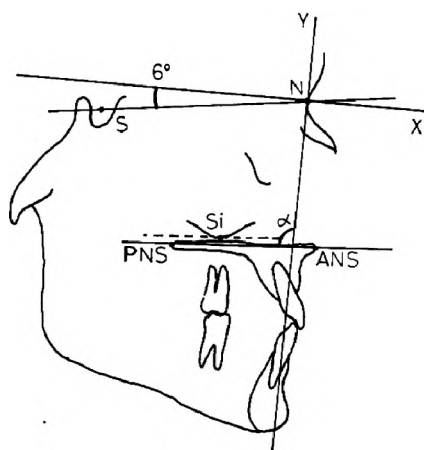


Fig. 8. For the cephalometric analysis, there andmarks are used: ANS (anterior nasal spine), N (nasion), PNS (posterior nasal spine), S (sella), Si (defined as the intersection between a parallel line to the palatal plane (ANS-PNS) and the lowest point of the maxillary sinus).

Coordinate system is defined by the X-axis constructed by drawing a line through N, rotated 6 degrees upward from the SN line, and the Y-axis as a perpendicular on the X-axis through N.

The angle α is defined as the angle between the Y-axis and the palatal plane (ANS-PNS).

Sagittal and vertical maxillary displacements, defined as sagittal and vertical movements of the posterior nasal spine (PNS), the point Si (defined as the intersection between a parallel line to the palatal plane (ANS-PNS) and the lowest point of the maxillary sinus) and the anterior nasal spine (ANS), were presented as linear measurements in millimeters on the X- and Y-axis.

Anterior and inferior movements of the examined points were indicated by positive values, and posterior and superior changes were indicated by negative values (see Table II).

Variables (n=20)		
Sagittal	Post distraction (mm)	6 M post distraction (mm)
	Mean \pm SD	Mean \pm SD
PNS – X	9.9 \pm 2.2	-0.7 \pm 0.5
Si – X	9.5 \pm 2.3	-0.1 \pm 0.6
ANS – X	9.3 \pm 2.4	-0.1 \pm 0.6
Vertical		
PNS – Y	1.4 \pm 2.5	-0.2 \pm 1.1
Si – Y	3.1 \pm 3.1	0.04 \pm 0.8
ANS – Y	4.2 \pm 4.3	-0.1 \pm 1.1

Table II. This table lists the linear maxillary changes (mm) of each cephalometric point. The column 'Post distraction' lists the differences between the preoperative cephalogram and the cephalogram acquired at the end of the distraction period, and the column (6M post distraction) the differences between the latter cephalogram and the follow-up cephalogram 6 months after distraction. Anterior and inferior movements of the examined points were indicated by positive values, and posterior and superior changes were indicated by negative values.

Changes in inclination of the palatal plane (ANS-PNS) were also observed by the angular measurement ANS-PNS / Y (α). Upward rotations were indicated by positive values; downward rotations by negative values (see Table III).

Variables (n=20)		
	Post distraction (degree)	6 M post distraction (degree)
	Mean \pm SD	Mean \pm SD
A	-4.1 \pm 4.7	0.1 \pm 1.2

Table III. This table shows the palatal plane changes ($\alpha = \text{ANS-PNS} / Y$) (degree) between the preoperative cephalogram and the cephalogram acquired at the end of the distraction period, and between the latter cephalogram and the follow-up cephalogram 6 months after distraction in the column 'Post distraction', resp. '6M post distraction'. Upward rotations were indicated by positive values, downward rotations by negative values.

Measurements on the preoperative cephalograms and on the cephalograms acquired at the end of the distraction period are compared to evaluate the distraction effect. The stability of the distraction is investigated by comparing measurements on the latter cephalograms with the measurements on the cephalograms up to 65 months after distraction.

In addition, to assess the stability, the Wit's appraisal was determined for each patient preoperatively, after distraction, 6 months after distraction and at different moments during the further follow-up period (see Fig. 9). The Wits appraisal (mm) is defined as the distance between the perpendicular projections of point A and point B on the occlusal plane on a lateral cephalogram. In a normal sagittal relationship Wit's measurement is 0 mm. In Class II relationships Wits measurement has a positive value and in Class III relationships Wits measurement has a negative value. The tracings and measurements were done by one investigator.

Results

A single surgeon (NN) performed all the surgical procedures. There were no surgical complications in any of the 20 patients. In the first treated patient (case nr. 20) the activation screwdriver fitted directly on the distraction screw. Therefore the activation had to be performed under local anesthesia. In the second treated patient (case nr. 17) a flexible activation arm (AA) was used. Distal end of the AA was hidden behind the upper lip. After 8 mm of activation the AA that apparently was not strong enough, bended, making further distraction impossible. In the subsequent prototype the AA was replaced with a rigid one. This AA was successful for all other 18 patients. Activation was either done by the patients or by their parents. All the patients could resume their daily activities within a week after distractor placement. The predicted hard tissue changes were achieved in all patients. This resulted in significant integumental changes. Forward movement of the upper lip resulted in an improved lip relationship. Changes in the nasolabial angle were satisfactory, and the nasal tip changes were desirable. Determination of the distraction vector beforehand made a

predictable final result possible in all cases. Figure 9 overviews a number of patients.

Table II shows the changes of the cephalometric measurements between the lateral preoperative cephalograms and the cephalograms at the end of the distraction period. The mean sagittal movement was for each variable positive, meaning a mean anterior movement. This anterior movement is about 10 mm.

The mean vertical movements had also positive values, indicating a downward maxillary movement. Moreover, the maxilla underwent in general a downward rotation indicated by a negative value for α (see Table III).

The changes of maxillary examination landmarks between the end of the distraction and six months after distraction are characterized by very small negative values, indicating a stable distraction effect (see Table II). Over this 6 months period, also the rotational effect was stable, as indicated by very small positive changes for α (see Table III).

The Wits' appraisal showed to be stable up to 5 years after distraction in the adult patients. The Wits' appraisal decreases again in the growing patients with longer follow up.

On the long term, the sagittal jaw relationship obtained through maxillary distraction osteogenesis showed to be stable in adults, and showed more or less CI III relapse in growing patients.

Discussion

This study is a critical evaluation of the clinical applicability of a trans-sinusal distractor^{11, 12}.

The heterogeneity by age of the patient group (between 8 and 48 years old) is suggesting that this type of distractor is useful in all age groups, when the volume of the maxillary sinus cavity allows for accommodation of the distraction screw. According to the literature the human sinus, even at the age of 6 to 8 years is deep enough to provide room for the distraction screw, and this is not significantly different in cleft patients. Harvold et al⁶ compared the maxillary sinus growth pattern in cleft palate patients with the normal population. He concluded that there was no developmental difference of the antrum of the cleft patient compared to the normal population. Duerinckx et al³ retrospectively evaluated the paranasal sinuses in 80 infants and children aged 0-17 years undergoing brain MRI. They showed that at the age of 4 years already more than two third (2/3) of the maxillary sinus was pneumatized (a measure of sinus development). There was relatively little change in the degree of pneumatization beyond the age of 11. Brånemark et al¹ showed in an experimental and clinical study that the insertion of implants where sinus or even nasal cavity penetration could not be avoided was justified. The result of their clinical

trials had shown that titanium screw penetrating the bone of sinus or nasal cavity caused no undesirable side effects during the healing, and no fistula formation. Wolf et al²⁰ concluded in their study of the sinuses in 102 pediatric skulls and cadaver heads that by the age of 8, pneumatization of the maxillary sinus has progressed considerably. The length (ventrodorsal) of the maxillary sinus ranges from 34 to 38 mm. By comparison with other types of intraoral devices, the major advantage of the TSMDTM is that the bulky part of the distractor is placed inside the maxillary sinus, so there is no interference with the periosteum, or irritation of surrounding soft tissue, or skin^{3,8}. Because of this 'low profile', it can be easily held in place as long as necessary during the retention period. This is in contrast with extraoral distraction devices or facial masks with elastic forces^{4, 5, 8, 9, 13, 19}.

Distraction was started after a latency period of five days although recent experimental findings suggest that immediate distraction could abbreviate the distraction period without adverse sequelae¹⁷.

A strict antibiotic protocol was maintained during the distraction period, because of a potential communication between the oral cavity and the maxillary sinus. No signs of infection, or fistula formation were found in any patient. This is in line with other findings concerning penetration of titanium implants or screws into the sinus cavity¹.

The skeletal anchorage of the TS-MD bypasses the dentoalveolar compensations and possible relapse of tooth borne distractor types. Orthodontic splints or bands are not needed at this point, which can be a problem in young children (mixed dentition) or in cases with inadequate dentition^{4, 5, 8, 9, 13, 15, 18, 19}. TS-MD is a valid alternative for patients who were formerly treated by conventional osteotomies and autogenous bone grafting techniques. Distraction in horizontal, vertical and sagittal planes can be achieved, only by changing the inclination of the distraction screw. This implies a preoperative vector planning. Correction of the midline can be achieved by distracting one side more than the other.

A cephalometric analysis was used as an indication for the maxillary distraction. ANS and PNS were used as skeletal landmarks to define the sagittal and vertical position of the maxilla to the coordinate axis; point A was not used for these linear measurements because of the influences of orthodontic treatment on this point. An additional maxillary reference point was defined (Si) and the results concerning the linear measurements to this point were in line with the other findings for ANS and PNS.

The Wits' appraisal was used to analyze the sagittal jaw relationship before and after distraction. This measurement is less influenced by vertical and sagittal changes, in growing individuals, especially in view of point N. Therefore Table II and III restricts to linear and angular measurements up to six months after distraction. Because of the fact that all cephalometric reference points are changing with time in growing

individuals, as well as the position of the coordinate axes, the results of linear and angular measurements after six months were judged to be unreliable.

The cephalometric data presented in this study showed predictable and stable long-term results in adults. In growing individuals ongoing growth of the facial skeleton has to be considered. These results supported the clinical findings that distraction, via an intraoral appliance is a reliable procedure and were in line with other previous studies^{16,22,23}.

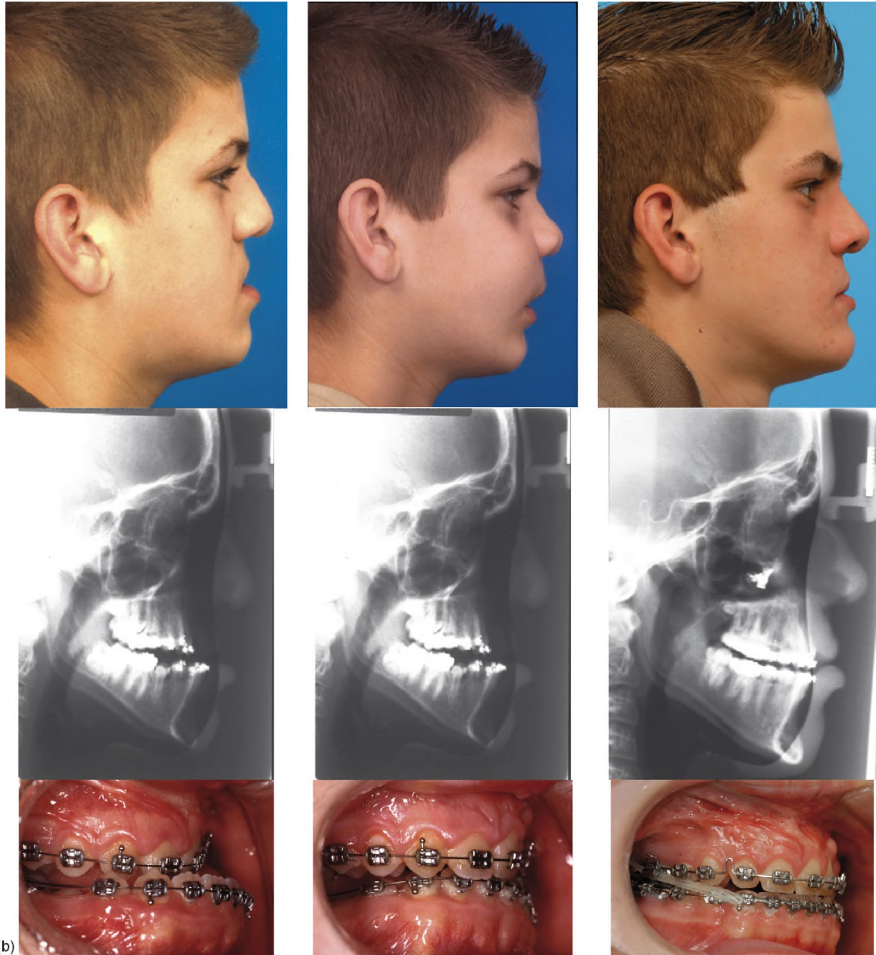
In conclusion, trans-sinusal maxillary distraction helps young children with severe midfacial hypoplasia to enter the adolescence with more or less normal facial proportions, although the distraction effect seems to relapse in growing patients. However, later orthognathic corrections might be necessary in this group of patients, the severity of the deformity has been decreased by distraction osteogenesis.

The distraction in adults showed a very stable result in the long term.

Acknowledgements. Part of this research was possible thanks to a grant for research specialization from the Flemish Institute for stimulation of the scientific-technological research in the industry (IWT) to Filip Schutyser.



Fig. 9.a. A sixteen-year old girl (patient 12) with a repaired left unilateral cleft lip and palate and moderate maxillary deficiency was treated with TS-MD. A high LeFort I osteotomy was performed. A total advancement of 8 mm, and a vertical extrusion of 2 mm were achieved. The photographs demonstrate correction of the sagittal and the vertical relationships, and harmonization of the face. A class I dental occlusion was achieved. The lateral cephalograms demonstrate optimal bimaxillary relationship, with long-term stable results (55 months).



(b)

Fig. 9.b. A fourteen-year old boy (patient 19) with a repaired left unilateral cleft lip and palate and severe maxillary deficiency with anterior open bite was treated with TS-MD™. A high LeFort I osteotomy was performed. The sagittal and vertical relationships were corrected. The anterior open bite was corrected by the clockwise rotation of the maxilla. Clinical photographs demonstrate a class I dental relationship, and the harmonization of the face. After 17 mm of activation a total advancement of 10 mm, and a vertical extrusion of 6 mm at the level of the central incisors were achieved. Long-term follow-up (55 months) showed stable results. The mandibular asymmetry was corrected.

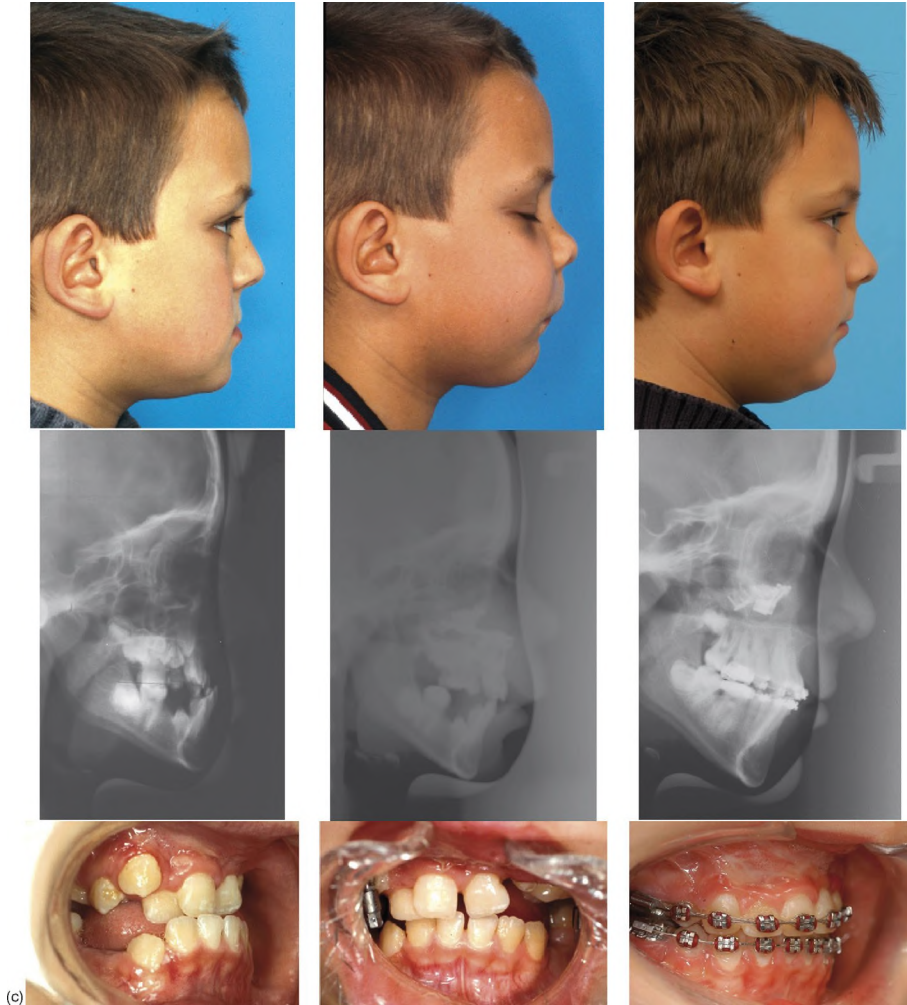


Fig 9.c. A ten-year old boy (patient 10) with a repaired left unilateral cleft lip and palate and moderate maxillary deficiency was treated with TS-MD. A high LeFort I osteotomy was performed. After 10 mm activation a total advancement of 8 mm, and a vertical extrusion of 2 mm was achieved. The photographs demonstrate correction of the sagittal and the vertical relationships, and harmonization of the face. A class I dental occlusion was achieved, and maintained after 30 months of follow up.



Fig 9.d. A thirteen-year old girl (patient 18) with a class III malocclusion and an anterior open bite is presented. There is also a shifted maxillary midline. A high LeFort I osteotomy was performed. Bilateral TS-MDs were placed. The vectors of distraction were parallel, but oriented to the right in order to correct the maxillary midline shift. A genioplasty was performed at the same time. The TS-MD™ was activated for 16 mm. This resulted in 10 mm advancement, 7 mm vertical extrusion at the level of central incisors, and a shift of 5 mm of the maxillary midline to the right. Clinical slides show correction of midfacial deficiency as well as inter arch asymmetry. The lateral cephalograms demonstrate the closure of the open bite and optimal bimaxillary relationship. The cephalometric analysis after 60 months shows a relapse of class III malocclusion, due to excessive mandibular growth. The patient has no functional nor aesthetic problem and wishes no orthognatic correction at this time.

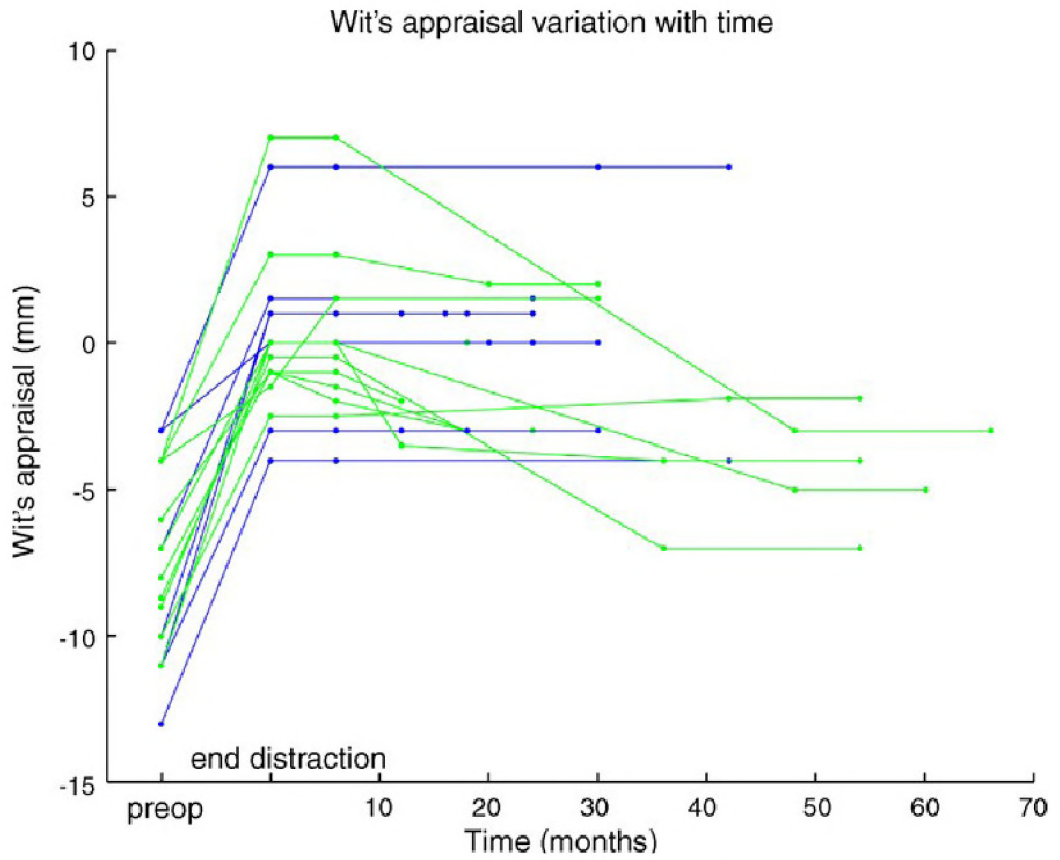


Fig. 10. The Wit's appraisal is given for each patient at different time intervals: before the distraction (pre), at the end of the distraction period (post), and respectively 6, 12, 14, ... months after distraction. Three patients, indicated with red lines, show a decreasing Wit's appraisal essentially due to excessive mandibular growth.

References

1. Brånemark PI, Adell R, Albreksson T, Lekholm U, Lindstrom J, Rockler B. An experimental and clinical study of osseointegrated implants penetrating the nasal cavity and maxillary sinus. *J Oral Maxillofac Surg* 1984; 42: 497-505
2. Cohen SR. Craniofacial distraction with a modular internal distraction system: evolution of design and surgical techniques. *Plast Reconstr Surg* 1999; 103: 1592-1607
3. Duerinckx AJ, Hall TR, Whyte AM, Lufkin R, Kangaroo H. Paranasal sinuses in pediatric patients by MRI: normal development and preliminary findings in disease. *Eur J Radiol* 1991 Sep-Oct;13(2): 107-112
4. Figueroa AA, Polley JW. Management of severe cleft maxillary deficiency with distraction osteogenesis : procedure and results. *Am J Orthod Dentofacial Orthop* 1999; 115: 1-12
5. Harada K, Baba Y, Ohyama K, Enomoto S. Maxillary distraction osteogenesis for cleft lip and palate children using an external, adjustable, rigid distraction device: a report of 2 cases. *J Oral Maxillofac Surg* 2001; 59: 1492-1496
6. Harvold E. Cleft lip and palate. Morphologic studies of the facial skeleton. *Am J Orthod* 1954; 40: 493
7. Kessler P, Wiltfang J, Schultze-Mosgau S, Hirschfeld U, Neukam FW. Distraction osteogenesis of the maxilla and midface using a subcutaneous device: report of four cases. *Br J Oral Maxillofac Surg* 2001; 39: 13-21
8. Krimmel M, Cornelius CP, Roser M, Bacher M, Reinert S. External distraction of the maxilla in patients with craniofacial dysplasia. *J Craniofac Surg* 2001; 12: 458-463
9. Molina F, Ortiz Monasterio F, De La Paz Aguilar M, Barrera J. Maxillary distraction: aesthetic and functional benefits in cleft lip-palate and prognathic patients during mixed dentition. *Plast Reconstr Surg* 1998; 101: 951-963
10. Nadjmi N, Prédicibilité de la distraction du maxillaire supérieur avec distracteur trans-sinusien. *Rev Stomatol Chir Maxillofac*. 2004; 105: 9-12
11. Nadjmi N, Van Erum R, Schoenaers J, Schepers E. Maxillary distraction using a trans-sinusual distractor: technical note. *Int J Oral Maxillofac Surg* 2003; 31: 553-559

12. Stalmans K, Van Erum R, Verdonck A, Nadjmi N, Schepers E, Schoenaers J, Carels C. Cephalometric evaluation of maxillary advancement with an internal distractor in an adult boxer dog. *Orthod Craniofac Res* 2003; 6: 104-111
13. Swennen G, Colle F, De May A, Malevez C. Maxillary distraction in cleft lip palate patients: a review of six cases. *J Craniofac Surg* 1999; 10: 117-122
14. Swennen G, Figureoa AA, Schierle H, Polley JW, Malevez C. Maxillary distraction osteogenesis: a two-dimensional mathematical model. *J Craniofac Surg* 2000; 11: 312-317
15. Swennen G, Schliephake H, Dempf R, Schierle H, Malevez C. Craniofacial distraction osteogenesis: a review of the literature: Part 1: clinical studies. *Int J Oral Maxillofac Surg* 2001; 30: 89-103
16. Trahar M, Sheffield R, Kawamoto H, Lee HF, Ting K. Cephalometric evaluation of the craniofacial complex in patients treated with an intraoral distraction osteogenesis device: a preliminary report. *Am J Orthod Dentofacial Orthop* 2003; 124: 639-650
17. Weinzweig J, Baker SB, Mackay GJ, Whitaker LA, Barlett SP. Immediate versus delayed midface distraction in a primate model using a new intraoral internal device. *Plast Reconstr Surg* 2002; 15: 1600-1610
18. Wen-Ching KO E, Figueroa AA, Polley JW. Soft tissue profile changes after maxillary advancement with distraction osteogenesis by use of a rigid external distraction device: a 1-year follow-up. *J Oral Maxillofac Surg* 2000; 58: 959-969
19. Wiltfang J, Hirschfelder U, Neukam FW, Kessler P. Long-term results of distraction osteogenesis of the maxilla and midface. *Br J Oral Maxillofac Surg* 2002; 40: 473-479
20. Wolf G, Anderhuber W, Kuhn F. Development of the paranasal sinuses in children: implication for paranasal surgery. *Ann Otol Rhino Laryngol* 1993; 102: 705 – 711
21. Wong GB, Nargozian C, Padwa BL. Anesthetic concerns of external maxillary distraction osteogenesis. *J Craniofac Surg* 2004 ; 15: 78-81
22. Rachmiel A, Aizenbud D, Peled M. Long-term results in maxillary deficiency using devices. *Int J Oral Maxillofac Surg* 2005; 34: 473–479

23. Krimmel M, Cornelius CP, Bacher M, Gulicher D, Reinert S. Longitudinal cephalometric analysis after maxillary distraction osteogenesis. *J Craniofac Surg* 2005; 16: 683-688
24. Cheung LK, Chua HD. A meta-analysis of cleft maxillary osteotomy and distraction osteogenesis. *Int J Oral Maxillofac Surg* 2006; 35: 14-24

CHAPTER 6

Predicting Soft Tissue Deformations for a Maxillofacial Surgery Planning System: from Computational Strategies to a Complete Clinical Validation.

W. Mollemans¹, F. Schutyser¹, N. Nadjmi², F. Maes¹, P. Suetens¹

1 Medical Image Computing (Radiology - ESAT/PSI)

Faculties of Medicine and Engineering,

University Hospital Gasthuisberg, Herestraat 49, B-3000 Leuven,
Belgium

2 Eeuwfeestkliniek, Harmoniestraat 68, B-2018 Antwerpen, Belgium

Medical Image Analysis 2007: 11: 282-301

Abstract

In the field of maxillofacial surgery there is a huge demand from surgeons to be able to pre-operatively predict the new facial outlook after surgery. Besides the big interests for the surgeon during planning, it is also an essential tool to improve the communication between surgeon and patient. In this work we compare the usage of four different computational strategies to predict this new facial outlook. These four strategies are: a linear Finite Element Model (FEM), a nonlinear Finite Element Model (NFEM), a Mass Spring Model (MSM) and a novel Mass Tensor Model (MTM). For true validation of these four models we acquired a data set of 10 patients who underwent maxillofacial surgery, including pre-operative and post-operative CT data. For all patient data we compared quantitatively the predicted facial outlook, obtained with one of the four computational models, with post-operative image data. During this quantitative validation distance measurements between corresponding points of the predicted and the actual post-operative facial skin surface, are quantified and visualised in 3D. Our results show that the MTM and linear FEM predictions achieve highest accuracy. For these models the average median distance measures only 0.60 mm and even the average 90% percentile stays bellow 1.5 mm . Furthermore, the MTM turned out to be the fastest model, with an average simulation time of only 10 seconds. Besides this quantitative validation, a qualitative validation study was carried out by 8 maxillofacial surgeons, who scored the visualised predicted facial appearance by means of pre-defined statements. This study confirmed the positive results of the quantitative study, so we can conclude that fast and accurate predictions of the post-operative facial outcome are possible. Therefore the usage of a maxillofacial soft tissue prediction system is relevant and suitable for daily clinical practice.

Keywords: Maxillofacial Surgery, Soft Tissue Simulation, Therapy planning, Mass Tensor Model

1 Introduction

1.1 Background

Maxillofacial surgery treats abnormalities of the skeleton of the head. Skull remodelling implies osteotomies, bone fragment repositioning, restoration of bone defects and inserting implants. Since the human face plays a key role in interpersonal relationships, people are very sensitive to changes to their outlook. Even very subtle malformations of facial proportions can strongly affect the appearance of a face¹⁶. Therefore planning of the operation and reliable prediction of the facial changes are very important in view of a better preparation, improved surgical outcome and shorter operation time.

Traditional computer-aided maxillofacial planning systems starts from 2D lateral X-rays. In these planning environments the surgeon can define an appropriate osteotomy line and derive the necessary displacement of each bone segment. Besides this bone-related planning, most commercial 2D cephalometric planning systems nowadays allow to analyse the facial profile of the patient and to do some sort of video overlaying^{40,12}. As such it becomes possible to give a first impression of the patient's expected post-operative outlook. Notwithstanding the better preparation of the surgeon and improved communication between surgeon and patient thanks to these 2D planning systems, these systems can not define the full 3D transformation of the bone parts. Especially for patients suffering from dysmorphism both in the coronal and sagittal planes, these 2D systems which rely on only 2D lateral images are insufficient. Moreover they demand from the surgeon good mental work and when communicating with the patient, they are limited to only lateral views of the patient's expected post-operative appearance.

Since the introduction of computed tomography in 1972 it became possible to acquire true 3D anatomical information for every patient. The development of 3D visualisation techniques in the late eighties, like the marching cubes algorithm²⁶, pushed the development of applications that used computer generated anatomical models. Soon the first craniofacial planning systems were born⁴. These first 3D computer aided planning systems made it possible to inspect the patient's skull and perform simple osteotomies in a 3D simulation environment. More advanced planning systems that allow complete manipulation of bone parts, were developed in the late nineties^{15,49}. In 2000 Schutyser *et al.*³⁸ reported on a 3D image-based planning system which includes osteotomy simulation with user-defined cutting trajectories, virtual distraction employing specific biomechanical models and evaluation tools based on a cephalometric reference frame. According to the surgeon's findings, different choices could be virtually redone in this environment in order to optimise the therapy. However, because of the high impact of maxillofacial therapy on the patient's face, not only this bone-related pre-operative planning of the surgery, but also the prediction of the deformation of the soft tissues became highly desirable.

1.2 3D Soft tissue modelling: State of the art

The idea of predicting the new patient's facial outlook with a computer aided maxillofacial planning system, was originally introduced by Vannier⁴⁴. At that moment, especially the computer animation world was expertised in facial modelling. Most of these facial modellers represented the face as a collection of regularly assembled mass-spring entities and were mainly focused on real-time output and realistic graphical behaviour^{41,25}.

The first maxillofacial soft tissue prediction systems, were strongly inspired by these computer graphics facial modellers. Koch *et al.*²⁴ presented a non linear finite-element approach to simulate the new facial outlook which provides a C^1 -continuous finite element surface. Linear springs were used to connect the facial surface with the underlying bone structures. He applied virtual maxillofacial interventions on the Visible Human Data Set¹ and qualitatively validated the new predicted facial outlook by visual inspection. Afterwards Keeve²² compared the two most popular soft tissue models for maxillofacial surgery, namely the mass spring model, that originated from the computer animation world and the finite element model, that was assumed to be a more biomechanical relevant model. His comparison was based on a qualitative visual inspection of the predicted facial outlooks calculated with each model. He concluded that although the mass spring model could never be biomechanically correct, the speed and the easy architecture of this model could be a serious advantage over the more accurate but computationally intensive finite element model. At the same moment Sarti³⁶ presented a volumetric finite element model applied on a cubic grid that coincide with the voxel grid of the CT data. This voxel-based modelling is advantageous from an image processing point of view (the data remain available on a voxel grid), but demands a large number of finite elements which is memory expensive. He implemented his model on a super computer and achieved good simulation results.

Despite these good results, it became clear that planning systems running on special designed computers, would never be accepted in daily clinical practice. Moreover, as already suggested for 2D soft tissue profile planning systems^{40,12}, it is important to also incorporate the changes in facial outlook during planning. The bone-related planning should be adjusted in function of the new predicted facial outlook which implies that the soft tissue prediction step needs to become part of the complete treatment planning. Therefore it is necessary that predictions are calculated in a fast and accurate way. A new goal, in the search of a good computer aided maxillofacial planning system, became the speed in which the new facial outlook could be calculated.

Also in other research fields, researchers tried to simulate accurately the deformation behaviour of soft tissues and tried to find a golden mean between accuracy and speed. Especially for surgical simulators used for training, where real-time simulations have to be performed, this trade-off became very clear. In this

research area a couple of novel computational strategies were presented^{3,11,32} in order to tackle this trade-off. More recent maxillofacial soft tissue planning systems were strongly inspired by these novel models.

Zachow⁴⁷ presented in 2000 a tetrahedral volumetric FEM model. These tetrahedral elements, which have less degrees of freedom than the prismatic elements that were often used before, are assumed to be better suited for simulation of the deformation of biological objects. By making a trade-off between the number of elements and the accuracy of the model, he was able to compute the new facial outlook of a real patient in less than 5 minutes. He noted that thanks to these short calculation times his model became appropriate for use in daily clinical practice. Two years later Teschner *et al.*^{42,28} reported on a multi-layer non-linear mass spring model. In his work he introduced the combination of using a mass spring model with a static constraint to calculate the soft tissue deformations. Until then mass spring models were typically combined with a time-integration scheme of the Newtonian motion equation to find the deformation of the soft tissues. Teschner suggested that only the deformation of the tissues were important and not the animation from the original position to the new deformed position. Consequently he proposed the use of an iterative scheme to directly find this new deformed position. By doing so and by lowering the number of mass points, he could reduce the simulation time of his mass spring model to less than 20 seconds. He used the planning system to predict the new facial outlook of one real patient and compared qualitatively the prediction result and the real post-operative facial outlook. Other important work for the field of maxillofacial soft tissue prediction systems was realised by Chabanas⁵. He was one of the first to present a complete maxillofacial planning system that incorporated the bone-related planning and the prediction of the new facial outlook. To overcome the difficult meshing step, he used a generic model that was elastically registered with patient specific data. A Finite Element solution was used to simulate the soft tissue deformation. The generic mesh contained 2284 mesh nodes and also muscle specific structures were incorporated in the mesh. This enabled not only prediction of the new facial outlook, but also simulation of the post-operative facial functional behaviour. This functional simulation of the facial expressions after surgery was introduced by Gladilin¹⁹ at the same moment.

More and more it became clear that before a maxillofacial soft tissue prediction system can be used in clinical practice, not only a qualitative validation of the predicted facial outlook is necessary, but also a real quantitative validation is required. Schutyser *et al.*³⁸ noted as first that this quantitative validation should be a numerical comparison between the predicted and real post-operative facial skin surface. After first registering the predicted and actual post-operative facial skin surface based on an unaltered subspace, he quantified distances between both surfaces in 3D. Later the relevance of this idea was confirmed by Chabanas⁶. In this work he quantitatively validated soft tissue predictions for three patients by measuring distances between the predicted facial surface and the real post-

operative outcome. More recently Zachow *et al.*^{48,46} reported on a quantitative validation for one relevant patient. He compared simulation results for different model parameters and concluded that a mean prediction error of 1 to 1.5 *mm* could be achieved with his model.

In previous work³¹ we presented a Tetrahedral Mass Spring Model (MSM) to simulate based on a bone-related planning, the new facial appearance after a maxillofacial procedure. A tetrahedral model build up was chosen to facilitate the meshing step compared to the multi-layered based models^{24,42} in which the meshing step, based on the approach of Waters⁴⁵, is typically rather tedious and error-prone. Our MSM directly calculates the new facial outlook by solving static force constraint, as introduced by Teschner⁴². A major advantage of this model is the combination of a large number of elements, for a better accuracy, and a fast simulation time. We quantitatively validated our MSM by measuring distances between predicted and post-operative facial surface for three patients and concluded that pretty good results could be achieved with this model³⁰. Nevertheless the usage of such a Tetrahedral MSM and MSM more generally, have some serious disadvantages, as discussed in^{34,29}. The most important drawback is that the MSM has no real bio-mechanical foundation.

1.3 Paper outline

This work mainly includes two parts. In the first part we present four different computational strategies used to model the deformation behaviour of facial soft tissues for a maxillofacial planning system: a linear Finite Element Model (FEM), a non-linear FEM, a MSM and a Mass Tensor Model (MTM) [10]. This last model, MTM, was introduced by Cotin *et al.*¹⁰. Two extensions to the original model are introduced in order to adapt it for our specific application. The MTM has the easy architecture of the MSM but keeps the bio-mechanical relevance of FEM, moreover as shown it beats both other linear models in computation time.

In the second part of this text we present a complete true validation work flow, including a quantitative and qualitative validation. Therefore, we acquired a data set of ten patients containing for each patient pre-operative and post-operative CT data. After first introducing the qualitative and quantitative validation methods, results for each of the four computational strategies are presented and discussed.

Our results show that the MTM achieves the same accuracy as the linear FEM, but clearly beats MSM and the linear FEM in simulation time. No significant improvement of the simulation accuracy was found, when using the non-linear FEM. The validation study denotes moreover an acceptable error of the predictions for the MTM and linear FEM when quantitatively measuring distances between the predicted and real post-operative facial outlook. These positive results were confirmed by the qualitative validation study, so that we are able to conclude that maxillofacial soft tissue prediction systems can be used in daily clinical practice.

2 Computational strategies for soft tissue modelling

Simulation of the deformation of the facial soft tissues due to bone movement, demands a mathematical model that is able to imitate the behaviour of the facial tissues. All approaches that have been proposed for this simulation, can be categorised in two main model types: Finite Element Models (FEM) and Mass Spring Models (MSM). Both methods have been investigated in our group in the past^{38,31}. In this section we briefly summarize these two models and highlight the main benefits and disadvantages of both methods. Next we introduce the Mass Tensor Model (MTM), as some sort of golden mean between both methods. Since one of the benefits of this MTM, compared to linear FEM or MSM, is the fast calculation time, we discuss this topic in more detail in the last part of this section.

2.1 Finite Element Model

To model the deformation behaviour of living soft tissues, we start from the mechanical equilibrium equations:

$$\begin{aligned}\frac{\partial \sigma_{xx}}{\partial x} + \frac{\partial \tau_{xy}}{\partial y} + \frac{\partial \tau_{xz}}{\partial z} + F_x &= 0 \\ \frac{\partial \tau_{xy}}{\partial x} + \frac{\partial \sigma_{yy}}{\partial y} + \frac{\partial \tau_{yz}}{\partial z} + F_y &= 0 \\ \frac{\partial \tau_{xz}}{\partial x} + \frac{\partial \tau_{yz}}{\partial y} + \frac{\partial \sigma_{zz}}{\partial z} + F_z &= 0\end{aligned}\tag{1}$$

with σ_{xx} , σ_{yy} , σ_{zz} , τ_{xy} , τ_{xz} and τ_{yz} the stress components and $\mathbf{F}(F_x, F_y, F_z)$ the volume forces. The material properties¹⁷ are introduced into these equations through the constitutive equations relating stresses and strains. Following the approach of³⁸ the soft tissue can be modelled as a homogeneous, linear and elastic material, such that we can use Hooke's law:

$$\begin{bmatrix} \sigma_{xx} \\ \sigma_{yy} \\ \sigma_{zz} \\ \tau_{xy} \\ \tau_{yz} \\ \tau_{zx} \end{bmatrix} = \frac{E}{(1+\nu)(1-2\nu)} \begin{bmatrix} 1-\nu & \nu & \nu & 0 & 0 & 0 \\ \nu & 1-\nu & \nu & 0 & 0 & 0 \\ \nu & \nu & 1-\nu & 0 & 0 & 0 \\ 0 & 0 & 0 & \frac{1-2\nu}{2} & 0 & 0 \\ 0 & 0 & 0 & 0 & \frac{1-2\nu}{2} & 0 \\ 0 & 0 & 0 & 0 & 0 & \frac{1-2\nu}{2} \end{bmatrix} \begin{bmatrix} \varepsilon_{xx} \\ \varepsilon_{yy} \\ \varepsilon_{zz} \\ \gamma_{xy} \\ \gamma_{yz} \\ \gamma_{zx} \end{bmatrix}$$

$$\Leftrightarrow \boldsymbol{\sigma} = \mathbf{D}\boldsymbol{\varepsilon} \quad (2)$$

with strain components ε_{xx} , ε_{yy} , ε_{zz} , γ_{xy} , γ_{xz} , γ_{yz} , Young's modulus E and Poisson coefficient ν . If we define $\{\mathbf{X}\}$ as the initial configuration at time t_0 and $\mathbf{x} = \mathbf{x}(\mathbf{X}, t)$ as the description of the point \mathbf{X} at time t , the displacement vector \mathbf{u} can be defined as $\mathbf{x} = \mathbf{X} + \mathbf{u}$. The Green-Lagrange strain tensor relates the strains $\boldsymbol{\varepsilon}$ to the displacement vector \mathbf{u} : $\boldsymbol{\varepsilon} = \frac{1}{2}(\nabla\mathbf{u} + \nabla\mathbf{u}^T + \nabla\mathbf{u}^T\nabla\mathbf{u})$. When assuming that displacements are relatively small the last term of this tensor can be neglected resulting in the linearised Green-Lagrange strain tensor: $\boldsymbol{\varepsilon} = \frac{1}{2}(\nabla\mathbf{u} + \nabla\mathbf{u}^T)$. In a large deformation setup, the full Green Lagrange tensor will be solved.

These equations are discretized using a 3D finite element method, resulting in a linear FEM when the linearised Green Lagrange tensor is solved or a non-linear FEM when solving the complete tensor. The continuum is modelled as a tetrahedral mesh. For the interpolation between the mesh nodes we use a basic linear, C_0 continuous shape function using 4 nodes for each tetrahedron⁵⁰.

For the linear FEM, the partial differential equations are reduced to a set of linear equations for the vertices of the tetrahedron mesh: $\mathbf{KU} = \mathbf{R}$ with \mathbf{K} the global stiffness matrix for the entire model and \mathbf{U} and \mathbf{R} the displacement and elastic force acting in each mesh node respectively. By defining a fixed displacement for a set of mesh nodes and demanding that in rest the total force in all other mesh nodes should be zero, the displacement of all mesh nodes can be found by solving the linear equations $\mathbf{KU} = \mathbf{R}$. To solve the finite element equations in a fast way we use a Jacobi preconditioned Krylov subspace method, namely GMRES (general minimum residual)³⁵.

For the nonlinear FEM, we use a commercial finite element analysis software package named CalculiX CrunchiX¹⁴, which is available under the terms of the GNU General Public License. The non-linear equations were solved iteratively using an Incomplete Cholesky preconditioning²³.

FEM is a general discretization procedure of continuum problems posed by mathematically defined statements. As a consequence this model has a very strong biomechanical relevance and is expected to be a very accurate model when simulating deformations of living tissues. These two properties make FEM an excellent choice from an accuracy point of view. Nonetheless it is known that FEM has a high computational cost and large memory usage, which could result in rather long simulation times and may hamper application of this approach in daily clinical practice as already argued in the introduction. FEM extensions based on pre-computing the matrix system, have been presented in order to improve the online simulation time¹¹. These extensions demand however a rather long pre-computation step.

2.2 Tetrahedral Mass Spring Model

A mass spring model assumes a discretization of the deformable object into n mass points and a set of m connections between each of these n mass points. For this we start from a tetrahedral discretization and assign to each mesh node a mass point and define a linear spring for each mesh edge. These linear springs follow Hooke's law:

$$F_s = k_s \Delta L \quad (3)$$

with F_s the magnitude of the elastic force working in the end points of the linear spring, k_s the linear spring constant and ΔL the difference between the rest length and the actual length of the spring.

In our model we distinguish two types of points: join points and free points (see also section 3.3). During simulation a well known displacement is applied to each of the join points, while the displacement of each free point is found by demanding that the total internal force \mathbf{F}_i^{int} in each free point should be zero when the deformable model is in rest. The total internal force \mathbf{F}_i^{int} of a free mass point i is given by:

$$\mathbf{F}_i^{int} = \sum_{\forall \mathbf{p}_j \in \mathcal{S}_i} k_j (\|\mathbf{p}_j - \mathbf{p}_i\| - L_j^0) \frac{\mathbf{p}_j - \mathbf{p}_i}{\|\mathbf{p}_j - \mathbf{p}_i\|} \quad (4)$$

with S_i denoting the set of springs connected to mass point i , \mathbf{p}_f the 3D coordinates of point f , and L_j^0 and k_j the rest length and spring constant of spring j , respectively.

Demanding that the total internal force in each free point should be zero, is solved as an iterative minimisation problem with a steepest-gradient solution scheme. To reduce the calculation time a dynamic cut-out was implemented. In each iteration step there are a lot of points in which the resulting force is very small. Moreover forces working in point i at the start of iteration j can only have been changed in comparison to the previous iteration step when point i or a neighbouring point has been moved during iteration $j-1$. Consequently only points with an internal force larger than some threshold value should be considered in each iteration step and secondly, only points which are neighbours of a point that has been moved in the previous iteration, have to be evaluated in the next step.

Since we want to model the behaviour of facial soft tissues, we have to choose an appropriate value for the spring constants in order to meet the correct stress-strain relationship. Van Gelder¹⁸ suggested a formula to compute the spring stiffnesses for a 3D tetrahedral mesh that is closest to an elastic continuous representation. Let E be the material's Young's Modulus, then the spring constant of spring i is given by,

$$k_i = \frac{E_i \sum_{\forall j \in \Omega_i} V_j}{(L_i^0)^2} \quad (5)$$

with Ω_i the collection of all tetrahedra containing spring i , V_j the volume of tetrahedron j and L_i^0 the rest length of spring i .

MSM finds its origin in the computer animation world^{22,42}. The very easy architecture and low memory usage make this model very attractive for fast simulators. However our Tetrahedral MSM and MSM more generally have also some important disadvantages. Three important disadvantages are distinguished:

1. In the Tetrahedral MSM an object is described into discrete mass points which are connected to each other by springs. A change of length of a spring induces a force in the direction of the spring. However since no volume behaviour of the tetrahedron is incorporated, this may cause a possible 'flip over' of a spring³⁴.
2. The value of the spring constant determines the elastic behaviour of the MSM. As shown in² there should be some kind of topology dependent

mapping of Young's Modulus to these spring constants. Although some suggestions are proposed how this can be done^{2,18}, the calculated value for the spring constant is only an approximation and has no true biomechanical relevance.

3. In a MSM there is no way to really control the volume conservation during simulation, even when the model is extended with extra 'volume springs', as described in³¹.

2.3 Mass Tensor Model

The fourth model introduced in this section, is a novel Mass Tensor Model (MTM) which can be seen as a mixture of FEM and MSM. On the one hand the model preserves the easy architecture of the MSM and on the other hand the model has the bio-mechanical relevance of FEM.

2.3.1 The original model

The original MTM was introduced by Cotin^{10,39}. In the MTM the modelled object is discretized into a tetrahedral mesh. Inside every tetrahedron T_i , the displacement field is defined by a linear interpolation of the displacement vectors of the four vertices of T_i , as defined by the finite element theory. The linear elastic energy of tetrahedron T_i can be expressed as a function of the displacements of the four vertices and of the two Lamé coefficients. These coefficients λ and μ are biomechanical elastic constants and directly proportional to the well known material dependent Young's Modulus E and Poisson coefficient ν , by the formula:

$$\lambda = \frac{\nu E}{(1+\nu)(1-2\nu)} \quad (6)$$

$$\mu = \frac{E}{2(1+\nu)} \quad (7)$$

The force applied at vertex j of tetrahedron T_i is defined as the derivative of the elastic energy of T_i .

$$\mathbf{F}_j^{T_i} = -\frac{\partial W_{elastic}(T_i)}{\partial \mathbf{p}_j} = \sum_{k=0}^3 [\mathbf{K}_{jk}^{T_i}] \mathbf{u}_{T_i(k)} \quad (8)$$

with \mathbf{p}_j the 3D coordinates of vertex j , $\mathbf{u}_{T_i(k)}$ the displacement of vertex k of tetrahedron T_i and $\mathbf{K}_{jk}^{T_i}$ the stiffness tensors for this tetrahedron. These tensors are completely determined by the initial position of each vertex of the tetrahedron and the Lamé coefficients, which are material specific. For details we refer to¹⁰.

For the whole mesh, the total elastic force \mathbf{F}_j at a vertex j is now simply the sum of the contributions of all tetrahedra containing this vertex j .

$$\mathbf{F}_j = \sum_{\forall T_i \in \Lambda_j} \mathbf{F}_j^{T_i} = \sum_{\forall T_i \in \Lambda_j} \sum_{k=0}^3 [\mathbf{K}_{jk}^{T_i}] \mathbf{u}_{T_i(k)} \quad (9)$$

with Λ_j the collection of all tetrahedra adjacent to vertex j . This expression can be rewritten into the following simple form:

$$\mathbf{F}_j = [\mathbf{K}_{jj}] \mathbf{u}_j + \sum_{\forall k \in \Psi_j} [\mathbf{K}_{jk}] \mathbf{u}_k$$

$$\text{with } [\mathbf{K}_{jj}] = \sum_{\forall T_i \in \Lambda_j} [\mathbf{K}_{jj}^{T_i}] \text{ and } [\mathbf{K}_{jk}] = \sum_{\forall T_i \in \Lambda_j} [\mathbf{K}_{jk}^{T_i}] \quad (10)$$

with Ψ_j the collection of all mass points neighbouring to mass point j . This MTM results in an easy implementation with mass points and model tetrahedra and a straightforward way to evaluate the force in each mass point during simulation.

During simulation the displacement for a set of mass points is set fixed (the join points, see section 3.3). The other model points (free points) will move due to elastic forces in these points induced by the displacement of these join points. The new rest position of these free points can then be found by time integrating the Newtonian motion equation¹⁰.

2.3.2 Extension 1: Direct computation of the deformation

As already suggested in^{42,31} the usage of a time integration scheme, as mentioned above, can lead to slow convergence and errors in the estimation of the final position. In a maxillofacial surgery planning system the prediction of this final rest position is more important than the exact animation of the deformation. Therefore we

combined the original Mass Tensor Model with a static constraint to directly estimate the deformation without calculating the animation.

The new rest position is now found by demanding that in each free point the total elastic force should be zero when the object is in rest.

$$\mathbf{u}_j^{new} = \operatorname{argmin} \|\mathbf{F}_j(\mathbf{u}_j)\| \quad \forall j \in \Gamma_{free} \quad (11)$$

with Γ_{free} the collection of all free mass points. To solve this optimisation problem, we use a local steepest gradient method which tries to minimise the total elastic force in each free point in every iteration step. So in iteration step p we get:

$$\mathbf{F}_j(\mathbf{u}_j^p) = 0 \rightarrow \mathbf{u}_j^p = -[\mathbf{K}_{jj}]^{-1} \left(\sum_{\forall k \in \Psi_j} [\mathbf{K}_{jk}] \mathbf{u}_k^{p-1} \right) \quad (12)$$

Since all $[\mathbf{K}_{jj}]$ and $[\mathbf{K}_{jk}]$ are only dependent on the initial mesh configuration and the two biomechanical constants, λ and μ , we can pre-compute all $[\mathbf{K}_{jj}]^{-1}$ and $[\mathbf{K}_{jk}]$. Hence the optimisation problem will be restricted to a series of matrix-vector multiplications and matrix summations.

2.3.3 Extension 2: A local dynamic stop criterion

A second improvement was introduced to the original MTM. Suppose we define a total elastic force threshold F_{thresh} . When the total elastic force $\|\mathbf{F}_j\|$ in each model point becomes smaller than this F_{thresh} , iterations will be stopped early. We name the difference between the predicted result when F_{thresh} is set to zero and the outcome when a non-zero value is assigned to F_{thresh} , the precision of the MTM. This definition of the term precision is consistent to the work of Hover *et al.*²⁰, where precision was defined as a measurement for the 'internal accuracy' of a model. It is needless to make this precision a lot higher than the achieved total accuracy, defined as the difference between the predicted outcome and the real post-operative new facial outlook. As a consequence iterations can be cut-off early, which will cause a serious gain in simulation time.

Defining a good overall value for F_{thresh} is however impossible, since this value will be dependent on the mesh topology and the biomechanical constants. Therefore we propose to look to the mean gradient of the displacement field over a number of iterations, to determine when iterations should stop. If this gradient becomes very small in every model point, we can conclude that we must be close to the real solution and can ensure that the error made by the limited precision is negligible to

the accuracy of the prediction. This dynamic stop criterion enables the combination of high accuracy with fast simulation times.

This threshold can be reached in different model points after a different number of performed iterations. Moreover the elastic force in point j at the start of iteration k can only have been changed since iteration $k-1$ when point j or a neighbouring point has been moved during iteration $k-1$. Due to the easy architecture of the MTM, storing information locally in each mass point, these two criteria can easily be incorporated in the iterative solution scheme and will result in a shorter simulation time.

2.3.4 Validation of the local dynamic stop criterion

We validated the local dynamic stop criterion of the MTM in two ways. In the first section we try to clarify the effect on the accuracy of the stop criterion. In the second part we highlight the gain in simulation time when comparing to FEM or MSM simulations.

Precision of MTM

For validation we arbitrarily selected five patient CT data sets and constructed for each data set a tetrahedral mesh which encloses the facial soft tissues, as explained in section 3.1. This tetrahedral mesh serves as input for our Tetrahedral Mass Tensor Model. For each patient boundary conditions, defining the joint and free model points, were generated based on a realistic bone-related planning (see section 3.3). After applying these conditions to the model, the soft tissue deformations were calculated by searching the new rest position for each free model point, as described in section 2.3.2. After each iteration step the new calculated position for each point was saved. Based on this saved data the maximal gradient of the displacement field and the minimal precision over all free model points were calculated during each iteration step. The precision of the prediction at iteration step n , was derived by measuring the distance between the final position, when the total elastic force is zero in each model point, and the position at iteration step n , for each model point. The graphs in figure 1 summarize the precision data for each of the five patients.

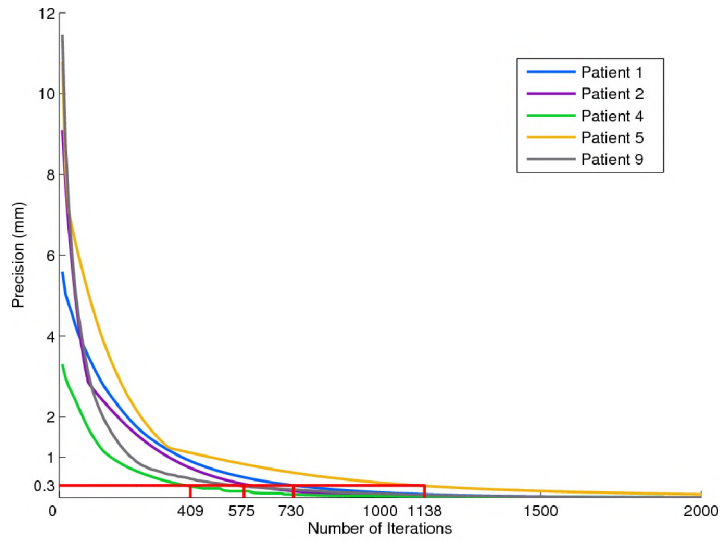


Fig. 1. The minimal precision in mm over all free model points after each iteration step for 5 arbitrarily chosen patient data sets. The red lines indicates when the minimal precision becomes smaller than $0.3 mm$.

As will be discussed in section 3, the mean accuracy of the Mass Tensor Model equals approximately $1.5 mm$ for this data set of 5 patients. When the minimal precision of our MTM becomes smaller than for example one fifth of this mean accuracy ($\approx 0.3 mm$), we can suppose that precision becomes negligible compared to the accuracy of the prediction and that iterations can be cut off. This cut-off boundary is indicated on each graph in figure 1 and summarized in table 1.

Patient	N_{its}	P_{min} (mm)	P_{mean} (mm)	G_{max}
1	727	0.30	0.058	0.0010
2	583	0.29	0.021	0.0015
3	409	0.28	0.065	0.0016
4	1138	0.28	0.011	0.00055
5	570	0.29	0.041	0.0017
Average	685.4	0.288	0.039	0.0012

Table 1: Table showing the number of performed iterations (N_{its}), the corresponding minimal (P_{min}) and mean precision (P_{mean}) of the current prediction and the maximal gradient (G_{max}) of the deformation field over all model points after Ω iterations.

Table 1 shows that when the minimal precision becomes smaller than 0.3 mm , the mean precision over all model points equals on average 0.039 mm . This very low mean value suggests that only a very small group of model points haven't reached their final rest position yet. Moreover the distance between the current position of these points and their final rest position is small compared to the real accuracy of the prediction and will therefore not influence the final prediction accuracy. As a consequence iterations can be stopped early. We can derive from table 1 that this boundary is reached when the maximal gradient of the displacement field becomes smaller than 0.001 .

Simulation time

To investigate in more detail the time gain due to the local stop criterion, we measured the time gain of the MTM compared to the linear FEM and MSM, in function of the numbers of tetrahedra used in the tetrahedral model. Therefore we created a set of virtual test cubes having the same dimensions but containing a different number of tetrahedra. During simulation the centre of the cube was moved 6 mm upwards. Simulation times were recorded for each biomechanical model and results are summarized in figure 2.

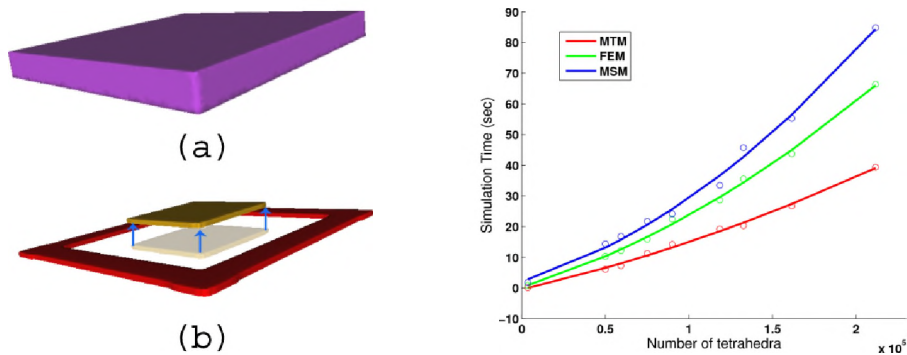


Fig. 2. Left: (a) Virtual test cube. (b) Boundary conditions applied to this cube. The centre of the cube (yellow) is moved 6 mm upwards, while the border (purple) is kept fixed. Right: Simulation time in function of the mesh size for all 3 biomechanical models.

These results reveal that the simulation time of FEM and MTM behaves more or less linear in function of the number of tetrahedra in our region of interest (30,000 – 200,000 tetrahedra). When the mesh size increases, and as a consequence the average tetrahedron size decreases, the maximum allowed step size in each iteration of the MSM, has to be decreased to prevent unwanted “spring-flipping”. This results in a more quadratic approximation for the MSM. It was noticed that a constant 40% time gain can be achieved with the MTM compared to FEM and MTM was on average 52% faster than MSM.

3 True Validation

Before a soft tissue simulator can be used in routine clinical practice, it has to be shown that this simulator is able to give an accurate prediction of the new facial outlook after surgery. The only way to truly measure this accuracy is by comparing post-operative data with the predicted data^{38,6,48}. This important validation step has often been lacking in other work. In this section we discuss how our validation data was acquired and processed. The validation work-flow includes following steps:

1. Data acquisition and pre-processing: Patients undergo a pre- and post-operative CT scan. Out of the two CT data sets the skull and skin surface are reconstructed. A tetrahedral volumetric mesh that serves as input for the soft tissue simulation, is built after first segmenting the facial soft tissues out of the pre-operative CT data
2. Bone-related planning: A maxillofacial bone-related planning that corresponds to the real performed procedure is generated.
3. Generating boundary conditions: Out of the bone-related planning boundary conditions for the biomechanical soft tissue model are generated.
4. Simulation: The new facial outlook is computed using a specific computational strategy.

5. Validation: The computed facial outlook is qualitatively and quantitatively compared with the real post-operative appearance.

While step 1 – 3 are more straightforward, we introduce in step four a novel method to combine a very fast simulation with a high resolution of the visualisation result. In the next subsection we discuss our validation methods. All simulations were qualitatively and quantitatively validated. To quantitatively validate the predicted facial outlook, we measured distances between corresponding points of the predicted and post-operative facial outlook. Finally, in the last part of this section, we present the results of using this validation set-up on a database of 10 patients who underwent a maxillofacial procedure.

3.1 Data acquisition and pre-processing

When a patient needs to undergo a maxillofacial surgery, pre-operatively a CT scan is acquired. Dense, highly detailed skin and bone surfaces are extracted with the marching cube algorithm with appropriately chosen thresholds²⁶.

To simulate the soft tissue deformations caused by a maxillofacial procedure, we also need a volumetric tetrahedral mesh containing all the facial tissues. Starting from the patients' CT data we automatically segment these facial soft tissues using a levelset segmentation algorithm²¹. Out of this segmented data we can build with the Amira software (TGS, Merignac Cedex, France) a tetrahedral mesh. Since our levelset segmentation algorithm produces a very smooth segmentation, we never experienced any problem in obtaining an appropriate tetrahedral mesh. The design of a simulator that can be applied in routine clinical practice imposes constraints concerning processing time and memory usage, i.e. on the dimensions of these tetrahedral volumetric meshes. Therefore it is interesting to restrict the tetrahedral mesh to the zone of the human face that will deform during surgery and to limit the number of tetrahedrons (typically less than 100000).

In their clinical routine, all patients had a post-operative CT scan four months after surgery, when swelling has disappeared. These post-operative images are also used during our validation procedure. Therefore the post-operative CT data is first rigidly registered to the pre-operative CT data, using maximization of mutual information on an unaltered subvolume²⁷. From these co-registered post-operative data, a surface representation of the skin and skull are generated.

3.2 Bone-related planning

Maxilim (Medicim, Sint-Niklaas, Belgium) is a 3D bone-related planning system for maxillofacial surgery, originating from development in our group over the last years³³. This software allows the maxillofacial surgeon to pre-operatively determine the necessary bone displacements and to see the effect of the procedure.

Since we want to validate the accuracy of our soft tissue simulator, we have to ensure that the planned procedure is exactly the same as the one performed by the surgeon. There are two critical parameters when planning a maxillofacial intervention: determination of the cut surfaces and determination of the displacements of the different skull parts. To define these parameters we use the pre-operative skull surface and the co-registered post-operative skull representation, generated as discussed in section 3.1.

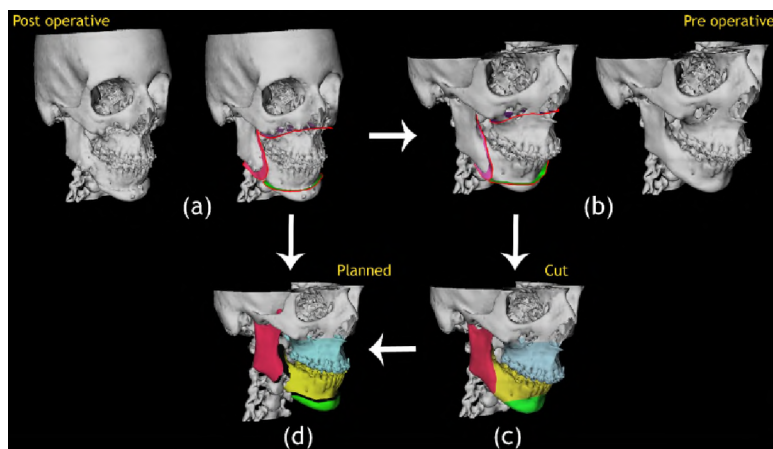


Fig. 3. Reconstruction of a bone-related planning that resembles the performed procedure as much as possible

During surgery the skull was cut into a number of separate parts which were displaced independently and which can be easily identified on the co-registered post-operative skull surface by visual inspection. To transfer the location of the cut surfaces from the co-registered post-operative to the pre-operative skull representation, we first divide this post-operative skull surface in different patches that each correspond to a separate skull part (see figure 3(a)). Each post-operative surface patch is then separately matched by manual alignment to the pre-operative skull representation. Afterwards the ICP algorithm¹³ is used to refine the rigid registration (figure 3(b)). The outline of each registered patch on the pre-operative skull surface as defined by ICP, is then used to define an initial cut surface on the pre-operative skull (figure 3 (c)). Then the pre-operative skull was virtually cut with these cut surfaces. Finally, the resulting bone fragments are again registered to the co-registered post-operative skull surface using ICP, to precisely determine the displacement of each skull part (figure 3(d)). The ICP algorithm was initialised by a manual allineation of the different skull parts.

This work-flow enables us to accurately reconstruct the performed surgery. However some differences between the planned procedure and the co-registered post-operative skull remained which can not be corrected by rigid displacements of bone parts. The most important reasons for these mismatches are: misplacement of a cut surface due to metal streak artifacts on the CT data, bone growth after surgery and

placement of screws in the bone during surgery. As a consequence the maximal distance between the planned skull and the co-registered post-operative skull, remained around 1 mm .

3.3 Boundary conditions

To simulate the effect of a maxillofacial surgery on the soft tissues, the bone-related planning has to be mapped to the tetrahedral soft tissue model. Therefore, we assume that the motion of a soft tissue point that adjoins the skull, equals the motion of that part of the skull. In this way two types of points can be distinguished: join points and free points (see figure 4).

- *Join points*: All points that join at a part of the skull. This skull part will be kept fixed or will be repositioned during surgery.
- *Free points*: All the other soft tissue points are free. During simulation their movement is completely determined by the resulting elastic force that exists in these points.

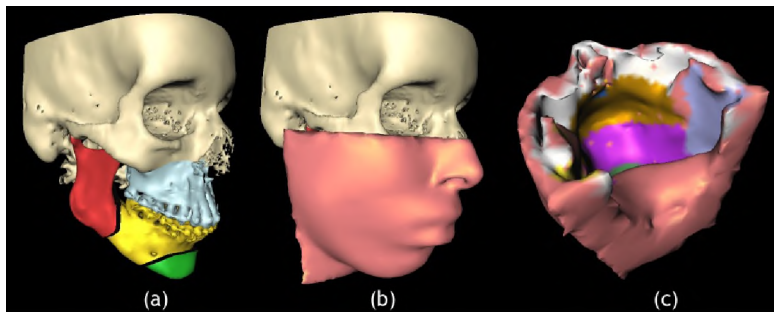


Fig. 4. Determination of the boundary conditions. (a) The bone-related planning. (b) The planning data is mapped to the soft tissue model. (c) Pink points are free points, the other coloured points are join points. The movement of a join point equals the movement of the corresponding skull part.

In the present simulator we do not model the exact contact behaviour between lips and teeth. At this moment teeth are treated as any other part of the skull, while a sliding contact behaviour would be more realistic and could probably improve simulation results.

3.4 Simulation

The created tetrahedral mesh and boundary conditions serve as an input for our soft tissue simulator. We used four different computational strategies (see section 2) to model the facial soft tissue behaviour and to predict the patient's post-operative appearance. These four models are: a linear FEM, a non-linear FEM, a MSM and a MTM. During simulation first join points are displaced as defined by the boundary conditions. Next the new position of each free model point is searched by demanding that the total elastic force should be zero in this point when the object is

in rest. Since we assume the facial tissues to be homogeneous and isotropic, it can easily be shown that the equations that need to be solved, are independent of Young's Modulus for all four computational strategies. For the linear and non-linear FEM and the MTM the Poisson Ratio was set to 0.46 during all simulations¹⁷.

As mentioned in section 3.1, for reasons of computational efficiency the tetrahedral mesh used for simulation is restricted to only the zone of the human face that will deform during surgery and is quite smooth due to the limited number of tetrahedrons. The recognition value of such a smoothed mesh is however rather low, as shown in figure 5(a). Moreover, since the perception of the human face is mainly determined by the relationship between different parts of the face, it is important for the surgeon to see the whole face and not just a part of it when inspecting the effect of a maxillofacial procedure. As a result, this tetrahedral mesh is unsuitable for clinical validation. To combine the advantages of a smooth sparse tetrahedral mesh for fast simulations and a very dense, highly detailed mesh for a good recognition, we introduce a volume/surface mapping method.

With the volume/surface mapping method, we first calculate the new facial outlook using a smooth sparse tetrahedral mesh and we then map this deformation field to a dense triangle representation of the human skin surface, that was also generated during pre-processing of the data (see section 3.1). Since the tetrahedral mesh is much sparser than the skin surface, we have to interpolate the calculated deformation field.

We suggest two different interpolation strategies. First the linear FEM shape functions⁵⁰ can be used to calculate the displacement in every point of the triangular surface. Second a Gaussian interpolation strategy is presented. Both methods enclose two steps: an initialisation procedure and an update process during which the displacement in each point of the triangular surface is calculated.

For the first method, the shape function method, we search during initialisation for each point P_i of the triangular skin surface the tetrahedron that is closest to this point P_i . To find this tetrahedron we project point P_i onto the outer triangular surface of the tetrahedral mesh and we define the tetrahedron that contains triangle k where point P_i was projected on, as the closest tetrahedron of this point. In the update stage the displacement of every surface point P_i is determined using the FEM shape functions of the closest tetrahedron:

$$u(P_i) = - \sum_{j=0}^3 \frac{m_j(P_i - q_{j+1}^0)}{6V_T} u_j \quad (13)$$

with $q_{j=0\dots3}^0$ and $u_{j=0\dots3}$ the initial position and displacement of the four vertices of this tetrahedron, V_T the initial tetrahedron volume and $m_{j=0\dots3}$ are the area vectors for each vertex as defined in¹⁰.

The second approach uses a more simple Gaussian interpolation strategy. We initialise the interpolation scheme by searching for each point Q_j of the outer surface of the tetrahedral mesh, the corresponding point P_i on the triangular skin surface. Since this skin surface is very dense, we can assume that the corresponding point P_i is simply the closest point on the triangular surface. To calculate the displacement of each surface point, we first map the displacement of each point Q_j of the tetrahedral mesh to its corresponding point of the facial skin surface. The displacement of n points of the facial skin surface is now known. Next the displacement of every point P_i of the facial skin surface is found by using following interpolation scheme between these n points:

$$u(P_i) = \frac{\sum_{\forall j \in \Theta_i(x,y)} \frac{u(P_j)}{d_{ij}}}{\sum_{\forall j \in \Theta_i(x,y)} \frac{1}{d_{ij}}} \quad (14)$$

with $u(P_i)$ the displacement of point P_i , d_{ij} the distance between point P_i and P_j and $\Theta_i(x,y)$ the collection of all points that lie in sphere with a radius of $x \text{ mm}$ around point P_i and have a connectivity with this point P_i lower than y . Empirically 3 mm and 5 were assigned to x and y , respectively.

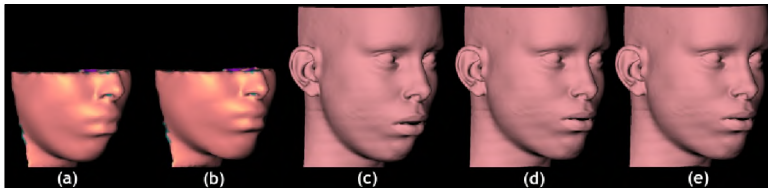


Fig. 5. (a) the initial tetrahedral mesh, (b) the deformed tetrahedral mesh, (c) the initial skin surface, (d) and (e) the deformed skin surfaces generated respectively with the shape function method and Gaussian interpolation approach.

In figure 5 we show the result of the volume/surface mapping visualisation method using both interpolation strategies. As can be seen, the high detail deformed skin surfaces (figure d and e) allow a much better and more realistic visual inspection of

the effect of the maxillofacial surgery. In section 3.6.1 both interpolation strategies will be quantitatively compared.

3.5 Validation procedure

We validated the predicted new facial outlook in two ways: quantitatively and qualitatively. For the qualitative validation surgeons were asked to rate the prediction result by visual inspection. Quantitative validation implies distance measurements between corresponding points of the predicted and real post-operative facial skin surface.

3.5.1 Quantitative validation

Quantitative validation incorporates measuring distances between the predicted and post-operative facial skin surface. Typically for these measurements, the predicted and post-operative facial skin surface are first rigidly registered based on an unaltered subvolume and subsequently the distance between both surfaces is determined. The distance measurement can be a two-sided Hausdorff distance⁴⁸ or a signed Euclidean distance^{38,6,30}. Afterwards the generated distance map can be visualised or statistically analysed.

As highlighted by Chabanas *et al.*⁶ the main problem of these distance maps is an underestimation of the real error, since the map is calculated as the minimal Euclidean distance between points of the predicted and the real post-operative skin surface and not as the distance between corresponding points. To overcome this problem, a method was elaborated that is capable of finding a better estimate of the correspondences between both facial surfaces.

First we rigidly register the pre-operative and post-operative CT data using maximisation of mutual information on an unaltered subvolume²⁷, typically the top of the skull, and extract out of these data sets the pre-operative and co-registered post-operative facial skin surface (see also section 3.1). During simulation the predicted facial skin surface is calculated by deforming the pre-operative facial skin surface (section 3.4). For finding 'true' correspondences between this predicted facial skin surface and the co-registered post-operative skin surface, we used a variant of the non-rigid TPS-RPM algorithm^{9,8}.

The original TPS-RPM algorithm finds correspondences between a moving and a target set of points A and B , by defining a regularized transformation $\mathbf{f}: A \rightarrow B$. This regularisation ensures that the internal structure of point set A is taken into account during the registration process, which can be achieved by minimising following cost-function:

$$E_{TPS} = \sum_{j=1}^N \mathbf{P} b_j - f(a_j) \mathbf{P}^2 + \lambda \iiint \left[\left(\frac{\partial^2 f}{\partial^2 x^2} \right)^2 + \left(\frac{\partial^2 f}{\partial y^2} \right)^2 + \left(\frac{\partial^2 f}{\partial z^2} \right)^2 \right]$$

$$+ 2\left(\frac{\partial^2 f}{\partial x \partial y}\right)^2 + 2\left(\frac{\partial^2 f}{\partial x \partial z}\right)^2 + 2\left(\frac{\partial^2 f}{\partial y \partial z}\right)^2] dx dy dz \quad (15)$$

with a_i and b_i corresponding points of sets A and B respectively. The second term is a measure for the total curvature of the transformation which constrains the smoothness of the transformation. The influence of this constraint is controlled by a parameter λ . The transformation function \mathbf{f} is defined as a thin-plate spline (TPS) function:

$$f(a_i) = a_i \mathbf{D} + \phi(a_i) \mathbf{W} \quad (16)$$

in which \mathbf{D} is an affine transformation matrix, $\phi(x)$ the used spline kernel and \mathbf{W} a non-affine transformation coefficient matrix.

At initialisation the correspondences between data set A and B are unknown. Hence, it is impossible to calculate the transformation \mathbf{f} in one step. Therefore the original TPS-RPM algorithm defines a correspondence matrix \mathbf{M} which keeps track of the current estimated correspondences between data set A and B . If point set A and B contain K and N points respectively, the new energy function that needs to be optimised is given as:

$$E_{TPS} = \sum_{j=1}^N \sum_{i=1}^K m_{ij} \mathbf{P} b_j - f(a_i) \mathbf{P}^2 - \zeta \sum_{j=1}^N \sum_{i=1}^K m_{ij} + \lambda \iiint \left[\left(\frac{\partial^2 f}{\partial^2 x^2}\right)^2 + \left(\frac{\partial^2 f}{\partial y^2}\right)^2 + \left(\frac{\partial^2 f}{\partial z^2}\right)^2 + 2\left(\frac{\partial^2 f}{\partial x \partial y}\right)^2 + 2\left(\frac{\partial^2 f}{\partial x \partial z}\right)^2 + 2\left(\frac{\partial^2 f}{\partial y \partial z}\right)^2 \right] dx dy dz \quad (17)$$

To minimise this energy function a deterministic annealing procedure is used. Starting at a high temperature value T for λ the algorithm will only allow the points to move in a group fashion way. As the temperature decreases this constraint loses its importance and this allows the points to move more locally to satisfy the minimum energy-condition.

Although this TPS-RPM algorithm has proven to be quite accurate in finding corresponding points, it is known to be quite resource-hungry and does not scale very well. As a consequence the original TPS-RPM algorithm can only be used for non-dense meshes. Usages of such non-dense meshes would induce a larger registration error, due to the discretization, that would strongly influence the final result of our quantitative validation. Therefore Tondeur *et al.*⁴³ implemented a variant of this TPS-RPM algorithm that uses the same TPS transformation but

searches correspondences between a point set and a continuous surface description.

Consider two point sets: a moving set A and a target set B . To obtain a continuous representation of the target set a Radial Basis Function (RBF) is fitted through this point set. Next following iterative scheme can be used, to obtain the transformation between both data sets:

Initialization

Load the moving set A (P_A)

$$P_{corr} = P_A$$

Fit a RBF through target set B (RBF_B)

Temperature parameter $T = T_{init}$

Outer Iteration : *Deterministic annealing*

Inner Iteration : *Register moving set at target set*

$$P_{temp} = P_{corr} + \mu(P_{corr}) \text{grad}(P_{corr})$$

(with grad the gradient of RBF_B and $\mu(x)$ the step size.

This step size is proportional to RBF_B in point x)

Use TPS (eq. 17) to calculate the transformation \mathbf{f} from P_A to P_{temp}

$$P_{corr} = \mathbf{f}(P_A)$$

Until Convergence

Decrease temperature T

Until final T is reached

All RBF and TPS calculations are performed using the Fast RBF Toolbox (Farfield Technology, Christchurch, New Zealand), which implements specialised fast evaluation and generation techniques for RBF's and makes these RBF's applicable for large data sets.

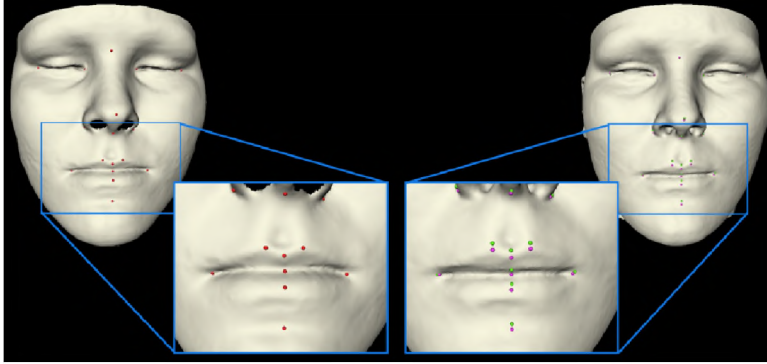


Fig. 6. Well-defined facial points were indicated on the predicted facial outlook (left). The corresponding points on the post-operative facial appearance (right) are searched with a traditional closest point algorithm (green points) and a variant of the non-rigid TPS-RPM algorithm (purple points).

The effect of the non-rigid warping, compared to a closest point search, can clearly be seen in figure 6. Left the predicted facial skin surface is shown. On this surface well defined facial points were manually indicated. Next the corresponding points on the real post-operative facial surface were searched using a traditional closest point approach (green points) and the introduced non-rigid algorithm (purple points). When zooming in on the lip area, a clear difference between both approaches is noticed. Thanks to the regularised warping of the algorithm, a better estimate of the 'true' correspondences between the predicted and real post-operative skin surface is achieved, resulting in a more correct distance measurement.

For our validation study we search correspondences between all mesh points of the predicted triangular skin surface, typically around 60.000 points, and the co-registered post-operative skin surface. Afterwards a signed euclidean distance between these corresponding points is measured. The measured distances are visualised by projecting these distances onto the facial skin surface by means of a color-code. This results in an easy interpretable image of the error distribution over the facial skin surface. Second, we calculate following statistical properties for each distance map: the mean, the variance, the 50% , 90% and 95% percentiles of the distance distributions.

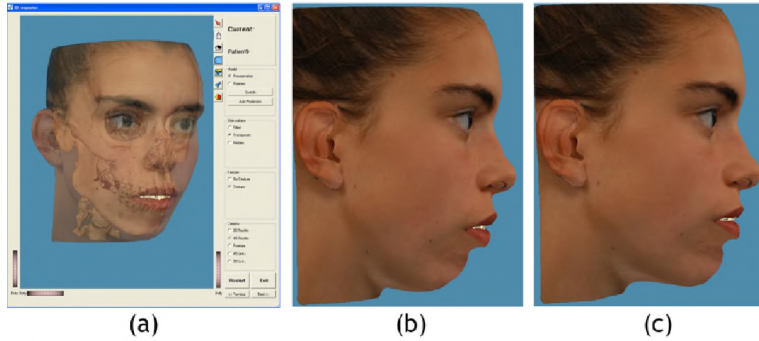


Fig. 7. Qualitative validation procedure: (a) Surgeons could inspect the pre-operative facial skin surface, pre-operative skull and planned skull surface in a 3D environment. Next they are asked to score the truthfulness of the predicted post-operative skin surface. (b) Shows the textured pre-operative facial skin surface of a patient and (c) the predicted post-operative facial appearance.

3.5.2 Qualitative validation

A validation procedure during which surgeons are asked to score the predicted facial outlook, was set up to measure the value of the soft tissue simulations qualitatively. Predictions of the new facial outlook were calculated using the MTM. The qualitative validation procedure includes two experiments:

Experiment 1: First for each patient the pre-operative facial skin surface, pre-operative skull and planned skull surface are shown to the surgeon. The surgeon can inspect these models in a 3D environment (see figure 7). Texture, obtained with a 3D camera system (Eyetrionics, Leuven, Belgium) was added to the facial skin surface to increase realism. Based on the inspection of these models and the planning data, the surgeon is asked to imagine the patient's post-operative facial appearance. When ready, we show him our predicted new facial outlook and ask him to score on a scale of 1 to 5 the truthfulness of this prediction. In the 3D environment it is possible to switch fast between the pre-operative and predicted facial skin surface to emphasise the deformation between both surfaces. Finally the surgeon is asked to indicate on the face the regions where he thinks big errors between the predicted facial skin surface and real post-operative skin surface are present.

Experiment 2: In the second experiment the surgeon is shown the pre-operative skin and skull surface, the predicted new facial outlook and the planned skull, like in the first experiment. However in this experiment also a second 3D viewer is given in which the real post-operative facial surface can be inspected (figure 8). Based on these shown data the surgeon has to score two statements on a 1 to 5 scale. First he has to validate the resemblance between the predicted facial outlook and real post-operative appearance. In a second stage we ask him to once again score the truthfulness of the predicted facial skin surface, after having now seen the real post-

operative facial appearance. At last he has to define the facial regions where the predicted and real post-operative skin surface differ the most, in his opinion.

With the first experiment we want to measure how correct and realistic our predictions are, not knowing the real post-operative appearance. In the second test we want to define what are most error-sensitive facial regions, e.g. maybe it does not matter if large errors arise in the cheek area, but is it important to accurately predict the chin contour. Furthermore we want to investigate if a facial skin surface that was scored as truthful in the first experiment, still gets a high score after seeing the real post-operative facial skin surface in the second experiment.

Besides these two experiments we asked the surgeon to answer some more general questions concerning the relevance and practicability of 3D soft tissue predictions for maxillofacial surgery.

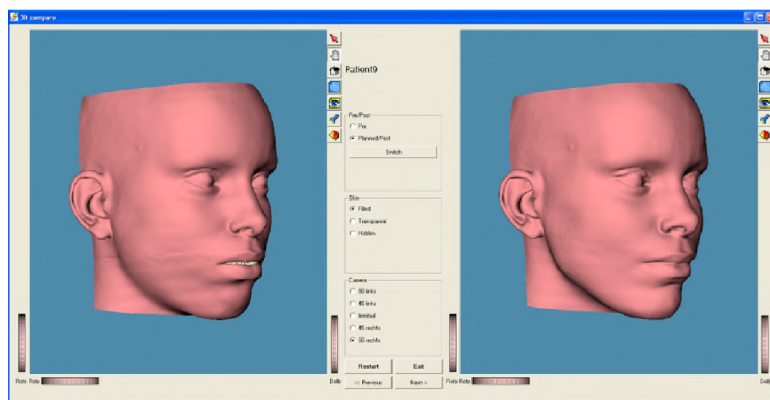


Fig. 8. The second qualitative validation experiment. Left the predicted facial skin surface is shown, right the real post-operative appearance is visualised.

3.6 Results

In close cooperation with Dr. N. Nadjmi (Eeuwfeestkliniek, Antwerpen, Belgium), we acquired data sets of 10 patients who underwent a maxillofacial procedure. For all patients we used the work-flow as described above, to process the data. The patient group counts two Class III and eight Class II patients³⁷.

The eight columns of table 2 summarize the data set number, the surgical procedure for each patient, the number of tetrahedrons used in each model, the maximal movement of the soft tissue points during simulation and the time needed to calculate the new facial outlook for each patient using one of the four computational strategies. All calculations were performed on a standard personal computer with an Intel Pentium 4 processor and 1 Gbyte RAM. As expected the nonlinear FEM is a lot slower as the three other linear computational strategies. Unexpectedly FEM turns out to be faster than MSM. The MTM clearly beats FEM and MSM in simulation

time. As shown in the last row of table 2 the average simulation time of the MTM equals more or less 10 seconds. These very short simulation times are a great advantage for an interactive maxillofacial surgery planning system.

Data set	Procedure	N_{tetra}	M_{max} (mm)	T_{FEM} (sec)	T_{MTM} (sec)	T_{MSM} (sec)	T_{NFEM} (sec)
P1	MSB+G	129955	8.1	24.7	16.5	68.35	893.6
P2	G+MxA	74232	9.5	11.9	7.6	24,3	233.4
P3	MSB + MxA	85213	4.9	16,8	6.6	22,7	449,1
P4	MA	66286	4.3	13.7	2.5	10.99	41.1
P5	MA+G+MxA	79716	16.7	19.2	12.9	47,6	1885.2
P6	MA+MxA	79125	6.3	19.5	5.4	33.1	913.5
P7	MA+MxA	75314	9.6	17.9	9.9	32.2	1001.6
P8	MA+G+MxA	303745	9.9	104.1	23.2	94.3	2712.3
P9	MA+G+MxSB	80654	13.8	11.5	8.2	42.3	897.3
P10	MA+G+MxA	91925	9.5	17.9	8.5	34.6	498.6
Mean		106616	9.26	25.7	10.2	35.1	952.6

Code	Description
MSB	Mandibular Set Back
MA	Mandibular Advancement
G	chin Genioplasty
MxSB	Maxillary Set Back
MxA	Maxillary Advancement

Table 2. A database of 10 patients was acquired. For each patient a soft tissue model was built and the new facial outlook was calculated based on the performed surgery and using one of the 4 computational strategies: FEM, MTM, MSM and NFEM. The first two columns show the performed maxillofacial procedure and the number of tetrahedra used in the facial soft tissue model. Column three lists the maximum movement over all soft tissue points during simulation. Time needed to calculate the new facial outlook is summarized for each strategy in the last four columns.

3.6.1 Quantitative Results

For the quantitative validation step the 10 data sets were processed as discussed in 3.5.1. To improve the validation the eye region and neck area of each patient were manually selected and omitted during processing. Differences in these regions are mainly due to opening or closing of the eyelids or a change in head position during acquisition of the pre-operative and post-operative CT scan and can not be simulated by our soft tissue prediction system. Figure 9 summarizes the outcome of the statistical analysis for all four computational models. In the first row we show the mean, the variance and the maximum of the distance maps for each patient. The second row presents the 50%, 90%, 95% percentiles of the distance distributions of the generated maps. In table 3 we summarize more numerical data of the outcome of the statistical analysis, showing average values over all data sets for the 50%, 90% and 95% percentiles of the distance distributions of the generated maps for FEM, MTM, MSM and NFEM.

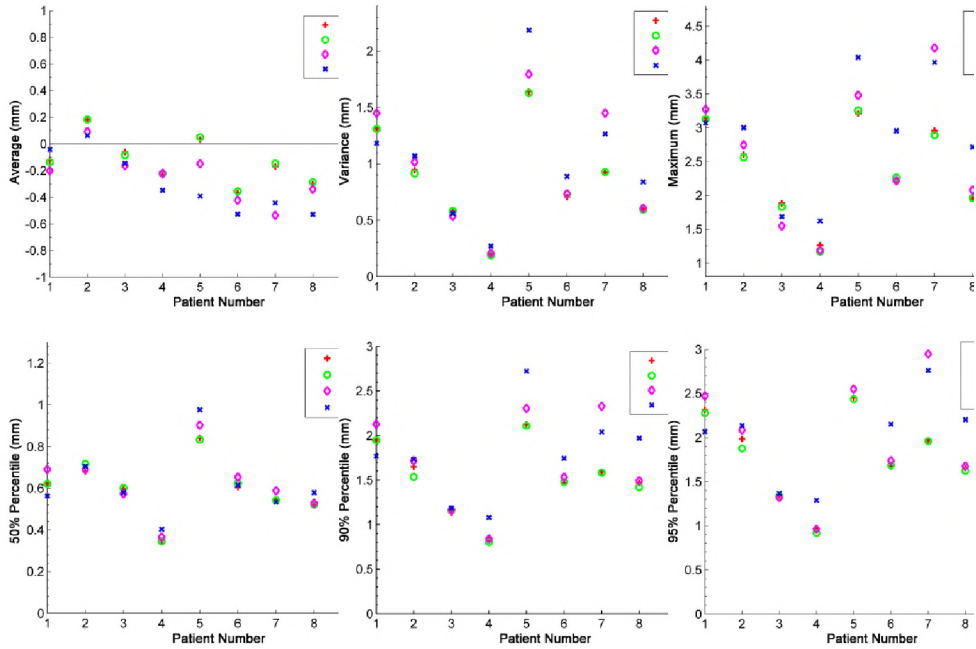


Fig. 9. For 10 patients, quantitative validation results of the predictions calculated using FEM, MTM, MSM or non-linear FEM, are presented.

Model	$T_{50\%}$	$T_{90\%}$	$T_{95\%}$
FEM	0,60	1,51	1,78
MTM	0,60	1,48	1,75
MSM	0,64	1,67	1,95
NFEM	0,63	1,71	2,05

Table 3. Average values, over all 10 patients, of the 50% , 90% and 95% percentiles of the distance maps calculated between the predicted and actual post-operative facial skin surface.

These results show that most accurate results are obtained with FEM and MTM and that both models calculate almost the same prediction result. Visual inspection of the predicted skin surfaces, showed that difference between both models are only located near the neck area, which is of less importance for the prediction quality. Also the prediction results obtained with the MSM are quite good. However when deformations become large (P2, P7, P9 and P10) the MSM is clearly less accurate

than FEM or MTM. Introduction of the nonlinear FEM didn't improve the simulation results. Only for P1 a better prediction was obtained when using the NFEM strategy. For all other data sets, the accuracy of the NFEM predictions was lower than those obtained with the three other computational strategies. As can be seen in table 3 the mean $T_{50\%}$ for FEM and MTM is only 0.6 mm and the average $T_{90\%}$ equals 1.50 mm . Keeping in mind the stability and predictability of a maxillofacial surgery (around 1 mm), these distance values show an acceptable accuracy.

Besides the statistical analysis of the generated distance maps we can also project these distance maps on the model by means of a color-code. This is shown for predictions calculated with the MTM, in figure 10. This figure shows the projected distance maps for each of the 10 patients. The color map ranges between -3 mm and 3 mm , where a negative error means that the predicted skin surface lies behind the post-operative skin surface. When inspecting these images, it can be noticed that there are some typical regions with large errors, namely: the tip of the chin, the lips and the two area's besides the nose wings.

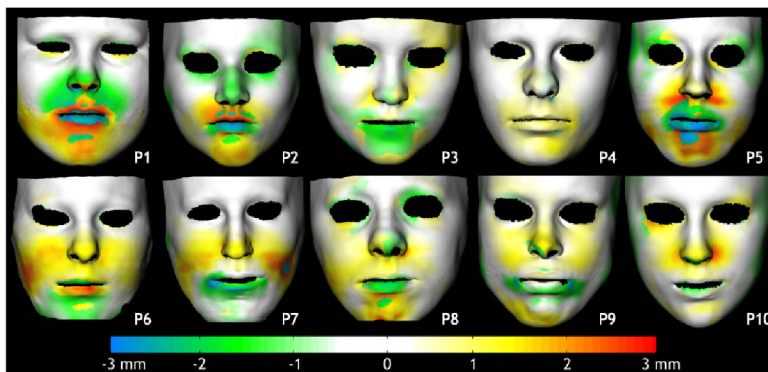


Fig. 10. Distance map visualised by color coding for the 10 patients. A negative error means that the predicted skin surface lies behind the post-operative skin surface.

To investigate the difference between the Gaussian and the shape function interpolation scheme, as introduced in section 3.4, we measured the accuracy of the prediction results calculated with the MTM in combination with one of both mapping strategies. These results are summarised in figure 11 showing the 50%, 90% and 95% percentiles of the calculated distance maps. Average differences between both methods were smaller than 0.05 mm for all three statistics. This difference is irrelevant for our application.

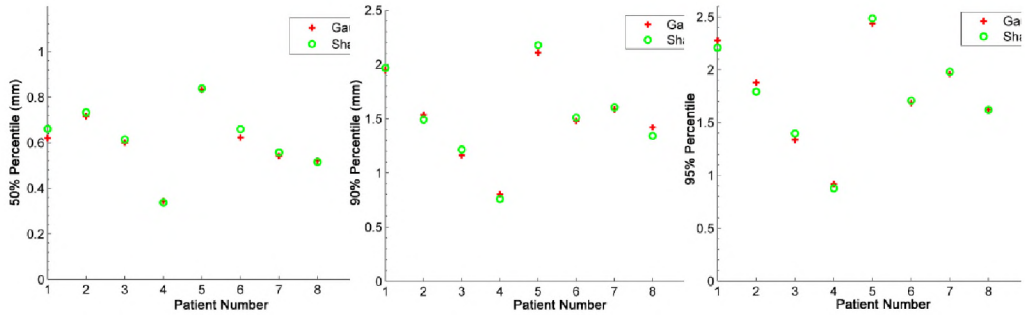


Fig. 11. The Gaussian and shape function interpolation scheme were used to map the deformations calculated on the $3D$ tetrahedral mesh to the dense triangular skin surface. For both methods differences between the predicted and actual post-operative skin surface were measured.

The time needed to calculate the interpolation can be separated in an initialisation step (step A) and an interpolation step (step B), as discussed in 3.4. These timing results are summarised for each patient in table 4. The Gaussian method clearly outperforms the shape function method in timing results with an average time gain of 85%. Considering the simulation times, listed in table 2, we can conclude that there is a significant difference in calculation time between both methods.

Data set	Gaussian		Shape function	
	A (msec)	B (msec)	A (msec)	B (msec)
P1	187	547	3813	1141
P2	63	109	859	219
P3	78	157	1188	344
P4	125	281	2203	688
P5	141	297	2094	625
P6	109	281	2172	594
P7	172	500	3532	1000
P8	140	312	3016	625
P9	156	454	3156	1047
P10	94	109	1094	250

Table 4. Calculation time results for the Gaussian and shape function interpolation scheme. Step A is the initialisation step, while in step B the actual interpolation is calculated.

3.6.2 Qualitative Results

Our qualitative validation study, as described above, was carried out by eight maxillofacial surgeons. Experiment 1 was always filled in first, next the surgeon carried out experiment 2 and finished with the more general questionnaire. During each experiment, the data of all 10 patients was presented to the surgeon in a randomised order.

Table 5 summarizes the most frequent scores given by all surgeons for each of the 10 patients for the most relevant statements of experiment 1 and 2. A statement, with which the surgeon completely agreed, was rated with 5, while a 1 indicates total disagreement with the statement. The scores of the more general questions are depicted in table 6.

Statement	P1	P2	P3	P4	P5	P6	P7	P8	P9	P10
The performed bone-related surgery is clearly visualised. (S1)	5	4	4.5	5	5	4.5	4	4	4.5	5
The prediction of the new facial outlook after surgery is correct. (S2)	3.5	3	3	4	4	4	3	4	3	4
The predicted outlook is a good prediction of the actual post-op outlook. (S3)	5	3	3	5	4	4.5	4	4	3.5	4

Table 5. Surgeons scored statements on a 1 to 5 scale. Statement S1 and S2 was scored during experiment 1. The last statement belongs to experiment 2.

Statement	Score
Prediction of the soft tissue deformations can improve the bone-related planning (S4)	5
This 3D soft tissue prediction system is useful in daily clinical practice. (S5)	4
This prediction system can greatly improves communication between surgeon and patient. (S6)	4.5

Table 6. General questions concerning our 3D soft tissue prediction system, were rated by surgeons

It is noticed that the most frequent scores over all patients for statement S2 are not lower than 3 and the overall median score for this statement is 3.75, which implies that the shown prediction corresponds well to what the surgeon expected to be the actual post-operative facial appearance. The most frequent score for statement S3 are even a little bit higher (overall median score is 4), indicating that our predictions are rated as good or even slightly better, after seeing the real post-operative outlook. The answers to the more general questionnaire (table 6), confirm these results. The interviewed surgeons agreed that this soft tissue prediction system could really help to make a better bone-related planning and to ameliorate communication between surgeon and patient.

4 Discussion

4.1 Computational strategies for soft tissue modelling

In this work we compared the usage of four different computational strategies for a 3D soft tissue maxillofacial planning system. These strategies are a linear Finite Element Model (FEM), a nonlinear Finite Element Model (NFEM), a linear Mass Spring Model (MSM) and a linear Mass Tensor Model (MTM). This last model, based on the work of Cotin *et al.*¹⁰, is some sort of golden mean between MSM and FEM.

MSM and FEM, are frequently used to predict the new facial outlook after maxillofacial surgery. MSM has an easy architecture and low memory cost, but isn't very biomechanical relevant and lack sufficient accuracy for our clinical application. FEM doesn't have this drawback but has on the other hand a more complex architecture. Moreover the speed of FEM is highly related to the sparsity of the global stiffness matrix, which may result sometimes in rather long simulation times. Although some authors state that reducing the simulation time can not be a goal of a maxillofacial soft tissue prediction system, we argue that soft tissue predictions

should be incorporated during bone-related planning, as confirmed in literature and by results of our qualitative validation study.

We introduced two novel extensions to the original MTM, a direct computation step and a local dynamic stop criterion, resulting in a very fast and accurate biomechanical model. As shown the usage of a stop criterion does not introduce new significant errors, since the MTM prediction can only have a limited accuracy. Moreover an average time gain of more than 40% could be achieved compared to FEM or MSM.

The presented MTM, MSM and FEM are homogenous biomechanical models, which do not incorporate tissue specific behavior. Zachow *et al.*⁴⁶ investigated the effect of an inhomogeneous tissue model. He differentiated between fat and muscle tissue and assigned for each tissue type different values to the Modulus of Young (E) and the Poisson Coefficient (ν). He concluded that the net improvement of using such inhomogeneous tissue models, did not significantly influence the prediction quality. Since his validation included only a single relevant data set, we hope to be able to affirm his results in the very near future by performing the same study on our more extensive database of 10 patients.

4.2 True validation

In the second part of this work, we presented results of a validation study for all four computational strategies on a data set of 10 patients, including pre-operative and post-operative image data. This validation study consists of two parts: a quantitative and qualitative validation.

For the quantitative validation we measured distances between corresponding points of the predicted and actual post-operative facial skin surface. Correspondences were searched using a variant of the non-rigid TPS-RPM algorithm. Measuring the minimal euclidean distance between both surfaces, would result in an underestimation of the prediction error, as highlighted in⁶.

Highest accuracy was obtained by usage of the FEM or MTM approach. For the MTM we showed that the median prediction error over all 10 patients was bellow 0.6 mm and even the 90% percentile was smaller than 1.5 mm . The MSM results were comparable to the MTM results when the displacement were relatively small. However for data sets with large displacements (P2, P5, P7 and P9) the accuracy of the MSM clearly decreased. Finally, introduction of an nonlinear model, NFEM, didn't improve the simulation accuracy. Only for data set $F1$ a slight increase in accuracy was recorded. The reduced accuracy for all other data sets, can perhaps be explained by the fact that this nonlinear modelling is much more sensitive to several criteria like the mesh (which should be refined in high stress areas), the boundary conditions and elastic parameters of the model. This same conclusion was

already made by Chabanas *et al.*⁷ based on some first results. Probably definition of more realistic boundary conditions, like the sliding contact behaviour between teeth and lips, is most necessary to further improve the simulation accuracy.

The quantitative validation study revealed that there are some typical regions with large errors: namely the tip of the chin, the lips and the two areas besides the nose wings. We think that the errors in chin and nose region are mostly due to the placement of screws on the bone during surgery; the extra displacement due to these screws, is not incorporated in our bone-related planning. Moreover derivation of correct boundary conditions for the nose region is a very difficult task, since the nose bone is very thin and can not be easily segmented. Finally when looking to the lips, we suggest two main reasons why the lip movement is wrongly simulated. A first reason is the connection between lower and upper lip: in our soft tissue model the two lips are not explicitly separated from each other during simulation. Secondly it was already noticed in clinical relevant literature that the lower lip becomes more straight when the mandible is advanced during surgery and becomes more relaxed when the opposite is performed, our present model is clearly not able to predict this effect correctly.

Finally during the quantitative validation study we compared prediction results obtained with two different interpolation strategies for the volume/surface mapping method. This volume/surface mapping enables the combination of short simulation times with a highly detailed visualisation of the deformed facial outlook. Results showed that using a Gaussian interpolation scheme is significantly faster without loss of prediction accuracy compared to the usage of a more theoretical based shape function interpolation. The Gaussian interpolation method has however as a drawback that it has to be tuned in function of typical mesh size of both the tetrahedral mesh and the triangular facial skin surface (see section 3.4).

Besides a quantitative validation, also a qualitative validation of the predicted facial outlook, calculated with the MTM, for all 10 patients was performed. This qualitative validation included two well defined experiments. The study was carried out by eight surgeons and we can conclude that our predictions were rated as 'good' and 'clinically relevant' for all 10 patients.

It is interesting to compare results of this qualitative validation study, with results obtained during the quantitative validation study. First we note that the patient with the highest scores (P4) is also the patient with the lowest distance values in the quantitative validation approach. On the contrary patients with the lowest scores (P2, P3 and P9) don't have the highest distance measurements in the quantitative analysis. Clearly a quantitative validation alone is not sufficient to separate good from bad predictions.

During experiment 1 and 2 of the qualitative validation, surgeons were asked to indicate regions of 'high errors' onto the predicted facial outlook. By comparing these

data with distance measurements of the quantitative validation we can define error-(in)sensitive facial regions. First, although patient P1, P6 and P7 have rather large errors in the cheek area these regions were never indicated as 'wrong' during the qualitative validation study by the surgeons. Secondly, it turned out that surgeons are very sensitive to errors in nose and lip region. For patient P1, P2 and P10 almost every surgeon indicated on the predicted facial skin surface the nose region as being wrongly simulated. Also when there was an inaccurate prediction of more than 1.5 mm of the lip contour, this was correctly noticed by the surgeons. At last for patient P2, P5, P8 and P9 there is a clear incorrect prediction of the post-operative chin outlook. It was noted that this inaccuracy probably arises from the fact that the patient's chin was in an unnatural tensed position during pre-operative CT acquisition, since patients were explicitly asked to close their mouth during this acquisition. Most surgeons stated that the soft tissue predictions would be strongly improved for these patients, if the chin had been more relaxed during CT acquisition.

Recently Zachow *et al.*^{48,46}, reported on a quantitative evaluation of 3D soft tissue predictions for maxillofacial surgery, based on a single data set. While their validation set-up is similar to ours and the simulation errors reported in⁴⁶ are comparable to ours, our validation is more extensive as it includes 10 patients, showing consistent accuracy of all 10 cases. Moreover, our error measure is a more realistic and clinically more relevant measure than the full head averaged measures used in⁴⁶, since we measure distances between corresponding points and only include the region of interest of the face, i.e. the deformed part of the face, and explicitly exclude the non-deformed parts such as the top of the skull.

Although most authors asked collaborating surgeons for feedback about their soft tissue simulations, none have presented an extensive qualitative validation. Since visualisation of the simulated facial appearance is the final goal of a maxillofacial soft tissue prediction system, we argue that a detailed qualitative validation study is essential. This validation should include well defined experiments, during which statements have to be scored by the surgeon. As shown, results of such a qualitative validation and quantitative validation are not necessarily coherent. This dis coherence enables the definition of new relevant research goals.

5 Conclusion

Maxillofacial surgery treats abnormalities of the skeleton of the head. Since the human face plays a key role in interpersonal relationships, people are very sensitive to changes to their outlook. Therefore planning of the operation and reliable prediction of the facial changes are very important. Recently, the use of 3D image-based surgery planning systems is more and more accepted in this field. Although the bone-related planning concepts and methods are maturing, prediction of soft tissue deformation needs further fundamental research.

In this work we compared four computational strategies to simulate the post-operative facial appearance: a linear Finite Element Model, a nonlinear Finite Element Model, a Mass Spring Model and a new Mass Tensor Model. We introduced this last model and observed a significant time gain in simulation time compared to the two traditional used models: the linear Finite Element Model and the Mass Spring Model.

Before a soft tissue simulator can be used in clinical practice, the accuracy of the prediction of the new facial outlook after surgery needs to be assessed. We presented a work-flow for a quantitative and qualitative validation procedure, based on pre-operative and post-operative image data. A database of 10 patients was acquired and the qualitative validation was carried out by 8 maxillofacial surgeons. For the quantitative validation distances between corresponding points of the predicted and actual post-operative facial outlook were measured for simulated data obtained with all four computational strategies. Best results were obtained by usage of the linear Finite Element Model or the Mass Tensor Model. We showed that for these model, the average median distance measures only 0.60 mm and the average 90% percentile stays bellow 1.5 mm . These results were confirmed by the qualitative validation study in which surgeons rated our predictions as 'good' and 'relevant' for usage in daily clinical practice.

In the near future we hope to improve our soft tissue simulations even more. First the usage an inhomogeneous biomechanical model, which distinguishes in mechanical behavior of fatty and muscle tissue, will be further investigated. Next special attention will go to the nose and lip region, since these regions were defined as being most error-sensitive during our validation study. Defining proper boundary conditions for those regions and separating the under and upper lip in our volumetric soft tissue model, will be our primary future goals. Finally we can conclude from this study that it is important that the patient's face is in a natural and relaxed position during CT acquisition. The definition of a clear clinical acquisition protocol is essential for further studies.

Acknowledgements. The authors would like to thank Dr. R. Steffens, Dr. M. Martini, Dr. T. Appel, Dr. M. Wenghoefer and Dr. T. Erdsach (Klinik für Mund-, Kiefer- und Gesichtschirurgie Universitätsklinikum, Bonn, Germany), Dr. W.A. Borstlap (UMC St Radboud, Nijmegen, Netherlands) and Dr. B. Vanassche (Eeuwfeestkliniek, Antwerpen, Belgium). They must be thanked for their voluntary participation in the qualitative clinical validation of this work. This work is part of the Flemish government IWT GBOU 020195 project on Realistic image-based facial modelling for forensic reconstruction and surgery simulation and K.U.Leuven/OF/GOA/2004/05.

References

1. Ackermann MJ. The Visible Human Project. Proceedings of the IEEE: Special Issue on Virtual and Augmented Reality in Medicine 1998: 86(3): 504-511
2. Bianchi G, Solenthaler B, Szekely G, Harders M. Simultaneous topology and stiffness identification for mass-spring models based on fem reference deformations. Lecture notes in computer science (MICCAI) 2004: 3217:293-301
3. Bro-Nielsen M, Cotin S. Real-time volumetric deformable models for surgery simulation using a finite elements and condensation. Computer Graphics Forum (Eurographics '96) 1996: 15(3): 57-66
4. Burk DL, Mears DC, Cooperstein LA, Herman GT, Udupa JK. Three-dimensional computed tomographic imaging and interactive surgical planning. J Comput Tomog 1986: 10(1): 1-10
5. Chabanas M, Luboz V, Payan Y. Patient Specific Finite Element Model of the Face Soft Tissues for Computer-assisted Maxillofacial Surgery. Med Image Anal 2003: 7(2): 131-151
6. Chabanas M, Marécaux C, Chouly F, Boutault F, Payan Y. Evaluating soft tissue simulation in maxillofacial surgery using preoperative and postoperative CT scans. Proc. of CARS, 2004: 419-424
7. Chabanas M, Payan Y, Marécaux C, Swider P, Boutault F. Comparison of linear and non-linear soft tissue models with post-operative CT scan in maxillofacial surgery. Lecture Notes in Computer Science (ISMS) 2004: 3078: 19-27
8. Chui H, Rangarajan A. A new point matching algorithm for non-rigid registration. Computer Vision and Image Understanding 2003: 89(2-3): 114-141
9. Chui H, Rangarajan A. A feature registration framework using mixture models. IEEE Workshop on Mathematical Methods in Biomedical Image Analysis (MMBIA) 2000: 190-197
10. Cotin S, Delingette H, Ayache N. A hybrid elastic model allowing real-time cutting, deformations and force-feedback for surgery training and simulation. The Visual Computer 2000: 16(8): 437-452
11. Cotin S, Delingette H, Ayache N. Real-time elastic deformations of soft tissues for surgery simulations. IEEE Transactions on Visualization and Computer Graphics 1999: 5(1): 62-73

12. Cousley RR, Grant E, Kindelan JD. The validity of computerized orthognathic predictions. *Journal of Orthodontics* 2003: 30(2): 149-154
13. De Groeve P, Schutyser F, Van Cleynenbreugel J, Suetens P. Registration of 3D photographs with spiral CT images for soft tissue simulation in maxillofacial surgery. *Lecture notes in computer science (MICCAI)* 2001: 2208: 991-996
14. Dhondt G. *The Finite Element Method for Three-Dimensional Thermomechanical Applications*. Wiley 2004
15. Everett P, Seldin E, Troulis M, Kaban LB, Kikinis R. A 3D System for Planning and Simulating Minimally-Invasive Distraction Osteogenesis of the Facial Skeleton. *Lecture Notes In Computer Science (MICCAI)* 2000: 1935: 1029-1039
16. Farkas LG. *Anthropometry of the Head and Face*. Lippincott Williams and Wilkins, 2 edition 1994
17. Fung YC. *Biomechanics: Mechanical Properties of Living Tissues*. Springer 1993: chapter 7: 242-320
18. Van Gelder A. Approximate Simulation of Elastic Membranes by Triangulated Spring Meshes. *Journal of Graphics Tools* 1998: 3(2): 21-42
19. Gladilin E. *Biomechanical Modeling of Soft Tissue and Facial Expressions for Craniofacial Surgery Planning*. PhD thesis, Fachbereich Mathematik und Informatik der Freien Universität Berlin, Konrad-Zuse-Zentrum für Informationstechnik Berlin (ZIB) 2002
20. Hofer M, Strauß G, Koulechov K, Dietz A. Definition of accuracy and precision - evaluating CAS-systems. *Proc. of CARS 2005*: 548-552
21. Ibanez L, Schroeder W, Ng L, Cates J. *The ITK Software Guide*. Kitware Inc. 2005
22. Keeve E, Girod S, Kikinis R, Girod B. Deformable modelling of facial tissue for craniofacial surgery simulation. *Computed Aided Surgery* 1998: 3(5): 228-238
23. Kershaw DS. The incomplete Cholesky-conjugate gradient method for the iterative solution of systems of linear equations. *Journal of Computational Physics* 1978: 26: 43-65

24. Koch RM, Gross MH, Carls FR, von Büren DF, Frankhauser G, Parish YIH. Simulating Facial Surgery Using Finite Element Models. Proc. of SIGGRAPH 1996: 421-428. ACM Press
25. Lee Y, Terzopoulos D, Walters K. Realistic Modeling for Facial Animation. Computer Graphics, 29 (Annual Conference Series) 1995: 55-62
26. Lorensen WE, Cline HE. Marching Cubes: a High Resolution 3D Surface Construction Algorithm. Proc. of SIGGRAPH 1987: 163-169
27. Maes F, Collignon A, Vandermeulen D, Marchal G, Suetens P. Multimodality image registration by maximization of mutual information. IEEE Transactions on Medical Imaging 1997: 16(2): 187-198
28. Meehan M, Teschner M, Girod S. Three-dimensional Simulation and Prediction of Craniofacial Surgery. Orthod and Craniofac Res 2003: 6(1): 102-107
29. Mollemans W, Schutyser F, Nadjmi N, Suetens P. Very Fast Soft Tissue Predictions with Mass Tensor Model for Maxillofacial Surgery Planning Systems. Proc. of CARS 2005: 491-496
30. Mollemans W, Schutyser F, Van Cleynenbreugel J, Suetens P. Fast Soft Tissue Deformation with Tetrahedral Mass Spring Model for Maxillofacial Surgery Planning Systems. Lecture notes in computer science (MICCAI) 2004: 3217: 371-379
31. Mollemans W, Schutyser F, Van Cleynenbreugel J, Suetens P. Tetrahedral Mass Spring Model for Fast Soft Tissue Deformation. Lecture notes in computer science (IS4TM) 2003: 2673: 145-154
32. Picinbono G, Delingette H, Ayache N. Non-linear anisotropic elasticity for real-time surgery simulation. Graphical Models 2003: 65(5): 305-321
33. Poukens J, Schutyser F, Van Cleynenbreugel J, Riediger D. 3D planning of distraction osteogenesis with Maxilim software. Proceedings 4th International Congress of Maxillofacial and Craniofacial Distraction 2003: 251-254
34. Roose L, De Maerteleire W, Mollemans W, Suetens P. Validation of different soft tissue simulation methods for breast augmentation. Proc. of Int J Comput Assist Radiol Surg 2005: 485-490

35. Saad Y, Schultz MH. A generalized minimal residual algorithm for solving nonsymmetric linear systems. *SIAM Journal on Scientific and Statistical Computing* archive 1986: 7(3): 856-869
36. Sarti A, Gori R, Lamberti C. A physically based model to simulate maxillo-facial surgery from 3D CT images. *Future Generation Computer Systems* 1999: 15(2): 217-221
37. Sarver D. *Esthetic Orthodontics and Orthognathic Surgery*. Mosby,1997: 1 edition
38. Schutyser F, Van Cleynenbreugel J, Ferrant M, Schoenaers J, Suetens P. Image-Based 3D Planning of Maxillofacial Distraction Procedures Including Soft Tissue Implications. *Lecture Notes In Computer Science (MICCAI)* 2000: 1935: 999-1007
39. Schwartz J, Deniger M, Rancourt D, Moisan C, Laurendeau D. Modeling Liver Tissue Properties Using a Non-Linear Visco-Elastic Model for Surgery Simulation. *Med Image Anal* 2005: 9(2): 103-112
40. Smith ID, Thomas PM, Proffit WR. A comparison of current prediction imaging programs. *Am J Orthod Dentofacial Orthop* 2004: 125(5): 527-536
41. Terzopoulos D, Walters K. Physically-based facial modelling, analysis and animation. *Visualization and Computer Animation* 1990: 1(4): 73-80
42. Teschner M. *Direct Computation of Soft-Tissue Deformation in CranioFacial Surgery Simulation*. PhD thesis, Shaker Verlag, Aachen, Germany 2001
43. Tondeur S, Claes P, Vandermeulen D, Suetens P. Regularized on-rigid ICP using variational implicit surfaces for model building. Technical report, KUL/ESAT/PSI/0601, Katholieke Universiteit Leuven, Belgium 2006
44. Vannier MW, Gado MH, Marsh JL. Three-dimensional display of intracranial soft-tissue structures. *Am J Neuroradiol* 1983: 4(3): 520-521
45. Waters K. *A Physical Model of Facial Tissue and Muscle Articulation Derived from Computer Tomography Data*. *Proc. of SPIE* 1992: 574-583
46. Westermark A, Zachow S, Eppley B. Three-Dimensional Osteotomy Planning in Maxillofacial Surgery Including Soft Tissue Prediction. *J Craniofac Surg* 2005: 16(1): 100-104

47. Zachow S, Gladiline E, Hege H-C, Deuffhard P. Finite-Element Simulation of Soft Tissue Deformation. Proc. of CARS 2000: 23-28
48. Zachow S, Hierl Th, Erdmann B. A Quantitative Evaluation of 3D Soft Tissue Prediction in Maxillofacial Surgery Planning. Proc. of 3 Jahrestagung der Deutschen Gesellschaft für Computer- und Robotor-assistierte Chirurgie 2004: 75-79, Munchen
49. Zachow S, Gladilin E, Zeilhofer H, Sader R. Improved 3D Osteotomy Planning in Cranio-maxillofacial Surgery. Lecture Notes In Computer Science (MICCAI) 2001: 2208: 473-48
50. Zienkiewicz OC, Taylor RL. The Finite Element Method: Volume 1 - The Basis. Butterworth Heinemann 2000: London, 5 edition

CHAPTER 7

Virtual occlusion in planning orthognathic surgical procedures.

**N. Nadjmi¹, W. Mollemans², A. Daelemans¹, G. Van Hemelen¹,
F. Schutyser² and S. Bergé³**

1. Department of Cranio-Maxillofacial Surgery, AZ MONICA, Harmoniestraat 68, B-2018 Antwerpen, Belgium;
2. Medical Image Computing (Radiology – ESAT\PSI), Faculties of Medicine and Engineering, University Hospital Gasthuisberg, Herestraat 49, B-3000 Leuven, Belgium;
3. Department of Oral & Cranio-Maxillofacial Surgery, Radboud University Nijmegen, Geert Grooteplein-Zuid 14, 6525 GA Nijmegen, The Netherlands

Int J Oral Maxillofac Surg 2010: 39: 457-462

Abstract

Accurate preoperative planning is mandatory for orthognathic surgery. One of the most important aims of this planning process is obtaining good postoperative dental occlusion. Recently, 3D image-based planning systems have been introduced that enable a surgeon to define different osteotomy planes preoperatively and to assess the result of moving different bone fragments in a 3D virtual environment, even for soft tissue simulation of the face. Although the use of these systems is becoming more accepted in orthognathic surgery, few solutions have been proposed for determining optimal occlusion in the 3D planning process. In this study, a 3D virtual occlusion tool is presented that calculates a realistic interaction between upper and lower dentitions. It enables the surgeon to obtain an optimal and physically possible occlusion easily. A validation study, including 11 patient data sets, demonstrates that the differences between manually and virtually defined occlusions are small, therefore the presented system can be used in clinical practice.

Keywords: Virtual surgery; 3D planning; Occlusion;

Introduction

Virtual planning of orthognathic surgery is an extremely challenging area of research that combines medical imagery, computer graphics and mathematical modeling. Recently, three dimensional (3D) image based planning systems^{3,15,19–23} have become available that enable the surgeon to define necessary osteotomy planes preoperatively and to assess different surgical scenarios virtually. Using this technology means orthognathic surgery can be optimized and surgery time can be reduced.

Obtaining a good and stable dental occlusion is one of the key goals of orthognathic surgery. Traditionally, the final occlusion is defined with plaster casts of the upper and lower dental arches. The surgeon manually searches for a relative position for both casts, to obtain a good and stable occlusion. Based on the defined occlusion, a surgical splint is manufactured and used during surgery, transferring the virtual surgical planning into the operating theatre. This method is accepted as the global 'gold standard' of practice, but working with plaster casts has some drawbacks. First the anatomical information from the complete skull is lost when looking at plaster casts. Second, although some information about the spatial orientation can be obtained from plaster casts mounted in an articulator, this simulation cannot fully enable a surgeon to visualize how the final occlusion may change the morphology of the surrounding hard and soft tissues in 3D. Third, storage of the plaster casts is problem. There is a need to make the manual procedure virtual. With the aim of bringing 3D imaging and computer-aided planning one step closer to practice, a new method to define the desired occlusion between the upper and lower dentition virtually was developed. An experimental study was performed to prove the validity of this new method.

Materials and methods

After making imprints (Alginoplast®, Heraeus Kulzer GmbH, Hanau, Germany), dental plaster casts (Fujirock®, GC, Japan) are manufactured. To obtain digital models of these casts, the upper and lower plaster casts are separately scanned using a Cone Beam CT (CBCT) scanner (i-CAT™ 3D Imaging System, Imaging Sciences International Inc., Hatfield, USA). The scanning resolution is set to 0.2 mm x 0.2 mm x 0.2 mm (voxel resolution). Based on the volumetric CBCT data, surface models of upper and lower dentitions are generated using the marching cubes algorithm with an appropriate threshold⁹(Fig. 1).

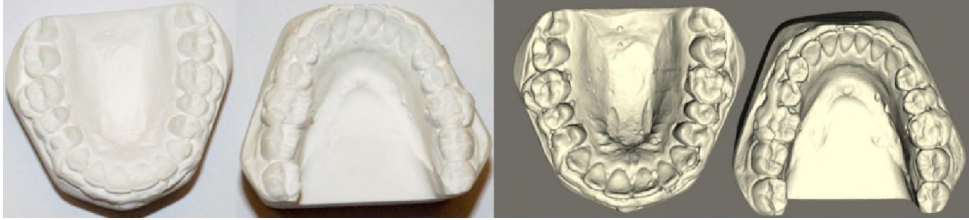


Fig. 1. To obtain digital dental models, plaster cast were separately CBCT scanned.

To allow the user to define a desired occlusion, contact behavior between the dental models should be modeled. Since occlusion is defined as the relative position of the lower and upper dental arches, it is sufficient to move the upper dental arch towards the lower dental arch. In the presented system this movement can be realized by free-hand movements or by guided movements. A combination of both methods is thought to be sufficient to define the desired occlusion virtually. With the free-hand movement tool, the user can freely translate and rotate the upper dental model in a 3D environment (Fig. 2).

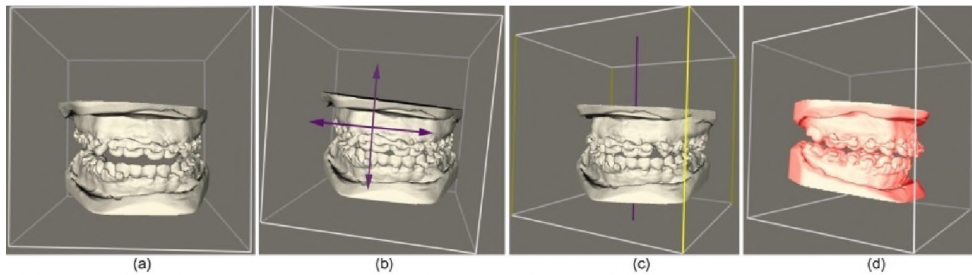


Fig. 2. (a) Initial setup in the 3D environment. (b) The dental model can be translated in any direction and (c) rotated round the X, Y and Z-axes. (d) When the dental models collide, they are colored red and penetration of the models is prevented.

A rigid motion engine is used to calculate whether the upper and lower dental models collide. If collision occurs, the motion applied by the user is cancelled, resulting in temporary fixation of the upper dental model. To emphasize that collision has occurred, both models are colored red. When the user moves the upper dental model to a non-colliding position, the red color disappears. This framework prevents virtual penetration of the upper and lower dental models. This system enables the user to obtain a rough estimate of a good occlusal position. Owing to the irregular shape of the teeth, it is almost impossible and very time consuming to achieve perfect occlusion by manual alignment in the virtual software tool.

An additional guided movement tool was implemented which enables the user to define the final desired occlusion starting from a good initial position. The tool allows the user to indicate corresponding points on the upper and lower dental models manually.

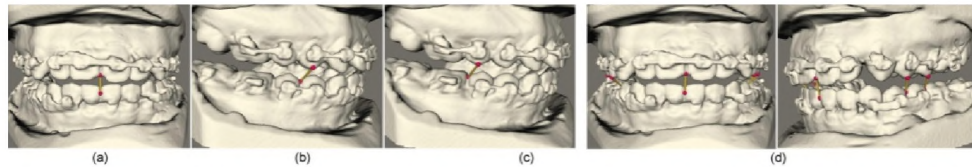


Fig. 3. (a–c) Corresponding points can be indicated manually on the upper and lower dentition models (d).

Typical correspondences are, for example, points on the midline between the upper and lower central incisors (Fig. 3a), the tip of the vestibular cuspid of the first upper premolar and contact points between the first and second lower premolar (Fig. 3b), and the tip of the cuspid of the second upper premolar and the contact point between the second lower premolar and first lower molar (Fig. 3c). After the user has indicated at least three corresponding pairs of points, the system calculates a new position for the upper dental model. This new position is found by minimizing the distance between the indicated correspondences while respecting the impenetrability of the dental models. To assure these requirements, the rigid motion engine is used. To each corresponding pair of points, a ‘spring connection’ is assigned. The forces generated by these springs are applied to the upper dental model. Next, the rigid motion engine is used to calculate the resulting movement of the upper dental model for a short time step. This procedure is successively approximated (iteration); in each approximation step, the spring forces are updated and a new position for the upper dental model is calculated. After a few iterations, the model reaches a stable position, when the forces applied by the springs equal the contact reaction forces defined by the rigid motion engine. If a stable position is found, the result is presented to the user (Fig. 4).

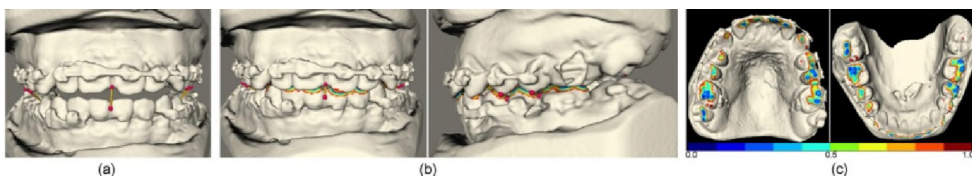


Fig. 4. (a) After defining an initial position with the first tool, correspondences were indicated. (b) Simulation result. (c) To facilitate the dentition of a good occlusion, an occlusionogram is shown.

For this position, the system generates an occlusionogram of the upper and lower dentition. This occlusionogram is a distance map between the upper and lower dentition and gives the user a good idea where the teeth make contact. In the presented occlusionogram, a specific color was assigned to all regions where the distance between both models measures less than 1 mm (Fig. 4c).

By combining the free hand and guided movement tool, the user can iteratively define a good initial starting position and perform several motion simulation steps, finally obtaining good occlusion. To verify this statement, a validation study was performed (Fig. 5).

The dental casts of 11 orthognathic patients were collected. To allow comparison between the manual and virtual approach, only casts that did not require occlusal adjustments of the dentition were selected. For each patient, the upper and lower plaster casts were separately digitized using a CBCT scanner (voxel resolution 0.2 mm x 0.2 mm x 0.2 mm). Three maxillofacial surgeons (A, B and C) were asked to position the upper and lower plaster casts manually in a desired final occlusion and to fix the models together using sticky wax (Associated Dental Products Ltd., Purton Swindow, Wiltshire, UK) (Fig. 5a, first row).

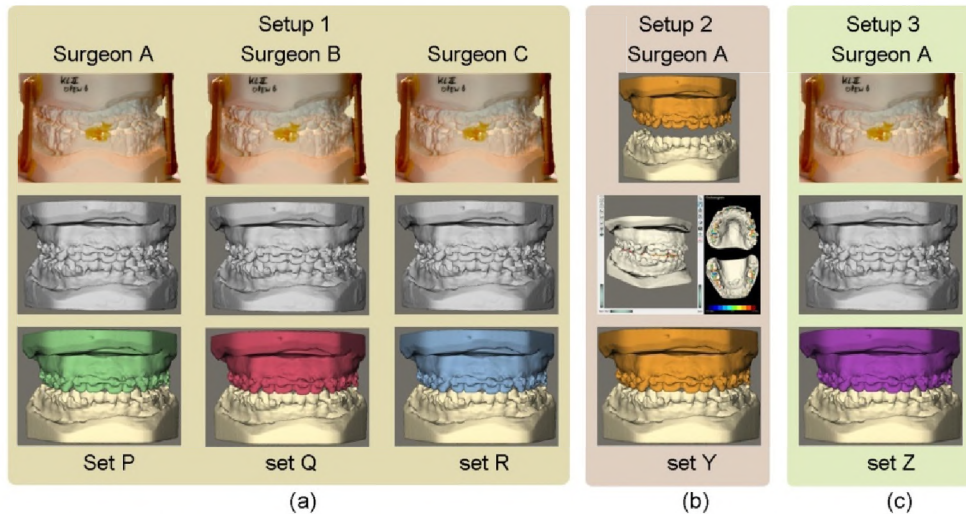


Fig. 5. (a) Manual procedure. First row: manually placed casts and fixed in final occlusion. Second row: digitized sets of casts. Third row: final coaligned casts with separated and color-coded upper casts. (b) Virtual procedure. (c) Repetition of setup 1 for surgeon A after 3 weeks.

The aligned casts, which were fixed in optimal occlusion, were digitized using a CBCT scanner (voxel resolution 0.2 mm x 0.2 mm x 0.2 mm). These CBCT data sets of the plaster casts were superimposed on the CBCT volume of the corresponding lower dental cast. It was ensured that the lower dentitions of all corresponding data sets shared the same position. These aligned data sets were called the co-aligned volumes (Fig. 5 a, second row). To obtain the superimposition, the maximization of mutual information criterion¹⁰ was used. This criterion measures the information redundancy between the image intensities of corresponding voxels between the different CBCT scans. This information is aimed to be maximal when the images are geometrically aligned. To measure the differences in the spatial position of the upper casts in the three different data sets, the upper casts were separated from the lower casts and were color-coded. To obtain this separation a second alignment step was introduced. Each digitized upper plaster cast was aligned to the corresponding co-aligned volume. A set of dentition models in occlusion could be obtained for each surgeon and for each patient (Fig. 5a, third row); these sets were called P, Q and R.

In a second setup, surgeon A was asked to define the desired occlusion for each data set with the presented software system (Fig. 5b). The relative initial position of the upper and lower dental models was randomized. This task resulted in a fourth set of aligned dentition models (set Y).

Finally, surgeon A repeated the first procedure, the manual definition of the desired occlusion for each patient data set (Fig. 5c). This task was performed 3 weeks after finishing the first validation procedure to prevent the surgeon from being biased. A fifth set of aligned dentition models (set Z) was obtained, after digitizing the aligned models and performing the alignment tasks.

The second phase of this study consisted of three steps. First, inter-observer reliability was defined by calculating the distance maps between sets P and Q and later on between P and R. In the second step, the same procedure was performed between sets P and Z to measure the intraobserver reliability. Third, the difference between a manually planned occlusion and an occlusion obtained with the software tool was revealed through the calculation of the distance maps between sets P and Y. For each distance map, the median distance and the 90% and 95% percentiles of the distance distribution were calculated. Since the differences close to the occlusal plane are of utmost importance, a region of interest was defined (Fig. 6a).

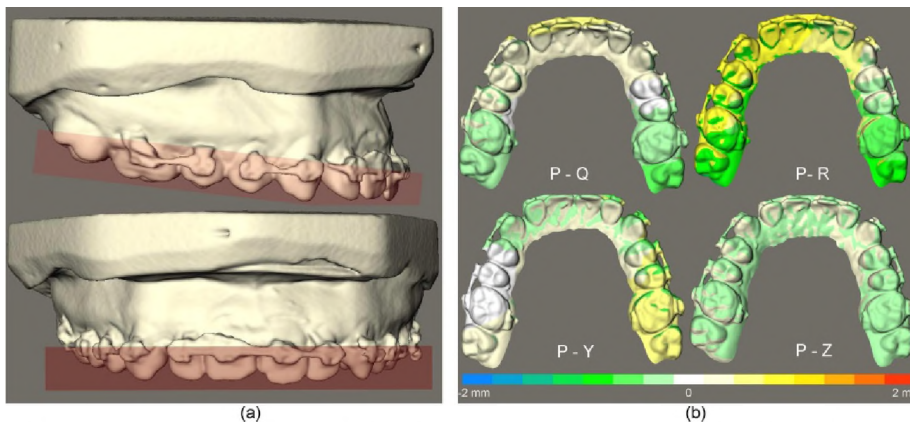


Fig. 6. (a) Distances were only calculated in a small region around the occlusal plane. (b) The distances calculated between different sets can be projected on top of the dental surface mesh by means of a color code. The color bar ranges from -2 mm to 2 mm.

The calculated distance maps are projected on top of the surface mesh by means of a color code.

The software tool was implemented in the Maxilim1 2.0 platform (Medicim NV, Mechelen, Belgium). All tests were performed on a standard personal computer (Pentium IV – 2.0 GHz).

Results

The desired occlusion could be obtained easily with the presented software tools for all 11 data sets (Fig. 6b). Table 1 summarizes the results; each column lists the mean value of the specified statistic over all patient data sets. The median intraobserver variability measured 0.46 mm. Even the 95 percentile statistic was less than 0.8 mm, indicating that the defined occlusions were almost identical. The interobserver variability was higher (average median value 0.72 mm). The median difference between a manual obtained occlusion and an occlusion defined with the software tool was 0.60 mm on average. It was concluded that the plaster-digital variability was slightly higher than the intra-observer variability, but was less than the interobserver variability.

			Median	P 90%	P 95 %
		P-Q	0.89	1.17	1.37
Plaster-	Inter-Variability	P-R	0.55	0.79	0.91
Plaster-	Intra-Variability	P-Z	0.46	0.65	0.76
Plaster-	Digital	P-Y	0.60	0.81	0.91

Table 1. The mean value over all patient data sets of the median, the 90% percentile and the 95% percentile of each distance distribution.

Discussion

Orthognathic surgery is a complex procedure, so accurate planning of the surgery is mandatory. Recently, 3D planning systems have been introduced. These systems start from 3D image data and enable the surgeon to perform 3D cephalometric analysis^{16,19,23}, to execute virtual osteotomies^{1,21,23} while moving bone fragments in a 3D environment, and to simulate the patient's postoperative facial appearance^{4,11,12,21}. These systems offer the surgeon better surgical preparation, but none include virtual planning of dental occlusion. Defining a good occlusion is one of the most important steps in the surgical planning procedure, since it defines the relative position of the mandibular and maxillary bone fragments.

Until now, there have been few reports of how occlusal planning can be combined with a computer-aided planning system. Bettegaet al.² presented a complete computer-aided planning system. Their system allowed the surgeon to perform a 3D cephalometric analysis, split the skull into separate bone fragments, move the bone fragments in 3D and define the position of the mandibular bone fragment based on a defined occlusion. To find this occlusion, plaster casts were used. After manually positioning the lower and upper casts so that the desired occlusion was obtained, the relative movement of the lower cast was transferred to the virtual planning by means of a 3D optical localizer. Later, Chapuiset al.⁵ used the same

concept and presented some case results. They showed that an occlusion could easily be defined with this concept, but their approach and the Bettega system have limitations. First, plaster casts of the upper and lower dentition are still necessary because they are used to define the occlusion. Second, a 3D optical localizer is necessary to transfer the defined occlusion to the computer-aided planning system. These optical systems are expensive and not available in every clinical practice. Third, errors arise in their systems when transferring the manually defined occlusion to the computer-aided planning process.

Pongracz & Bardosi¹⁴ tried to omit the use of plaster casts and created a fully virtual occlusal planning tool. To define a good occlusion, they aligned upper and lower dental models based on corresponding points that were manually indicated. The accuracy of their method is hard to confirm since the contact behavior between the upper and lower dentition is not modeled and the impenetrability of teeth is not guaranteed.

In this study a novel method that virtually defines the occlusion is presented. A rigid motion simulation engine ensures the impenetrability of the dental models. This engine enables the user to identify the desired occlusion semi-automatically. The motion engine allows almost real-time simulations.

The results of the validation study of 11 patient data sets showed that the plasterdigital reliability was slightly higher than the intra-observer reliability, but was less than the inter-observer reliability. It can be concluded that the presented system allows for the reliable determination of the desired occlusion. For less stable occlusions, where an occlusal adjustment in the form of teeth grinding could be necessary, a virtual grinding module was implemented, but not tested in this setup.

Despite these results, the authors acknowledge that virtual planning is not the same as manual planning. During manual planning, the surgeon 'feels' the models as he or she sets the real models in the desired occlusion; during virtual planning, the surgeon has to 'see' the occlusion. Although the presented system offers some solutions to facilitate this detection (e.g., with the occlusionogram), it is admitted that a learning curve is associated with this virtual occlusal planning system.

The system can run on any standard personal computer and no specialized expensive hardware is required. In this way, the presented method can be introduced easily into daily clinical practice. The system is completely virtual and no interactions with plaster casts are necessary. Based on the virtually defined occlusion, one can generate a virtual surgical splint^{6,8}. These surgical splints are used to transfer the planned occlusion to the operation theatre. Since the presented system is completely digital, it should be easy to generate splints in a fully automated process, as opposed to producing them by manufacturing. Recent efforts on realizing skeletal virtual models including accurate dental surface information have been published^{7,13,17}. The presented system enables the user to define the

desired occlusion for these 'augmented models'¹⁸. Once plaster casts are no longer required their generation and storage will no longer be necessary.

Having integrated the presented system into an orthognathic planning system (that allows 3D cephalometrics, the performance of osteotomies and the movement of bone fragments), the first complete orthognathic planning system is now a reality.

References

1. Bell WH, Guerrero CA. Distraction Osteogenesis of the Facial Skeleton. BC Decker Inc. 2007: 55–79
2. Bettega G, Payan Y, Mollard B, Boyer A, Raphael B, Lavallee S. A simulator for maxillofacial surgery integrating 3D cephalometry and orthodontia. *Comput Aided Surg* 2000; 5: 156–165
3. Burk DL, Mears DC, Cooperstein LA, Herman GT, Udupa JK. Threedimensional computed tomographic imaging and interactive surgical planning. *J Comput Tomogr* 1986; 10: 1–10
4. Chabanas M, Luboz V, Payan Y. Patient specific finite element model of the face soft tissues for computerassisted maxillofacial surgery. *Med Image Anal* 2003; 7: 131–151
5. Chapuis J, Schramm A, Pappas I, Hallermann W, Schwenzer-Zimmerer K, Langlotz F, Caversaccio M. A new system for computer-aided preoperative planning and intraoperative navigation during corrective jaw surgery. *IEEE Trans Inform Technol Biomed* 2006; 11: 274–287
6. Gateno J, Teichgraeber Jf, Xia J. Method and apparatus for fabricatingorthognathic surgical splints (US patent no. 6,671,539), in USPTO Patent Full- Text and Image Database. December 30, 2003, US Patent and Trademark Office.
7. Gateno J, Xia J, Teichgraeber JF, Rosen A. A new technique for the creation of a computerized composite skull model. *J Oral Maxillofac Surg* 2003; 61: 222–227
8. Gateno J, Xia J, Teichgraeber JF, Rosen A, Hultgren B, Vadrnais T. The precision of computer-generated surgical splints. *J Oral Maxillofac Surg* 2003; 61: 814–817
9. Lorensen WE, Cline HE. Marching cubes: a high resolution 3D surface construction algorithm. *Proc of SIGGRAPH*. 1987: 163–169
10. Maes F, Collignon A, Vandermeulen D, Marchal G, Suetens P. Multimodality image registration by maximization of mutual information. *IEEE Trans Med Imaging* 1997; 16: 187–198
11. Meehan M, Teschner M, Girod S. Three-dimensional simulation and prediction of craniofacial surgery. *Orthodont Craniofacial Res* 2003; 6 (1):102–107

12. Mollemans W, Schutyser F, Nadjmi N, Maes F, Suetens P. Predicting soft tissue deformations for a maxillofacial surgery planning system: from computational strategies to a complete clinical validation. *Med Image Anal* 2007; 11: 282–301
13. Nkenke E, Zachow S, Benz M, Maier T, Veit K, Kramer M, Benz S, Hausler G, Neukam FW, Lell M. Fusion of computed tomography data and optical 3d images of the dentition for streak artefact correction in the simulation of orthognathic surgery. *Dentomaxillofac Radiol* 2004; 33: 226–232
14. Pongracz F, Bardosi Z. Dentition planning with image-based occlusion analysis. *Int J Comput Assist Radiol Surg* 2006; 1: 149–156
15. Schutyser F, Van Cleynenbreugel J, Ferrant M, Schoenaers J, Suetens P. Image-based 3D planning of maxillofacial distraction procedures including soft tissue implications. *Lecture Notes Computer Sci (MICCAI)* 2000; 1935: 999–1007
16. Swennen G, Schutyser F, Hausamen JE. *Three-Dimensional Cephalometry. A colour Atlas and Manual.* Springer 2005: 7-32
17. Swennen G, Mommaerts M, Abeloos J, Clercq CD, Lamoral P, Neyt N, Casselman J, Schutyser F. The use of a wax bite wafer and a double computed tomography scan procedure to obtain a three-dimensional augmented virtual skull model. *J Craniofac Surg* 2007; 18: 533–539
18. Swennen G, Mollemans W, De Clercq C, Abeloos J, Lamoral P, Lippens F, Neyt N, Casselman J, Schutyser F. A cone-beam computed tomography triple scan procedure to obtain a three-dimensional augmented virtual skull model appropriate for orthognathic surgery planning. *J Craniofac Surg* 2009; 20: 297–307
19. Troulis MJ, Everett P, Seldin EB, Kikinis R, Kaban LB. Development of a three-dimensional treatment planning system based on computed tomographic data. *Int J Oral Maxillofac Surg* 2007; 31: 349–357
20. Westermark A, Zachow S, Eppley B. Three-dimensional osteotomy planning in maxillofacial surgery including soft tissue prediction. *J Craniofac Surg* 2005; 16: 100–104
21. Xia J, Samman N, Yeung RW, Shen SG, Wang D, Ip HH, Tideman H. Three-dimensional virtual reality surgical planning and simulation workbench for orthognathic surgery. *Int J Adult Orthodon Orthognath Surg* 2000; 15: 265–282

22. Xia JJ, Gateno J, Teichgraeber JF. Three-dimensional computer-aided surgical simulation for maxillofacial surgery. *Atlas Oral Maxillofac Surg Clin North Am* 2005; 13: 25–39
23. Zachow S, Hege H, Deuhard P. Computer assisted planning in cranio-maxillofacial surgery. *J Comput Inform Technol—Special Issue on Computer-Based Craniofac Model Reconstruct* 2006; 14: 53–64

CHAPTER 8

Quantitative validation of a computer aided maxillofacial planning system, focusing on soft tissue deformations

N. Nadjmi¹, E. Defrancq¹, W. Mollemans², G. Van Hemelen¹, S. Bergé³

1. Cranio-Maxillofacial Unit, AZ MONICA, Harmoniestraat 68, B-2018 Antwerp, Belgium
2. Medical Image Computing (Radiology - ESAT/PSI), Faculties of Medicine and Engineering
University Hospital Gasthuisberg, Herestraat 49, B-3000 Leuven, Belgium
3. Department of Oral and Maxillofacial Surgery, Radboud University Nijmegen, Medical Centre, Nijmegen, the Netherlands

Submitted 2011 Int J Oral Maxillofac Surg

Abstract

The aim of this study was to evaluate the accuracy of 3D soft tissue predictions generated by a computer aided maxillofacial planning system in patients undergoing orthognathic surgery. Twenty patients with dentofacial dysmorphism were treated with orthognathic surgery, after a preoperative orthodontic treatment. Surgeries were planned with the Maxilim software. Computer assisted surgical planning was transferred to the patient by digitally generated splints. The validation procedures were performed in different steps: 1) Standardized registration of the pre- and postoperative Cone Beam CT volumes; 2) Automated adjustment of the bone related planning to the actual operative bony displacement; 3) Simulation of soft tissue changes accordingly; 4) Calculation of the soft tissue differences between the predicted and the postoperative results by distance mapping. Eighty four percent of the mapped distances between the predicted and actual postoperative results measure between -2 mm and +2 mm. The mean absolute linear measurements between the predicted and actual postoperative surface was 1.18. Our study shows that the overall prediction was not dependent on the surgical procedure. Despite some shortcomings in prediction of the final position of the lower lip and cheek area, this software promises a clinically acceptable soft tissue prediction of orthognathic surgical procedures.

Keywords Virtual surgery, 3D planning, Orthognathic surgery, Soft tissue prediction

Introduction

Achieving optimal results in orthognathic surgery depends among others on the accuracy of the surgical planning in addition to the used surgical technique. The scanning of the patients in natural head position (NHP) with cone-beam computed tomography (CBCT), accurate visualization of the interocclusal relationship in the 3-dimensional (3D) model of the patient's skull⁸, adding highly detailed texture information to the skin that is segmented out of the CBCT by using 3D photographs or mapping of traditional 2-dimensional (2D) photographs, and virtual occlusion planning⁷ have made the 3D maxillofacial planning systems an indispensable part of the modern orthognathic practice. 3D virtual treatment planning allows a better preparation that might improve surgical outcome and shorten operation time⁶. The aim of this study was to quantitatively evaluate the accuracy of 3D soft tissue predictions generated by a computer aided maxillofacial planning system in patients undergoing orthognathic surgery.

Materials and Methods

The study protocol was approved by the local ethics committee (DIRSEC/EC/119, AZ Monica, Antwerp, Belgium). A total of 20 consecutive patients aged 15–42 years with dentofacial malformations, who underwent orthognathic surgery, between mid-November and December 2008 were included in the study. Informed consent was obtained from the participating patients who met the study criteria.

Inclusion criteria

- Generally healthy patients
- Completed preoperative orthodontic treatment
- Patients selected for: Le Fort I ± Bilateral Sagittal Split Osteotomy ± Genioplasty

Exclusion criteria

- Syndromic patients
 - Previous orthognathic surgery
 - Patients who did not met the inclusion criteria
-

A full extended height cone-beam CT (CBCT) (i-CATTM, Imaging Sciences International, Inc., Hatfield, USA) was used for the standard scanning protocol (field of view, 17 cm diameter/22 cm height; scan time, 2 x 20 seconds; voxel size 0.4 mm). A multidimensional hard and soft tissue patient-specific virtual model was computed⁸. All procedures were planned in Maxilim (Medicim NV, Mechelen, Belgium). The bony surgery was virtually performed and transferred to the patients by using computer-generated surgical splints². A postoperative CBCT-scan was taken four months after surgery with orthodontic brackets still in place. In order to minimize the effect of the head position on the intermaxillary relationship and facial soft tissues, the following standard protocol was used during preoperative and

postoperative scanning procedures: the preoperative and postoperative scans were taken with patient in natural head position (NHP), while gently biting on a very thin wax wafer in centric relation. The NHP was obtained by asking the patient to stand up and look at his/her image in the mirror. Then the distance between the supra-sternal notch and the soft tissue pogonion was measured. We called this distance, the natural head distance (NHD), and made sure that NHD was respected during the pre- and postoperative scanning procedure (Fig. 1).



Fig. 1. Patient positioned in NHP, NHD was respected during the pre- and post-operative scanning procedure.

Furthermore all the steps during validation process were automated and incorporated in the software to eliminate human errors. The calculations were performed on a standard personal computer with an Intel Centrino processor and 2 GB RAM. The entire validation process was executed by one single examiner (ED) and included 4 steps as described below.

Step 1: Standardized Registration

To compare the pre-operative simulation of the soft tissue changes and the post-operative data, both image data sets had to share the same spatial reference frame, therefore a registration of the pre- and post-operative CBCT volumes was executed. This registration process was fully automated and incorporated in the software. Basically it involved maximization of mutual information which is a well known registration algorithm⁵. The registration is applied on an unaltered sub-volume, manually defined as the region between the infraorbital rim and the rest of the scanned viscerocranium. After defining the registration parameters for this sub-volume, the transformation was applied to the whole post-operative dataset (Fig. 2).

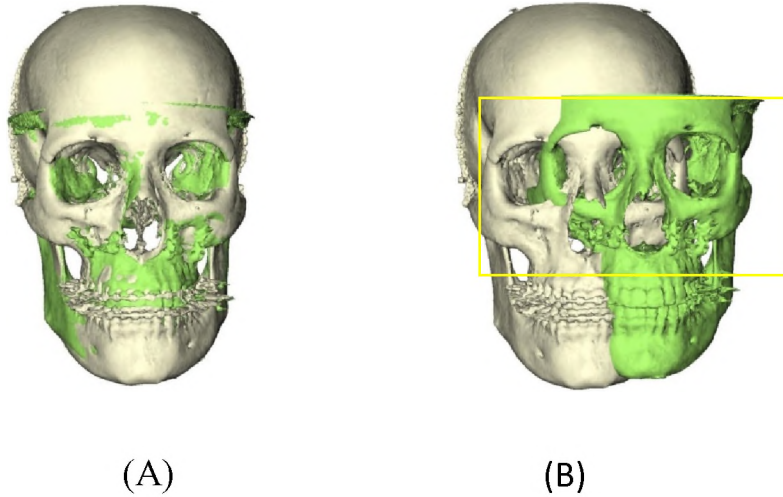


Fig. 2. 3D reconstruction of the pre- (white) and post- (green) operative skull before (A) and after registration(B). The yellow frame indicates the selected registration area

Step 2: Automated adjustment of the bone related planning

Since the validation of the accuracy of the soft tissue simulator was the aim of this study, the simulated planned procedure had to be the same as the one performed by the surgeon per-operatively. Therefore in the second stage of the validation procedure the virtually osteotomised bone fragments were moved to the real postoperative position, using the rigid Iterative Closest Point (ICP) algorithm to get the best alignment between simulated and postoperative bone segments and to align the surfaces^{2,6} (Fig. 3).

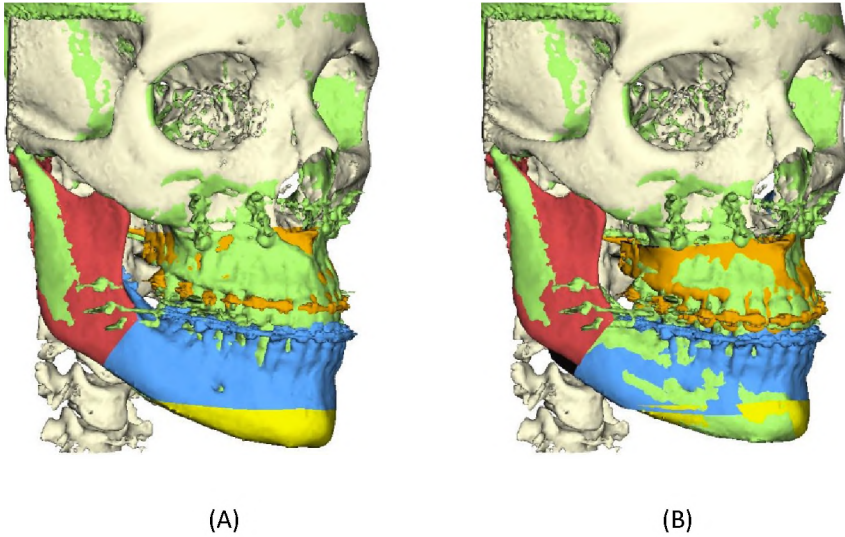


Fig. 3. The rigid Iterative Closest Point (ICP) algorithm was used to align the surfaces of osteotomised maxilla (brown) and the proximal segment of the mandible (blue) with the postoperative bony segments (green). (A) before alignment and (B) after alignment. White area shows the unaltered bony structures. Yellow color shows the osteotomised chin.

Step 3: Simulation of soft tissue changes

The soft tissue changes caused by the movement of the osteotomised bony segments as derived in the previous step, were automatically simulated by the software(Fig. 4).

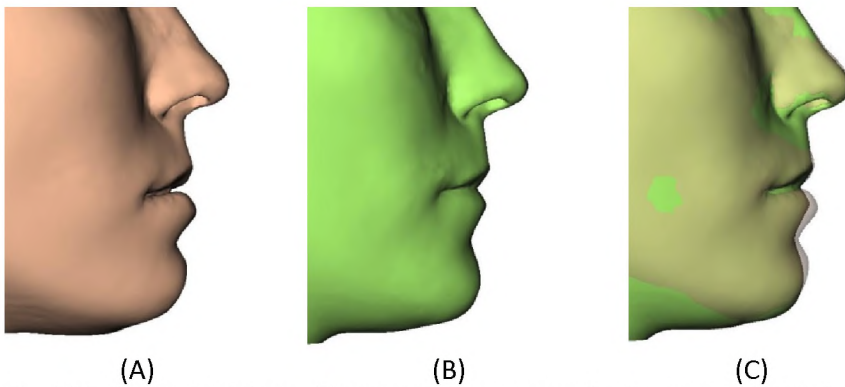


Fig. 4.(A): simulated soft tissue, (B): actual postoperative. profile, (C): overlap simulated-actual postoperative profile.

The software uses a biomechanical simulation model to calculate these changes⁶. This biomechanical model uses no hard/soft tissue movement ratios, but directly triesto mimic the 3D elastic deformation behaviour of facial soft tissues.

Step 4: Calculation of differences

In the final stage of the validation process the distances between the closest points of the simulated and the post-operative facial outlook were computed. Typically

around 8000 points uniformly spread around the patient's face were used. The measured distances were visualized by projecting these distances onto the postoperative facial skin surface by means of a colour code⁶, which resulted in an easy interpretable image of the error distribution over the facial skin surface (Fig. 5). In addition the statistical properties for each distance map were calculated using Matlab (MathWorks Inc, Natick, United States).

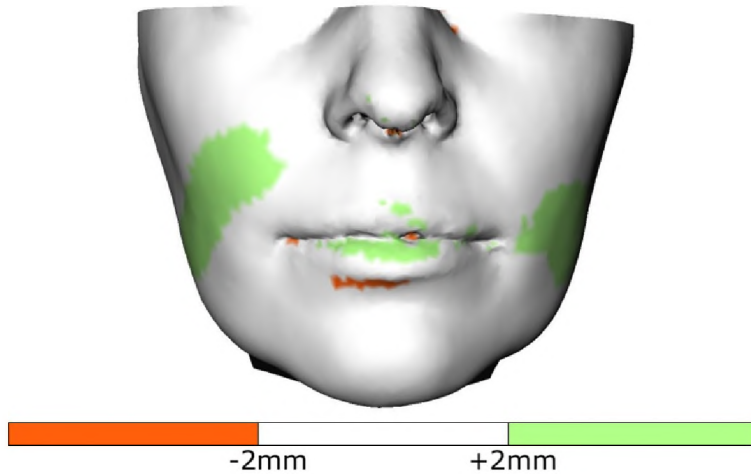


Fig. 5. Distance map with the measured errors projected on to the post-operative facial skin surface. Green indicates under-simulated regions (postoperative in front of prediction).

In order to describe the distribution of the errors, the mean signed distance of the absolute value, the 25-75% distance range, and the 5-95% distance range for each data set were computed (fig 6).

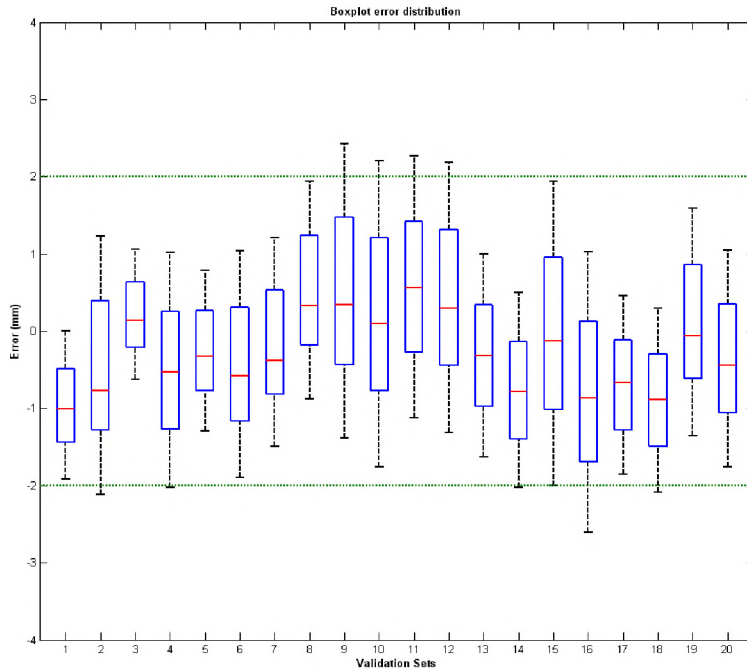


Fig. 6.: The boxplot presents the mean signed distance (red bar), the 25-75% distance range (blue box) and the 5-95% distance range (dotted lines) for each data set.

Results

Twenty patients, 14 females and 6 males, age 14 to 43 years (mean age 23 years; SD 9) met the inclusion criteria. In 11 patients a bimaxillary procedure was performed. In 6 patients this was combined with a genioplasty. Two patients underwent a bilateral sagittal osteotomy and in one of those 2 patients this was combined with a genioplasty.

Averaging over all 20 patients, the mean absolute difference between the predicted and actual postoperative surface was 1.18 mm. In fig. 6 the boxplot presents the mean signed distance (red bar), the 25-75% distance range (blue box) and the 5-95% distance range (dotted lines) for each data set. Visual inspection of the predicted skin surfaces, shows areas of inaccuracy are mostly around the lips and in the cheek area (Fig. 7).

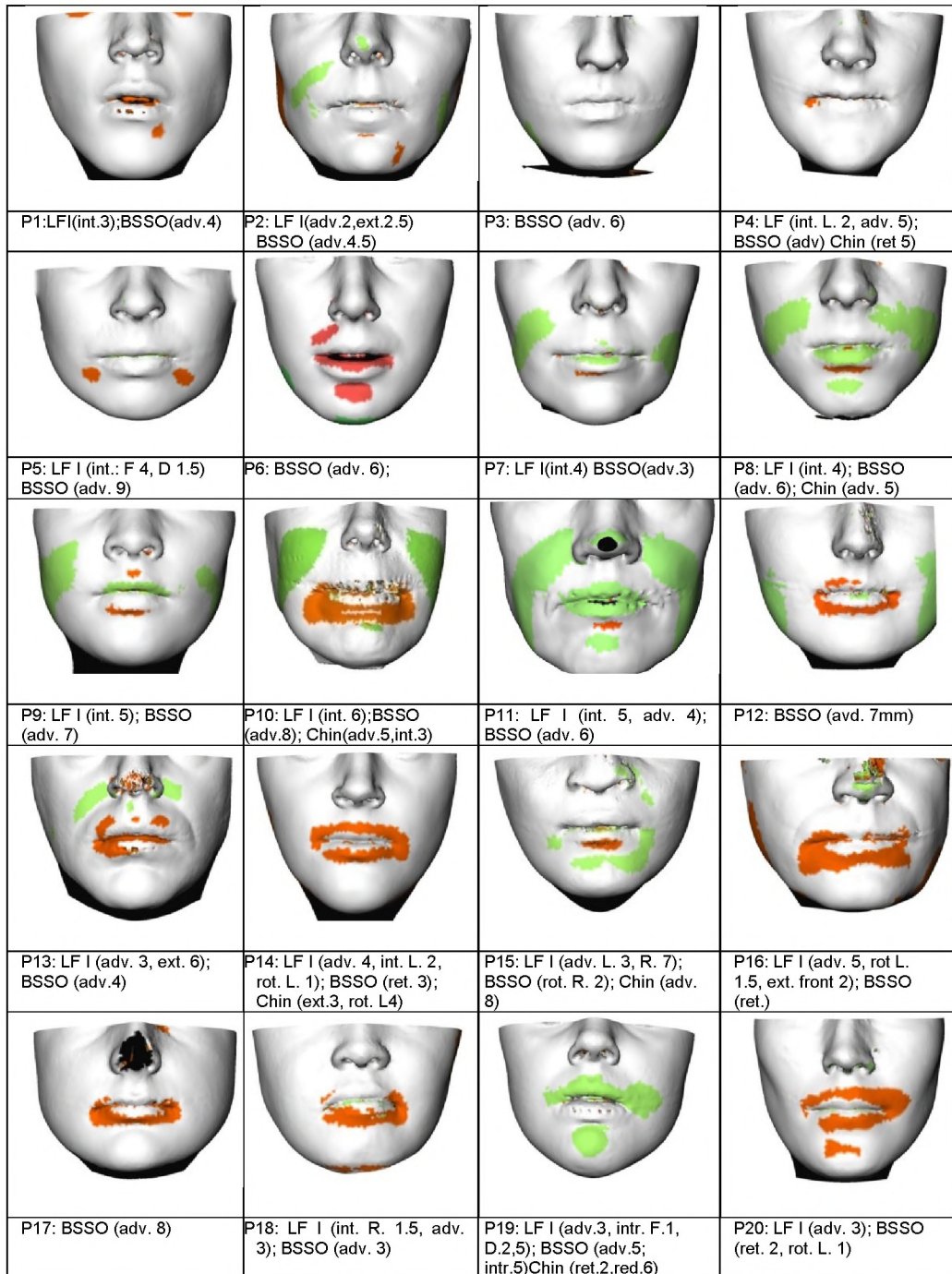


Fig. 7. Colour coded distance maps for all patients. Green is -2mm and red is +2mm. The performed procedure is mentioned below each distance map. The definition of the abbreviation is as follows: LF I: Le Fort I, BSSO: bilateral sagittal split osteotomy, int.: intrusion, ext.: extrusion, adv.: advancement, rot.: rotation, L.: left, R.: right.

The performed procedure and the amount of movements are as well depicted. Visual analysis of the distance maps showed that the inaccuracy in the prediction increased with the amount of bony displacement. The overlapped simulated and actual post-operative profiles are demonstrated in fig. 8.

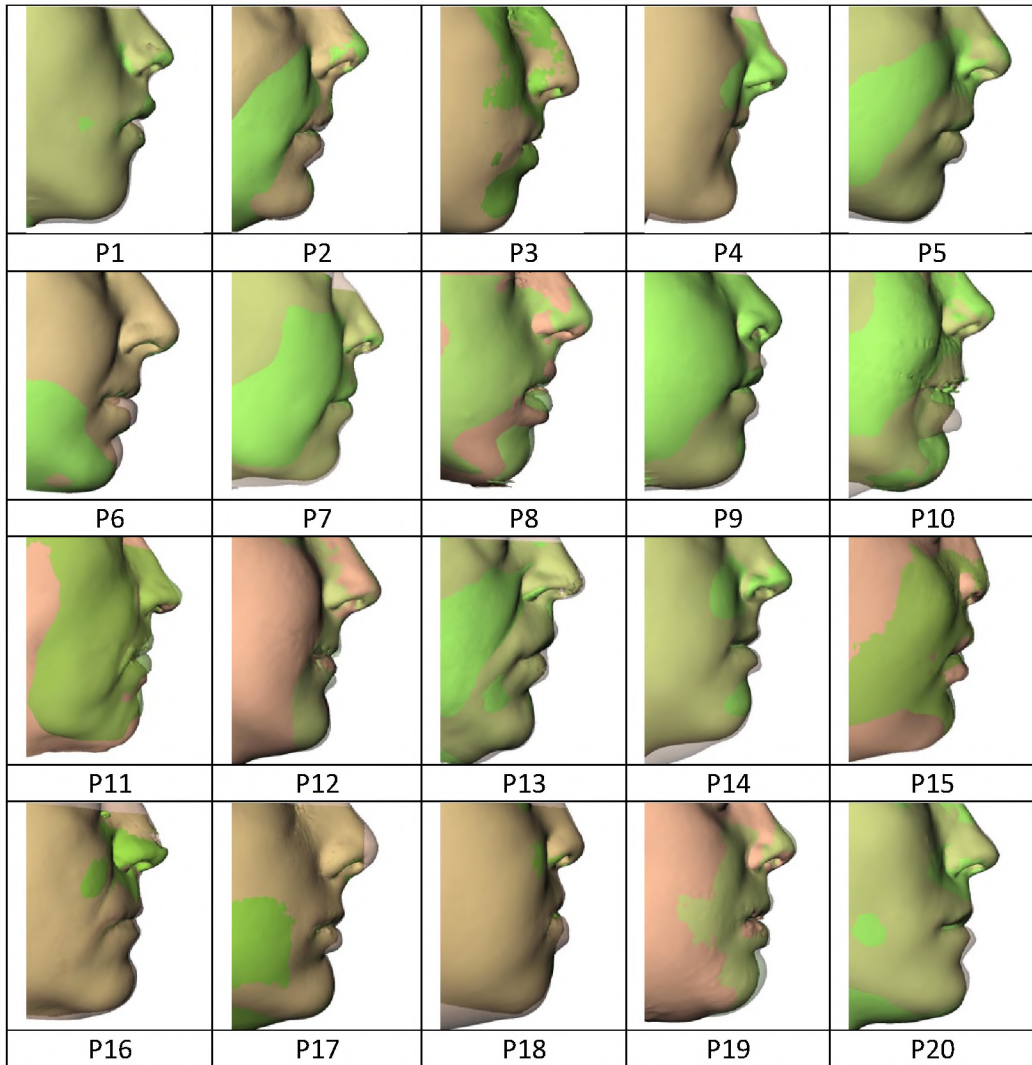


Fig. 8. The overlapped simulated (brown) and actual post-operative (green) profiles.

Discussion

The success of complex orthognathic surgical procedure is, among other factors, dependent on careful planning that could be reproduced in the operating room¹⁰. Common practice in 3D assisted orthognathic surgery revealsthe planning of bony structures and predicting the soft tissue changes. A few important questions rise in this concern: 1) How accurately can the computer assisted bone surgery be transferred to the patient? 2) How reliable is the soft tissue simulation? 3) Is this simulation reliable enough, in order to enhance (change) the original orthognathic planning? 4) Shouldn't we after all be working the other way round: making a patient specific 'ideal' aesthetic soft tissue contour and volume and measure and predict the amount of bony movement we need to achieve the ideal?

The aim of this study was to find an answer to the 2nd and the 3th question, while eliminating the first question by virtually ensuring that the planned procedure is the same as the one performed by the surgeon. Therefore the bone-related planning was adapted so that it resembled the performed surgery as much as possible.

The first study that systematically evaluated the accuracy of computer prediction programs was published recently by Kaipatur and Flores-Mir⁴. They concluded that the most significant area of error in prediction through the available computer prediction programs was the lower lip area. However the measurements in their selected studies were performed only in 2-dimentionis, being horizontal and vertical mean measurements. Furthermore the measurement on the same axis of two equal prediction errors in a different direction will neutralize each other and would result in a 0 mean value which would falsely presume a perfect prediction result. In other words the mean value should be taken from the absolute prediction error and this would always be a positive value. In the study of Kaipatur⁴ some of the mean values of prediction error were negative, which could indicate this conceptual mistake was made in several reviewed articles.

Xia et al.⁹ reported the accuracy of their computer-aided surgical simulation system in a pilot study, but failed to report the absolute mean value of the error in their results. Therefore, the mean of the absolute error, as presented in our analysis, can't be compared to the one presented by Xia et al.⁹

In this study only areas that were altered during surgery where included in the error map. Including the complete skull would 'falsely' improve our simulation results, because non-altered areas would be good 'simulated'. Generally a difference within 2 mm between the predicted and actual postoperative soft tissue result is considered to be clinically acceptable¹. In our study, averaging over all 20 patients, the mean absolute difference between the predicted and actual postoperative surface was 1.18mm, and 84% of the prediction errors were situatedbetween -2 mm and +2 mm. Our study revealed that although the quality of the prediction varied

between the patients, the overall prediction error was not dependent on the surgical procedure. This is in contrast to the study performed by Jacobson et al.³.

The visual evaluation of the colour coded distance maps and the overlapped profile images for all patients, showed that the nasal and paranasal areas are better simulated than the areas around the lips (particularly the lower lip, P6, P8, P10, P11, P18). We suggest three main reasons why the lip movement is less accurately simulated. The first reason is the connection between lower and upper lip: the current soft tissue model cannot explicitly separate the lips from each other during simulation. This causes problems when the lips are in contact and not in a relaxed position during preoperative CT. Secondly, lack of optimal definition of boundary condition, like sliding contact behaviour between teeth and lips, may be another reason. So even when the lips are in a relaxed position during the preoperative CT, still the upward movement, and inward rotation of the lower lip is not precisely simulated. Thirdly, lack of proper simulation of the adaptation of mental and orbicularis oris muscles after harmonization of occlusion may negatively influence the results. Besides the errors in the lower lip, another error region was observed in the cheek area. These were observed in intrusion cases where the impaction of the upper jaw exceeded 4 mm (see green bands on the distance maps of P7, P8, P9 and P10 in Fig. 6). Our hypothesis is that the soft tissues adjusted to the area of bony impaction are less cranially displaced as simulated by the biomechanical model used in this software. We believe what happens to the soft tissue surrounding the maxilla after impaction procedure depends on the suturing technique of the subcutaneous soft tissue and the elasticity of the overlying cutaneous tissue. So far, these factors cannot be incorporated in the current biomechanical model.

In conclusion, the results of this study, despite the shortcomings explained above, encourages the use of this software in all different combinations of orthognathic surgical procedures. Further intensive research is mandatory to enhance the prediction results of the lower lip region and the cheek area where maxillary impaction of more than 4mm is performed.

References

1. Donatsky O, Bjørn-Jørgensen J, Holmqvist-Larsen M, Hillerup S. Computerized cephalometric evaluation of orthognathic surgical precision and stability in relation to maxillary superior repositioning combined with mandibular advancement or setback. *J Oral Maxillofac Surg* 1997; 55(10): 1071-9: discussion 1079-1080
2. Gateno J, Xia J, Teichgraeber JF, Rosen A, Hultgren B, Vadvais T. The precision of computer-generated surgical splints. *J Oral Maxillofac Surg* 2003; 61(7): 814-817
3. Jacobson, R. and D.M. Sarver. The predictability of maxillary repositioning in LeFort I orthognathic surgery. *Am J Orthod Dentofacial Orthop* 2002; 122(2): 142-154
4. Kaipatur, N.R. and C. Flores-Mir. Accuracy of computer programs in predicting orthognathic surgery soft tissue response. *J Oral Maxillofac Surg* 2009; 67(4): 751-759
5. Maes F, Collignon A, Vandermeulen D, Marchal G, Suetens P. Multimodality image registration by maximization of mutual information. *IEEE Trans Med Imaging* 1997; 16(2): 187-198
6. Mollemans W, Schutyser F, Nadjmi N, Maes F, Suetens P. Predicting soft tissue deformations for a maxillofacial surgery planning system: from computational strategies to a complete clinical validation. *Med Image Anal* 2007; 11(3): 282-301
7. Nadjmi N, Mollemans W, Daelemans A, Van Hemelen G, Schutyser F, Bergé S. Virtual occlusion in planning orthognathic surgical procedures. *Int J Oral Maxillofac Surg* 2010; 39(5): 457-462
8. Swennen GR, Mollemans W, De Clercq C, Abeloos J, Lamoral P, Lippens F, Neyt N, Casselman J, Schutyser F. A cone-beam computed tomography triple scan procedure to obtain a three-dimensional augmented virtual skull model appropriate for orthognathic surgery planning. *J Craniofac Surg* 2009; 20(2): 297-307
9. Xia J, Samman N, Yeung RW, Wang D, Shen SG, Ip HH, Tideman H. Computer-assisted three-dimensional surgical planing and simulation. 3D soft tissue planning and prediction. *Int J Oral Maxillofac Surg* 2000; 29(4): 250-258

10. Xia J, Wang D, Samman N, Yeung RW, Tideman H. Computer-assisted three-dimensional surgical planning and simulation: 3D color facial model generation. *Int J Oral Maxillofac Surg* 2000; 29(1): 2-10

General discussion and future perspectives

Introduction

The aim of treating abnormalities of the dento-craniofacial complex, is to improve the patient's function and aesthetics. The skeletal remodeling in the course of these treatments implies performing osteotomies, bone grafting, distraction osteogenesis, implant placement, and other treatment modalities. The effect of these treatments has a direct influence on the patients personal and social wellbeing³. Therefore the challenge of maxillofacial surgeons in the 21st century is to achieve excellence in treating more than ever demanding patients. Patient's demands and expectations have risen dramatically in the past decade, especially when it comes to the changes in facial appearance after maxillofacial procedures⁰. Due to the complexity of the surgical procedures, careful pre-operative planning of the surgical intervention is mandatory to ensure an optimal outcome. Implementation of technical advances in medical three-dimensional (3D) imaging in the field of distraction osteogenesis and orthognathic surgery has been the motivation of this work. This thesis summarizes my research work of the past 12 years that has been performed in two phases.

In the first phase (1998-2004), I tried to use the available knowledge in 3D imaging at that time to introduce a computer planning system to simulate distraction osteogenesis (DO) in patients with maxillary hypoplasia, in particular cleft patients. This initial research resulted in the development of the Maxilim software (Medicim, Mechelen, Belgium), which was unique in its type in those days. It was first used to simulate a maxillary DO, using a trans-sinusal maxillary distraction (TSMD) device developed by myself in 2000^{12,12,19}. As this 3D bone-related planning system proved to be reliable in surgical planning of DO, I assumed, it might as well be useful in the planning of complex cases in orthognathic surgery.

Ideally, the software should be able to virtually predict the effect of orthognathic procedures in exceptionally complex situations, and where necessary to adapt them to ensure an excellent outcome.

In the second phase of my work (2004-2010), and with the help of many other researchers^{11,16} the Maxilim software was adapted to help in planning and simulation of hard and soft tissue changes after orthognathic procedures.

The first phase

The Initial work was concentrated in the field of distraction osteogenesis (DO) in patients with maxillary hypoplasia, in particular patients with clefts. Shortly after the introduction of extraoral DO, research on the development of intraoral devices started. The external devices, were cumbersome, highly visible, and were mostly not well tolerated by patients¹⁹. The suggested intraoral devices had two main disadvantages. Firstly, they were still too bulky, and were placed completely under the periosteum. The activation rods were either in continuous contact with lips, causing pain and irritation, or had to be delivered through the skin in the nasolabial region^{5,9,18}. Secondly, they were all unidirectional, which required a perfect preoperative vector planning.

To overcome the first disadvantage, I designed a distractor in a way that the distraction screw could be placed inside the sinus cavity, and would significantly diminish the size of the subperiosteal portion of the device. Furthermore according to the literature the human sinus, even at the age of 6 to 8 years would be deep enough to provide room for the distraction screw. This is not significantly different in patients with clefts^{1,6,20}. Keeping these facts in mind, the first intraoral, trans-sinusal prototype was made and used in an animal study (Chapter 2 & 3). The positive results of this study encouraged the use of the device in distraction of the maxilla in children and adults with midfacial hypoplasia. Subsequently a clinical prototype was designed and manufactured by KLS-Martin Medizin-Technik, Tuttlingen, Germany.

The second challenge that had to be overcome, was the prediction of the distraction vector pre-operatively and transferring it to the patient per-operatively. In cooperation with ESAT KULeuven, Belgium, software, that could virtually place the distractor device on the maxilla of the patient after a virtual Le Fort I type osteotomy, was developed. The distractors were virtually positioned at the Le Fort I level and the distraction was simulated by using a vector that was determined based on clinical examinations. Furthermore the entry point of the screw, the depth of the sinus, the position of the tooth buds and the roots of the teeth could be studied carefully. The unique information provided by the 3D environment made the procedures not only more predictable, but also safer to perform, especially in younger individuals. Subsequently different clinical studies were undertaken and were published as preliminary results and later on as a critical evaluation of the clinical applicability and the long-term follow up of the Trans Sinusal Maxillary Distractor (TS-MD)^{12,13,19} (Chapter 4 & 5).

The second phase

Development of a biomechanical model for soft tissue simulation

Although the above mentioned 3D bone-related planning system proved to be reliable in surgical planning of DO, it was not possible at that time to predict the

changes of the overlying soft tissue envelop during the DO. In other words, one could not foresee or judge the final esthetic results. As a consequence, the next step was the development of a biomechanical simulation model that would use no hard/soft tissue 2D movement ratio's, but would attempt to simulate the 3D elastic deformation behaviour of facial soft tissues after bony displacement¹¹(Chapter 6).

Four computational strategies were compared to simulate the post-operative facial appearance: a linear Finite Element Model, a non-linear Finite Element Model, a Mass Spring Model and a new Mass Tensor Model. The introduction of this last model showed a significant time gain in simulation time compared to the two traditional used models: the linear Finite Element Model and the Mass Spring Model. Further the accuracy of the prediction of the new facial outlook after surgery was assessed. The best results were obtained by usage of the linear Finite Element Model or the Mass Tensor Model.

These results were confirmed by the qualitative validation study in which surgeons rated the predictions as 'good' and 'relevant' for usage in daily clinical practice. However, further improvements were needed in the nasal and perioral area, since these regions were defined as being most error-sensitive during the validation study¹¹.

Implementation of the hard-soft tissue simulator in orthognathic surgery

In order to make this software beneficial in the daily practice of orthognathic surgery two main additional developments had to be implemented. Firstly the occlusal surface of the teeth had to be visualized with high precision, and secondly a virtual planning of dental occlusion was mandatory. Swennen et al. succeeded to implement the first change in the software using their triple scanning technique¹⁶. It was now necessary to define the virtual occlusion in order to predict the final facial appearance after the ideal positioning of the maxilla in complex bimaxillary procedures was determined. This would allow the simulation of the final soft tissue changes. The first challenge was to make the virtual occlusal surfaces impenetrable, so that they would resemble the use of dental casts when put into an optimal position. A novel method that virtually defined the occlusion was therefore developed¹⁴. A rigid motion simulation engine ensured the impenetrability of the dental models. Moreover, this engine enabled the user to identify the desired occlusion semi-automatically. The motion engine allowed almost real-time simulations. This software tool was validated and the result showed that the presented system allowed a reliable determination of the desired occlusion¹⁴.

Since the system was completely virtual, and incorporated the occlusal surface information precisely by using augmented models¹⁶, no additional interactions with dental casts were necessary. Further, based on the virtually defined occlusion, one could generate a virtual surgical splint as already presented by Gateno et al.³

However, splints could now be generated in a fully automated process in contrast with producing them by manufacturing.

After having integrated the presented system into an orthognathic planning system (that allows 3D cephalometrics, the performance of osteotomies and the movement of bone fragments), the first complete orthognathic planning system became a reality.

A validation of the soft tissue changes after prediction of the precise intermaxillary relationship became the subject of chapter 8 of this thesis. In contrast to the recent studies^{8,21} the absolute mean value of the error was presented in our validation study. In the earlier studies some of the mean values of prediction error were negative, which could indicate a conceptual mistake in the analysis of their data. In contrast to other studies our study revealed that although the quality of the prediction varied between the patients, the overall prediction error was not dependent on the surgical procedure. This is in contrast to other studies in the literature^{7,8}.

In the present model the nasal and paranasal areas were better simulated than the areas around the lips. Particularly the lower lip was less accurately predicted. Our hypothesis and suggested reasons for these inaccuracies are discussed in chapter 8 of this thesis.

In conclusion, the work presented in this thesis reveals the evolution of a 3D maxillofacial planning system that has proven to have some advantages. It is an indispensable tool that improves the diagnostic value in the daily practice of maxillofacial surgery. It helps the clinicians to virtually perform different types of osteotomies and visualize the effect of the movement of the osteotomised bony segments on the whole maxillofacial complex. It has proven to be very reliable in the prediction of the vector of maxillary distraction. It provides tools to bring the planned surgery to the operating theatre, and despite its shortcomings, it can be used in all different combinations of orthognathic and distraction surgical procedures. Further research is mandatory to enhance the prediction results of the lower lip region and the cheek area when maxillary impaction of more than 4mm is performed.

Future Directions

The creation of the Maxilim software package has brought many new insights and ideas to the field of 3D assisted orthognathic treatment planning and execution. It is the result of the cooperation of many professionals and although presenting a satisfying outcome yet, it is just the beginning. Still many improvements and fundamental research are needed to improve the present software and enhance its clinical applications. Future improvements should focus on the following main areas.

The simulation of the bony displacements could be refined. The axis of autorotation of the mandible after vertical maxillary displacement should be calculated and implemented in the software. This is important in order to find the autorotated and final position of the mandible after maxillary impaction or extrusion, before the eventual mandibular osteotomy.

Moreover, when the virtual mandibular osteotomy is performed, and the distal segment is moved to its final and desirable position, the eventual bony interferences between the distal and proximal segments should be visualized. These interferences can have an adverse effect on the condyles, which could result in flaring of the mandibular angle and cause adverse esthetic outcome. These effects can be avoided by changing the design of the virtual osteotomies during the planning procedures.

Furthermore, the final result of orthognathic surgery is not only dependent on bony displacement, but also on the soft tissue handling. This is of particular importance in the Le Fort I osteotomy. The type of incision, the effect of maxillary impaction on the nasal tip, the type of procedures to improve the esthetic effect on the nose and to prevent an adverse effect on it, and wound closure are, among others, important factors that would influence the final esthetic outcome¹⁰. So far, these factors cannot be incorporated in the current biomechanical model. In the present model the soft tissues that are not attached to the bone, such as the lips and the buccal areas, are treated as the soft tissues that are connected to the bone. For teeth and lips a sliding contact behavior would be a more correct approximation of the interactions between both. Roose et al¹⁶ implemented such a sliding contact for a breast implantation planning system and could be adapted for usage in our simulator. Secondly, the behavior of the mentalis and orbicularis muscles during mandibular and/or chin movements should be studied and incorporated in the simulation software as well.

Final remark

It should not be forgotten that we still look at 3D images on 2D screens and that it is in fact our brain that adds the 3rd dimension. Nevertheless, taking the recent IT-advances into account it will not take very long before we will virtually be able to handle our planning in a real 3D environment. On the other hand, it will take much longer before the 4th dimension will be computerized. That is the ability of the software to propose an initial planning of the surgical treatment based on the surgeons' input of his/her clinical findings and radiological measurements. The future path of the evolution of 3D maxillofacial planning concepts must be laid in close collaboration between the medical and technical world.

References

1. Donatsky O, Bjorn-Jorgensen J, Holmqvist-Larsen M, Hillerup S. Computerized cephalometric evaluation of orthognathic surgical precision and stability in relation to maxillary superior repositioning combined with mandibular advancement or setback. *J Oral Maxillofac Surg* 1997; 55: 1071-1079
2. Duerinckx AJ, Hall TR, Whyte AM, Lufkin R, Kangaroo H. Paranasal sinuses in pediatric patients by MRI: normal development and preliminary findings in disease. *Eur J Radiol* 1991; 13: 107-112
3. Farkas LG, *Anthropometry of the Head and Face*. Lippincott Williams and Wilkins 1994: 2nd edition
4. Gateno J, Teichgraeber JF, Xia J. Method and apparatus for fabricating orthognathic surgical splints (US patent no. 6,671,539), in USPTO Patent Full-Text and Image Database. December 30, 2003, US Patent and Trademark Office
5. Guerrero CA, Bell WH, Meza LS. Intraoral distraction osteogenesis: maxillary and mandibular lengthening. *Atlas Oral Maxillofac Surg Clin North Am* 1999; 7: 111-151
6. Harvold E. Cleft lip and palate. Morphologic studies of the facial skeleton. *Am J Orthod*. 1954; 40: 493-506
7. Jacobson R, Sarver DM. The predictability of maxillary repositioning in LeFort I orthognathic surgery. *Am J Orthod Dentofacial Orthop* 2002; 122(2): 142-154
8. Kaipatur NR, Flores-Mir C. Accuracy of computer programs in predicting orthognathic surgery soft tissue response. *J Oral Maxillofac Sur*. 2009; 67: 751-759
9. Kessler P, Wiltfang J, Schultze-Mosgaus, Hirschfelder U, Neukam FW. Distraction osteogenesis of the maxilla and midface using a subcutaneous device: report of four cases. *Br J Oral Maxillofac Surg* 2001; 39: 13-21
10. Mitchell C, Oeltjen J, Panthaki Z, Thaller SR. Nasolabial aesthetics. *J Craniofac Surg*. 2007; 18: 756-765
11. Mollemans W, Schutyser F, Nadjmi N, Maes F, Suetens P. Predicting soft tissue deformations for a maxillofacial surgery planning system: from computational strategies to a complete clinical validation. *Med Image Anal* 2007; 11: 282-301

12. Nadjmi N. Predictability of maxillary distraction with the trans-sinusoidal distractor. *Rev Stomatol Chir maxillofac* 2004; 105: 9-12
13. Nadjmi N, Schutyser F, Van Erum R. Trans-Sinusoidal Maxillary Distraction for correction of midfacial hypoplasia: Long-term clinical results. *Int J Oral Maxillofac Surg* 2006; 35: 885-896
14. Nadjmi N, Mollemans W, Daelemans A, Van Hemelen G, Schutyser F, Bergé S. Virtual occlusion in planning orthognathic surgical procedures. *Int J Oral Maxillofac Surg* 2010; 39:457-462
15. Reyneke JP. *Essentials of Orthognathic Surgery*. Quintessence Publishing Co 2003: 1 edition
16. Roose L, De Maerteleire W, Mollemans W, Maes F, and Suetens P. Incorporating implant deformation for a better soft tissue simulation of breast augmentation planning. *Int J Comput Assist Radiol Surg* 2006; 1:148–150
17. Swennen G, Mommaerts M, Abeloos J, Clercq CD, Lamoral P, Neyt N, Casselman J, Schutyser F. The use of a wax bite wafer and a double computed tomography scan procedure to obtain a three-dimensional augmented virtual skull model. *J Craniofac Surg* 2007; 18: 533–539
18. Weinzweig J, Baker SB, Macky GJ, Whitaker LA, Bartlett SP. Immediate versus delayed midface distraction in a primate model using a new intraoral internal device. *Plast Reconstr Surg* 1999; 109: 1600-1610
19. Wenghoefer M, Martini M, Nadjmi N, Schutyser F, Kuijpers-Jagtman AM, Berge S. Transsinusoidal maxillary distraction in three cleft patients. *Int J Oral Maxillofac Surg* 2006; 35: 954–960
20. Wolf G, Anderhuber W, Kuhn F. Development of the paranasal sinuses in children: implication for paranasal surgery. *Ann Otol Rhino Laryngol* 1993; 102: 705-711
21. Xia, J., et al. Computer-assisted three-dimensional surgical planing and simulation. 3D soft tissue planning and prediction. *Int J Oral Maxillofac Surg* 2000; 29(4): 250-258

Samenvatting

Inleiding

Het doel van de behandeling van dento-craniofaciale afwijkingen is het verbeteren van het functionele en esthetische aspect bij patiënten. Een skeletale correctie van deze afwijkingen houdt het uitvoeren van osteotomieën, bot enten, distractie-osteogenese, plaatsing van implantaten en andere behandelingen in. Het effect van deze ingrepen heeft een directe invloed op het persoonlijk en maatschappelijk welzijn van de patiënten. Daarom is het voor de maxillofaciaal chirurg van de 21ste eeuw een uitdaging om perfectie na te streven in de behandeling van de meer dan ooit veeleisende patiënten. De eisen en verwachtingen van de patiënt zijn dramatisch gestegen in het afgelopen decennium, met name als het gaat om de veranderingen in de gelaatsuitdrukking na maxillofaciale procedures⁸. Vanwege de complexiteit van de chirurgische ingrepen zijn zorgvuldige preoperatieve planningen verplicht om een optimaal resultaat te garanderen. Het implementeren van de technische vooruitgang in de medische driedimensionele (3D) beeldvorming, op het gebied van distractie-osteogenese en orthognatische chirurgie, is de motivatie van dit werk. Dit proefschrift geeft een overzicht van het onderzoekswerk uit de periode 1998-2010, wat grosso modo kan worden opgedeeld in twee fasen.

In een eerste fase (1998-2004) werd de beschikbare kennis in de 3D-beeldvorming gebruikt om een computer planningssysteem voor de simulatie van distractie-osteogenese (DO) bij patiënten met maxillaire hypoplasie, in het bijzonder schisis patiënten, te ontwikkelen. Dit initiële onderzoek resulteerde in de ontwikkeling van Maxilim software[®] (Medicim, Mechelen, België). Deze software werd voor het eerst gebruikt om de simulatie van een maxillaire DO met behulp van een transsinusale maxillaire distractor^{4,5,7} (TSMD) uit te voeren. Omdat dit 3D planningssysteem betrouwbaar bleek te zijn voor de chirurgische planning van DO, werd verondersteld, dat het ook voor de planning van complexe gevallen in orthognatische chirurgie inzetbaar zou zijn. Idealiter moest de software in staat zijn om het effect van orthognatische procedures te voorspellen en daar waar nodig aan te passen.

In de tweede fase (2004-2010) werd de Maxilim software verder ontwikkeld met het oog op planning en simulatie van orthognatische procedures, dit vooral op het gebied van de verandering van harde en zachte weefsels enerzijds en het ontwerpen van een occlusie-tool anderzijds^{4,9}.

De eerste fase

Het initiële werk concentreerde op DO bij patiënten met een maxillaire hypoplasie, in het bijzonder schisis patiënten. Kort na de introductie van de extraorale DO werd onderzoek naar de ontwikkeling van intra-orale apparaten gestart. Enerzijds waren de externe systemen omslachtig, goed zichtbaar en werden meestal niet goed verdragen door patiënten². Anderzijds hadden ook de voorgestelde intra-orale apparaten meerdere belangrijke nadelen. Ten eerste waren ze te volumineus. Voorts werden ze volledig onder het periost geplaatst. De activatiestaafjes waren voortdurend in contact met de lippen, wat irritatie, soms zelfs pijn veroorzaakte. Soms moesten de activatiestaafjes in de nasolabiale regio^{1,3,11} transcutaan gelokaliseerd worden. Tenslotte waren alle intra-orale DO-apparaten unidirectioneel, waardoor een absoluut perfecte preoperatieve vectorplanning noodzakelijk was.

Als oplossing voor de bovenvermelde problemen werd een distractor ontwikkeld waarbij de distractieschroef binnen de holte van de sinus maxillaris kon worden geplaatst. De positieve resultaten van het initiële, experimentele werk vormden de aanzet tot de ontwikkeling van een trans-sinusaal apparaat voor de distractie van de bovenkaak voor patiënten met een ernstige midfaciale hypoplasie (in samenwerking met KLS-Martin Medizin-Technik, Tuttlingen, Duitsland) (**hoofdstuk 2 & 3**).

Om de volgende uitdaging aan te pakken, was de preoperatieve transfer van de preoperatief berekende distractievector. In samenwerking met ESAT (KU Leuven, België) werd software ontwikkeld, waardoor het distractie apparaat virtueel op de bovenkaak van de patiënt kon worden geplaatst na het plannen en digitaal uitvoeren van een virtuele osteotomie op het niveau van Le Fort I. In aansluiting hierop werden verschillende klinische studies gepubliceerd, eerst als voorlopige resultaten, later als lange termijn follow-up en tenslotte als een kritische evaluatie van de klinische toepasbaarheid van de TS-MD^{4,5,7} (**hoofdstuk 4a, 4b & 5**).

De tweede fase

Hoewel het hierboven genoemde 3D planningsstelsel bewees betrouwbaar te zijn in de chirurgische planning van distractieosteogenese, was het op dat ogenblik niet mogelijk de veranderingen van de bedekkende weke delen te voorspellen tijdens een DO. Er moest dus een biomechanisch simulatiemodel worden ontwikkeld om de simulatie van de 3D-elastische vervorming van de weke delen van het gezicht na benige verplaatsing uit te voeren. Vier computer strategieën, te weten een lineaire finite element model, een niet-lineaire finite element model, een mass spring model en een nieuwe mass tensor model, werden vergeleken. De invoering van het nieuwe mass tensor model toonde een significante simulatie tijdwinst in vergelijking met de anderen. Verder werd de nauwkeurigheid van deze computer gestuurde simulatie software beoordeeld. De beste resultaten werden verkregen door het gebruik van het lineaire finite element model cq. Het mass tensor model⁴ (**hoofdstuk 6**).

Er waren nog twee belangrijke aanvullende ontwikkelingen noodzakelijk om de software nuttig te maken in de dagelijkse praktijk van de orthognatische chirurgie. In de eerste plaats moest de precieze visualisatie van het occlusale oppervlakte van de tanden in beeld gebracht worden. Ten tweede moest de virtuele planning van de definitieve occlusie gerealiseerd worden. Nadat Swennen et al. er in waren geslaagd om met behulp van een 'triple scan procedure'¹⁰ de digitale gebitsmodellen op de juiste plaats met de digitale schedel te fusioneren, bestond de volgende stap er in de virtuele occlusie te definiëren. De oplossing werd gevonden door het ontwikkelen van een 'rigid motion simulation engine'. De validatie van deze software toonde dat het gepresenteerde systeem resulteerde in een betrouwbare bepaling van de gewenste occlusie⁶ (**hoofdstuk 7**).

Na de integratie van de gepresenteerde occlusie module in een orthognatisch planningssysteem werd een eerste serie van complete digitale orthognatische planning uitgevoerd. Een validatie van de weke delen veranderingen na de voorspelling van de exacte intermaxillaire relatie zoals hierboven beschreven, werd gerealiseerd (**hoofdstuk 8**).

Summary

Introduction

The aim of treating abnormalities of the dento-craniofacial complex is to improve the patients' function and aesthetics. The skeletal remodeling in the course of these treatments implies performing osteotomies, bone grafting, distraction osteogenesis, implant placement and other treatment modalities. The effect of these treatments has a direct influence on the patients' personal and social wellbeing. Therefore the challenge of maxillofacial surgeons in the 21st century is to achieve excellence in treating more than ever demanding patients. Patients' demands and expectations have risen dramatically in the past decade, especially when it comes to the changes in facial appearance after maxillofacial procedures⁸. Due to the complexity of the surgical procedures, careful pre-operative planning of the surgical intervention is mandatory to ensure an optimal outcome. Implementation of technical advances in medical three-dimensional (3D) imaging in the field of distraction osteogenesis and orthognathic surgery has been the motivation of this work. This thesis summarizes research work from 1998 through 2010 that basically has been performed in two phases.

In the first phase (1998-2004), the available knowledge in 3D imaging at that time was used to introduce a computer planning system to simulate distraction osteogenesis (DO) in patients with maxillary hypoplasia, in particular cleft patients. This initial research resulted in the development of the Maxilim software[®] (Medicim, Mechelen, Belgium). It was first used to simulate a maxillary DO, using a trans-sinusal maxillary distraction (TSMD) device^{4,5,7}. As this 3D bone-related planning system proved to be reliable in surgical planning of DO, it was assumed that it might as well be useful in the planning of complex cases in orthognathic surgery. Ideally, the software should be able to virtually predict the effect of orthognathic procedures in exceptionally complex situations, and, if necessary to adapt it to ensure an excellent outcome.

In the second phase (2004-2010), the Maxilim software[®] was further developed to support planning and simulation of hard and soft tissue changes of orthognathic procedures. In addition an occlusal defining tool was developed and implemented in the software^{4,9}.

The first phase

The initial work focused on the field of distraction osteogenesis (DO) in patients with maxillary hypoplasia, in particular patients with clefts. Shortly after the introduction of extraoral DO, research on the development of intraoral devices started. The external devices, were cumbersome, highly visible, and were mostly not well tolerated by patients². The suggested intraoral devices had two main disadvantages. Firstly, they were still too bulky, and were placed completely under the periosteum. The activation rods were either in continuous contact with lips, causing pain and irritation, or had to be delivered through the skin in the nasolabial region^{1,3,11}. Secondly, they were all unidirectional, which required a perfect preoperative vector planning.

To overcome the above-mentioned disadvantages, a distractor was designed in a way that the distraction screw could be placed inside the maxillary sinus cavity. The positive results of the initial, experimental work resulted in the development of a trans-sinusal device for distraction of the maxilla in children and adults with mild to severe midfacial hypoplasia (in cooperation with KLS-Martin Medizin-Technik, Tuttlingen, Germany (**chapter 2 & 3**)).

The following challenge that had to be overcome was the prediction of the distraction vector pre-operatively on one hand and transferring this vectorplanning to the patient per-operatively on the other hand. In cooperation with ESAT KULeuven, Belgium, software was developed, that could virtually place the distractor device on the maxilla after a virtual Le Fort I type osteotomy was planned and virtually performed. Subsequently different clinical studies were undertaken and were published as preliminary results and later on as a critical evaluation of the clinical applicability and the long-term follow up of the TS-MD^{4,5,7} (**chapter 4a, 4b & 5**).

The second phase

Although the above mentioned 3D bone-related planning system proved to be reliable in surgical planning of DO, it was not possible at that time to predict the changes of the overlying soft tissue envelop during the DO. As a consequence, the next step was the development of a biomechanical simulation model that would attempt to simulate the 3D elastic deformation behaviour of facial soft tissues after bony displacement. Four computational strategies were compared to simulate the post-operative facial appearance: a linear finite element model, a non-linear finite element model, a mass spring model and a new mass tensor model. The introduction of this last model showed a significant gain in simulation time compared to the other models. Further the accuracy of the prediction of the new facial outlook after surgery was assessed. The best results were obtained by using the linear finite element model or the mass tensor model⁴ (**chapter 6**).

In order to make this software beneficial in daily practice of orthognathic surgery, two main additional developments had to be implemented. Firstly the occlusal surface of the teeth had to be visualized with high precision, and secondly a virtual planning of dental occlusion was mandatory. Swennen et al.¹⁰ succeeded to implement the first change in the software using their triple scanning technique. It was now necessary to define the virtual occlusion. This was realized by the development of a 'rigid motion simulation engine'. A rigid motion simulation engine ensured the impenetrability of the dental models. Moreover, this engine enabled the user to identify the desired occlusion semi-automatically. The motion engine allowed almost real-time simulations. This software tool was validated and the result showed that the presented system allowed a reliable determination of the desired occlusion⁶ (**chapter 7**).

After having integrated the presented occlusal model into an orthognathic planning system, the first complete orthognathic planning system became a reality and was taken into the clinical application. A validation of the soft tissue changes after prediction of the precise intermaxillary relationship became the subject of **chapter 8**.

References

1. Guerrero CA, Bell WH, Meza LS. Intraoral distraction osteogenesis: maxillary and mandibular lengthening. *Atlas Oral Maxillofac Surg Clin North Am* 1999; 7: 111-151
2. Jacobson R, Sarver DM. The predictability of maxillary repositioning in LeFort I orthognathic surgery. *Am J Orthod Dentofacial Orthop* 2002; 122(2): 142-154
3. Kessler P, Wiltfang J, Schultze-Mosgaus, Hirschfelder U, Neukam FW. Distraction osteogenesis of the maxilla and midface using a subcutaneous device: report of four cases. *Br J Oral Maxillofac Surg* 2000; 39: 13-21
4. Mollemans W, Schutyser F, Nadjmi N, Maes F, Suetens P. Predicting soft tissue deformations for a maxillofacial surgery planning system: from computational strategies to a complete clinical validation. *Med Image Anal* 2007; 11(3): 282-301
5. Nadjmi. N. Predictability of maxillary distraction with the trans-sinusoidal distractor. *Rev Stomato Chir maxillofac* 2004; 105(1): 9-12
6. Nadjmi N, Mollemans W, Daelemans A, Van Hemelen G, Schutyser F, Bergé S. Virtual occlusion in planning orthognathic surgical procedures. *Int J Oral Maxillofac Surg* 2010; 39:457-462
7. Nadjmi N, Schutyser F, Van Erum R. Trans-Sinusal Maxillary Distraction for correction of midfacial hypoplasia: Long – term clinical results. *Int J Oral Maxillofac Surg* 2006; 35: 885-896
8. Reyneke JP, *Essentials of Orthognathic Surgery*. Quintessence Publishing Co, 1 edition, 2003
9. Roose L, De Maerteleire W, Mollemans W, Maes F, and Suetens P. Incorporating implant deformation for a better soft tissue simulation of breast augmentation planning. *Int J Comput Assist Radiol Surg* 2006; 1:148–150
10. Swennen G, Mommaerts M, Abeloos J, Clercq CD, Lamoral P, Neyt N, Casselman J, Schutyser F. The use of a wax bite wafer and a double computed tomography scan procedure to obtain a three-dimensional augmented virtual skull model. *J Craniofac Surg* 2007; 18: 533–539
11. Weinzweig J, Baker SB, Macky GJ, Whitaker LA, Bartlett SP. Immediate versus delayed midface distraction in a primate model using a new intraoral internal device. *Plast Reconstr Surg* 1999; 109: 1600-1610

List of abbreviations

2D	2-Dimensional
3D	3-Dimensional
AA	Activation Arm
AH	Activation Head
ANS	Anterior Nasal Spine
BCLP	Bilateral Cleft Lip and Palate
CBCT	Cone Beam CT
CLP	Cleft Lip and Palate
CP	Consolidation Period
DO	Distraction Osteogenesis
DP	Distraction Period
FEM	Finite Element Model
GMRES	General Minimum Residual
MSM	Mass Spring Model
MTM	Mass Tensor Model
NFEM	Nonlinear Finite Element Model
NHD	Natural Head Distance
NHP	Natural Head Position
OR	Operating Room
PI	Point of Intersection
PNS	Posterior Nasal Spine
RED	Rigid External Device
SD	Standard Deviation
STL	Stereolithographic
TS-MD	Trans-Sinusal Maxillary Distractor
UCLP	Unilateral Cleft Lip and Palate

Acknowledgement

It would not have been possible to write this doctoral thesis without the help and support of the kind people around me, to only some of whom it is possible to give particular mention here.

I still remember very vividly, sitting at the stern of the training ship crossing the Atlantic Ocean, watching the stars above and lost in my dreams. I was 19 and although in training to become a sea captain, continuously reminded of my childhood dream to become a physician and a researcher. '*Daneshmand*' as we call it in Persian. A dream that seemed to be unattainable at the time.

But eventually this dream became the aim of my life as I kept on trying to give it dimensions in the reality. Almost four years later, the decision was made. I would stay in Belgium to fulfill my dream. During the last months of my training at the Nautical School in Antwerp (Hogere Zeevaartschool), I travelled to Tehran and discussed the consequences of my decision with my parents. Those were emotionally very tough to accept, not to mention the financial consequences. My country was in war and I would not be able to travel back home if I would break with the company who sponsored my nautical studies in Antwerp. Neither my family would be able to travel to Belgium, because of the harsh economical situation during the war. My parents did not hesitate a second to accept all the consequences and would support and respect my decision. At the time I could not even imagine how hard it had been for them. Now, being a father myself, I realise how unconditional their love had been. Their love gave me wings to fly and discover the world and myself. Therefore, I would like to express my sincere thanks and love to the both of them.

I would like to thank my children, Julie and Kian. They had to miss their fathers' attention during so many weekends and evenings. Just a few weeks ago Kian told me: "Papa, you are almost there and I know you can make it..." It was a beautiful moment of my life. Also, I would like to mention my gratitude to their mother, Katherine, for taking care of them with love during all of those moments.

I am indebted to Professor Bergé for his friendship and professional guidance. Dear Stefaan, this thesis would not have been possible without your brilliant advices that lighted my way throughout this work, not to mention your patience and accuracy in reviewing this thesis. I have enjoyed our many discussions during the past years.

The good advice, support and friendship of my co-supervisor, Professor Kuijpers-Jachtman, have been invaluable, for which I am extremely thankful.

I am most grateful to Dr. Ria Van Erum for her unsurpassed kindness and support from the very beginning of my research work.

Her positive attitude and professional insight were extremely valuable for the start of the experimental study and further clinical work.

Without the cooperation with the medical image computing group (ESAT, KULeuven, Belgium) under guidance of Professor P. Suetens, and the hard work of Filip Schutyser and Dr. Wouter Mollemans, my imaginations and ideas would have never become a reality, for which my utmost gratitude.

Not to forget are all the members of our wonderful team of MKA at AZ Monica and AZ KLINA for their support and extremely good care of our patients, those who participated in our studies and others. Beside the very busy clinical activities in our practice, scientific work was made possible by their hard work and professionalism. My special thanks goes to Claudia who spend hours of her free time helping me with the typing and layout of this work and to Kim for organizing 'D-day'!

For any errors or inadequacies that may remain in this work, of course, the responsibility is entirely my own.

Curriculum Vitae



Nasser NADJMI
MD, DDS, FEBOMFS

Nasser Nadjmi was born on 27th of March 1965 in Tehran, Iran, where he lived until the age of 18. After finishing his high school in Iran and due to the post-revolution circumstances in his country he could not start the medical studies in Iran. He did the selection exams to get a scholarship to come to Belgium for nautical studies. Those exams took seven months and in the meanwhile he got the diploma of building surveying from a private institution in Tehran.

In October 1984 he came to Antwerp, Belgium, after being selected for the studies of merchant marine at the Higher Nautical College Antwerp. He was graduated as an aspirant officer for merchant marine in July 1987.

In August of the same year he followed an intensive course on the Dutch language at 'Centrum voor Levende Talen' in Leuven, Belgium.

In September 1987, after a successful entrance exam, he was admitted at the dental school of the Catholic University of Leuven. In September 1988 he was admitted to the Medical school of the same university and combined the medical and dental studies. In June 1992 he got his dental degree and in June 1995 his medical degree from the KUL.

In July 1995 he started his training in Oral and Maxillofacial Surgery at the Saint John Hospital in Bruges, Belgium, which was affiliated with the KUL. In July 1997 he was graduated as Stomatologist and in August of the same year he was granted a Chief Residency position at the department of Oral and Maxillofacial Surgery at the University of Houston, Texas, USA. From December 1997 through March 1998 he functioned as a chief resident at the Department of Plastic and Craniofacial Surgery of the Providence Hospital in Southfield, Michigan. He also had a three months rotation at the ENT department of MD Anderson Cancer Center in Houston, Texas. After his return from the United States in August 1998 he started as a Chief Resident at the Department of Oral and Maxillofacial Surgery in Leuven, Belgium. In July 1999 he was graduated as an Oral and Maxillofacial Surgeon from KUL. After that and through December of the same year he followed a fellowship in Facial Plastic Surgery at the private clinic for Plastic Surgery of Dr. Backer and Dr. Stuzin in Miami, USA.

In January 2000 he joined the Craniofacial Association in Antwerp, Belgium. In the same year he founded the Cleft team at the University of Antwerp (UA). Since May 2010 he has become the coordinating program director for Oral and Maxillofacial Surgery through the UA. Currently he is a full member of the Craniofacial Association in Antwerp and functions as Director of the Cleft team at the UA and Director of the Department of Oral and Maxillofacial Surgery at AZ KLINA in Brasschaat, Belgium. He teaches at the University of Antwerp, school of medicine: 4th year medical students, since 2002 on the subject of “Congenital Craniofacial Deformities” and postgraduate course on “Maxillofacial Surgery” since 2004 at the same University.

Nasser has two children, Kian (10 years) and Julie (9 years) and lives in Antwerp, Belgium.

List of publications

1. Nadjmi N, Mommaerts MY, Abeloos JVS, De Clercq CAS, Neyt LF. Prediction of Mandibular Autorotation. *Int J Oral Maxillofacial Surg* 1998; 56:1241-1247
2. Mommaerts MY, Nadjmi N, Abeloos JVS, De Clercq CAS, Neyt LF. 6 years of experience with the Zygomatic Sandwich Osteotomy. *Int J Oral Maxillofacial Surg* 1999; 57: 8-13
3. Nadjmi N. and Jackson IT. Split thickness skin graft in the secondary reconstruction of the bilateral cleft lip. *Int J Oral Maxillofac Surg* 1999; 28: 176-178
4. Schutyser F, Van Cleynenbreugel J, Nadjmi N, Schoenaers J, Suetens P. 3D image-based planning for unilateral mandibular distraction. *Excerptamedica, international congress series 1214, proceedings 14th international congress and exhibition on computer assisted radiology and surgery CARS 2000: 899-904, San Francisco, USA*
5. Nadjmi N, Schutyser F. Mid-facial distraction with an intra-oral trans-sinusoidal distractor. Cranial and facial bone distraction processes, proceedings of the 3rd international congress of craniofacial and maxillofacial distraction - 2001 distraction odyssey: 419-424 June 14-16, 2001
6. Nadjmi N, Schutyser F, Defrancq J, Noorman van der Dussen F, Vanassche B, Van Hemelen G, Vercruysse H. Mid-facial distraction : easy and predictable. *Int J Oral Maxillofac Surg* 2003; 32: supplement 1: (16th international conference on oral and maxillofacial surgery - ICOMS May 14-20, 2003, Athens, Greece)
7. Nadjmi N, Van Erum R, Schoenaers J, Schepers E. Maxillary distraction using a trans-sinusal distractor: technical note. *Int J Oral Maxillofac Surg* 2003; 31: 553-9
8. Stalmans K, Van Erum R, Verdonck A, Nadjmi N, Schepers E, Schoenaers J, Carels C. Cephalometric evaluation of maxillary advancement with an internal distractor in an adult boxer dog. *Orthod Craniofacial Res* 2003; 6: 104-11.
9. Nadjmi N. Prédicibilité de la distraction du maxillaire supérieur avec distracteur transsinusien. *RevStomatoChirMaxillofac.* 2004; 105: 9-12
10. Mollemans W, Schutyser F, Nadjmi N, Suetens P. Very fast soft tissue predictions with mass tensor model for maxillofacial surgery planning systems. *Proceedings 19th international congress and exhibition on computer assisted radiology and surgery - CARS June 22-25, 2005, Berlin, Germany*

11. Mollemans W, Schutyser F, Nadjmi N, Maes F, Suetens P. 3D soft tissue prediction with a tetrahedral mass tensor model for a maxillofacial planning system : a quantitative validation study. SPIE medical imaging 2006 conference, February 11-16, 2006, San Diego, California, USA
12. Wenghoefer M, Martini M, Nadjmi N, Schutyser F, Jagtman A. K, Bergé S. Transsinusoidal maxillary distraction in three cleft patients. *Int J Oral Maxillofac Surg* 2006; 35: 954–960
13. Nadjmi N, Schutyser F, Van Erum R. Trans-Sinusoidal Maxillary Distraction for correction of midfacial hypoplasia: Long – term clinical results. *Int J Oral Maxillofac Surg* 2006; 35: 885-896
14. Mollemans W, Schutyser F, Nadjmi N, Maes F and Suetens P. Predicting soft tissue deformations for a maxillofacial surgery planning system: from computational strategies to a complete clinical validation. *Medical Image Analysis* 2007; 11: 282-301
15. Kurpershoek T, Wojcieckowski M, Nadjmi N, Vleminck I, Marien S, Claes J. Recurrent nasal bridge abscesses due to nasal dermoid sinus cyst. *Proceedings van de Belgische Vereniging voor Kindergeneeskunde - Societe Belge de Pediatrie* 2008; 1: 96-97
16. Nadjmi N, Mollemans W, Daelemans A, Van Hemelen G, Schutyser F, Bergé S. Virtual occlusion in planning orthognathic surgical procedures. *Int J Oral Maxillofac Surg*. 2010; 39(5): 457-62
17. Nadjmi N, Defrancq E, Mollemans, Van Hemelen G, Bergé S. Quantitative validation of a computer aided maxillofacial planning system, focusing on soft tissue deformations. Submitted to *Int J Oral Maxillofac Surg*.

Appendix

Development of Trans-Sinusal Maxillary Distractor

During my last year of residency (1998-99) at the University of Leuven, Belgium, I designed a maxillary distraction device that could be placed intra-orally, with the activation screw placed into the sinus cavity. The prototype device was built by Titamed, Antwerp, Belgium. The device was applied on a Boxer dog since they do inherently have a maxillary retrusion. The experimental animal study proved to be successful (Chapter 1 and 3).

From the very beginning of the success story of DO, KLS Martin, Tuttlingen, Germany, proved to be the leading company in developing and manufacturing distraction devices. Based on the success of the animal study, they agreed to build a clinical prototype, which turned out to be a long and difficult process. Some of the main designs of the developing process, in cooperation with the KLS Martin company, on the way to the final Trans Sinusal Maxillary Distraction (TSMD) device, are depicted (Fig. 1-7).

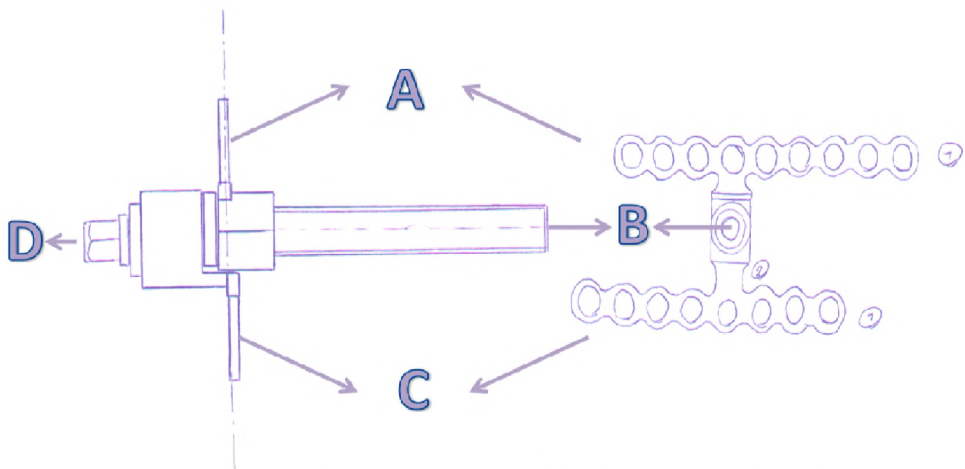


Fig. 1. One of the first hand drawn designs of the device: the distraction device consisted of two parts: an upper plate (A), fixed cranial to the osteotomy line, which is attached to a cylinder in which screw rods are tapped. The second part consists of a distracting screw (B), which is attached to a caudal plate (C) and an activation head (D). This plate is fixed caudal to the osteotomy line. The distraction screw is placed inside the maxillary sinus. In the original drawing the activation head was directly attached to the distractor.



Fig. 2. In the first prototype, the distance between the plates and the distractor was too short, so that it was impossible to adapt them properly to the anterior maxillary wall. The activation head was not long enough and was easily submerged under the mucosa.



Fig. 3. Although the distance between the plates and the distractor was made longer, it was still difficult to adapt them to the anterior maxillary wall. The activation head was now connected to the activating rod by a universal joint. The length of the activation arm turned out to be still too short

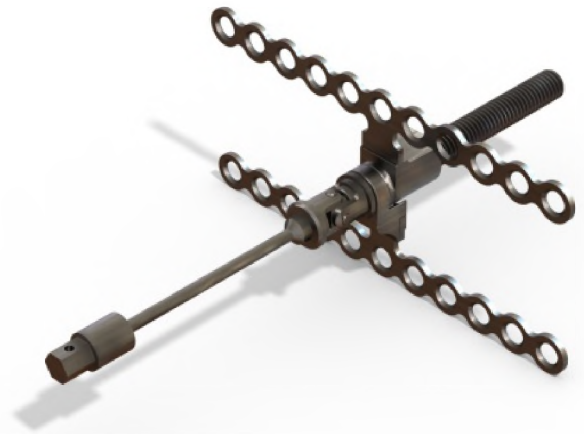


Fig. 4. Next, the plates were made significantly thinner so that the adaptability became easier, but it became apparent that they would bend too easily during the activation period. The activation arm was constructed longer, but was too thin and would also bend during distraction

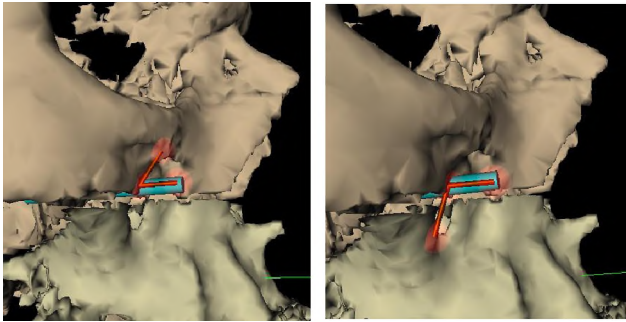


Fig. 5. The inclination of the anterior maxillary wall was measured on the 3D scan of multiple cleft patients with maxillary retrusion.

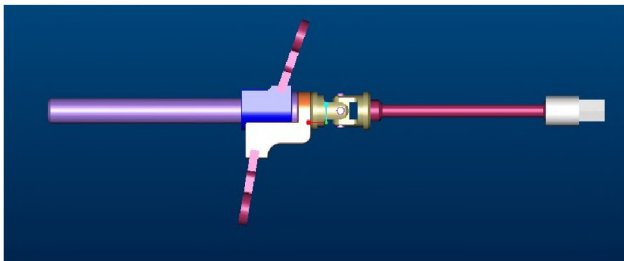


Fig. 6. The mean value of the measurements was applied to both the distraction plates, in order to make a universal prototype



Fig. 7. The final prototype with obliquely oriented plates, that made the adaptation to the anterior maxillary wall much easier, was more stable than the one depicted in figure 4.

The final prototype (Fig.7) had the potential to be used clinically and was a unidirectional device.

This document was created with Win2PDF available at <http://www.win2pdf.com>.
The unregistered version of Win2PDF is for evaluation or non-commercial use only.
This page will not be added after purchasing Win2PDF.